The Structure and Function of GLFGs in the Nuclear Pore Complex of Yeast

MATTHEW CHARLES SPINK

The Structure and Function of GLFGs in the Nuclear Pore Complex of Yeast

Matthew Charles Spink

Submitted for the degree of MSc in the School of Biological and Biomedical Sciences 2012

Abstract

The nuclear pore complex (NPC) is a large multiprotein complex which perforates the nuclear envelope. The NPC is made up of nuclear pore proteins (Nups), one third of which are phenylalanine-glycine (FG) containing. The NPC has a role in controlling movement of molecules between the nucleus and the cytoplasm. The FG Nups fill the NPC's centre and regulate translocation. There are many different proposed models of how FG Nups may regulate translocation from them reeling cargo complexes into the NPC to inter FG repeats binding to create a gel-like meshwork into which specific cargo can enter and translocate. Using transmission electron microscopy the glycine-leucine-phenylalanine-glycine (GLFG) domains of Nups are mapped, showing a cytoplasmic bias within the wild type (WT) NPC and also in FG domain deletion mutants. FG deletion mutants have higher percentages of GLFG labelling towards the NPC edge than WT and lower percentages towards the middle than WT. GLFG domain labelling is also observed 'reaching' to membrane structures from the NPC. Serial sectioning of individual NPCs confirmed that individual NPCs had different distributions of GLFG labelling, which was on the nucleoplasmic or cytoplasmic side, or on both sides. Mutants which are defective in the nucleotide exchange activity of the RanGEF, Prp20, have a deficiency of the active RanGTP molecular switch. This causes a shift in the GLFG labelling from the cytoplasmic side towards the nucleoplasmic side. Similarly the import of Kap121-dependant import cargo causes a shift from cytoplasmic to nucleoplasmic labelling. This is observed as the cargo reaches the midplane of the NPC. Field emission scanning electron microscopy shows GLFG labelling to be associated with filaments (cytoplasmic, internal and nucleoplasmic) and possibly also the transporter. Finally, a model based on the shift in GLFG labelling is developed. This model suggests that there is a collapse and 'reel in' of import cargo as in the reversible collapse model, there is then a restructure of GLFG domains into the nucleoplasm due to potentially passing cargo on.

Contents

Abbreviations

AA	amino acid
AFM	atomic force microscopy
CF	cytoplasmic filament
CT/P	central plug
DBR	distal basket ring
FESEM	field Emission Scanning Electron Microscopy
FG	phenylalanine-glycine
GDP	guanine di-phosphate
GLFG	glycine-leucine-phenylalanine-glycine
GTP	guanine tri-phosphate
IBB	importin-β binding domain
INM/ONM	inner/outer nuclear membrane
Kap	karyopherin
LR	luminal ring
MT	microtubule
mRNP	messenger ribonucleoprotein
NCT	nucleocytoplasmic transport
NE	nuclear envelope
NES	nuclear export signal
NLS	nuclear localization signal
NPC	nuclear pore complex
NR	nuclear ring
Nup	nuclear pore protein
OD	optical density
PBS	phosphate buffer saline

Pom	pore membrane protein
Ran	a ras related nucleo-protein
RanGAP	a RanGTPase activating protein
RanGEF	ran guanine exchange factor
RT	room temperature
SPB	spindle pole body
TEM	transmission electron microscopy
TF	transport factor
Tpr	translocated promoter region
WT	wild type
YPD	yeast extract peptone dextrose

Chapter 1 Introduction

I will begin by discussing the nuclear pore complex (NPC) structure in various species, with particular focus on yeast. The structure differs between eukaryotes, however there is a high degree of conservation. Structural information for each component of the NPC is given. I explain what Ran is and its role in translocation through the NPC. Finally I summarise the many translocation models which differ on the role of the FG Nups.

1.1 The NPC Structure

NPC structure

The nuclear pore complex (NPC) perforates the nuclear envelope (NE), which consists of two membranes separated by a lumen. The NPC has a role in controlling movement of molecules between the nucleus and the cytoplasm. The NPC is a large multiprotein complex with an estimated mass of at least 60MDa in vertebrates (Cronshaw *et al* 2002) and in the region of 44MDa (Rout *et al* 2000) to 55MDa in yeast (Yang *et al* 1998). NPCs contain 456 individual protein molecules and are composed of ~30 different proteins (Alber *et al* 2007[2]; Rout *et al* 2000). These proteins are termed nucleoporins (Nups) and 1/3 of them are phenylalanine-glycine (FG) containing. These fill the pore's centre and regulate translocation. The NPC has eight-fold rotational symmetry around a central channel (~38nm in yeast) (Alber *et al* 2007[2]). There are several coaxial rings which perforate the NE. From the most cytoplasmic of the rings 8 filaments are attached and extend into the cytoplasm, these are known as cytoplasmic filaments. From the most nucleoplasmic ring 8 filaments extend, joining to make a basket in the nucleus. Another set of filaments (internal filaments) has also been observed extending from the coaxial rings towards the NPC centre (Goldberg *et al* 1996) (Structure reviewed in Lim *et al* 2008).

Studies have shown the NPC to be largely conserved amongst all studied eukaryotes. However there are some differences; for example yeast NPCs are smaller than vertebrate NPCs (Yang *et al* 1998). Two thirds of the Nups are conserved between yeast and vertebrates. Some of the Nup

associated proteins are also conserved (Cronshaw *et al* 2002). Some studies of NPCs in various organisms include:

- *Xenopus* (Akey *et al* 1993; Goldberg *et al* 1996; Hinshaw *et al* 1992; Stoffler *et al* 2003)
- Birds (Goldberg *et al* 1997)
- Plant (Fiserova *et al* 2009)
- Yeast (Alber *et al* 2007[2]; Kiseleva *et al* 2004; Rout *et al* 2000; Yang *et al* 1998)
- *Dictyostelium discoideum* (Beck *et al* 2004, 2007)

Yeast NPC similarities and differences from higher eukaryotes

Many studies look at yeast NPCs and it is important to take into account why they may differ from NPCs in higher eukaryotes. Yeast cells are smaller, have rapid cell division and have a cell wall so require a much less complex cytoskeleton in comparison to vertebrates. Also, yeast have a closed mitosis as the NE does not break down. One consequence of this is that there is no need to disassemble NPCs. On the other hand, vertebrate cells have a lamina and larger nuclei, they do not have a closed mitosis as the NE does break down and NPCs must disassemble. Vertebrate cells can also specialise from stem cells by differentiating to fulfil a particular role, whereas yeast cells are unable to do this. The NE lumen appears to be thinner in yeast at ˜25-30nm (Yang *et al* 1998), this is based on 31 measurements, compared to 50-60nm in vertebrate (Goldberg and Allen 1996). Yeast NPCs therefore have a thinner NE to span and so have a smaller vertical spoke size. The vertebrate NPC (~105nm diameter) has a generally greater dimensionality than the yeast NPC (~95 nm diameter) (Kiseleva *et al* 2004). Reconstructions have shown some thin coaxial rings to be missing in yeast (Yang *et al* 1998), however in Kiseleva *et al* (2004) and Alber *et al* (2007[2]) they were observed to be present. It is reported that yeast have no nuclear lamina (Strambio-de-Castillia *et al* 1995). If this is true or there is no interaction of lamina with the NPCs, then there would be no yeast homologue of vertebrate lamina interacting parts of the NPC for example Nup153. However, the lamina in yeast is not yet fully understood.

Coaxial rings making the core scaffold of the pore and luminal spoke ring

Alber *et al* (2007[1]) models the yeast NPC giving structural information about the core scaffold and luminal spoke ring of the NPC (the results are presented in Alber *et al* (2007[2])). Modelling based on experimental evidence such as sedimentation analysis gives information on Nup shapes, immuno EM gives Nup position and affinity purification providing arrangement and interactions of Nups (Alber *et al* 2007[1]). Data is generated in experimental evidence then modelled using spatial

restraints. The data is then analysed to see how the Nups best fit together, giving a model of the NPC (Alber *et al* 2007[1]). This modelling suggests that the NPC consists of 8 spokes; each spoke can mostly be divided into two parallel columns (Alber *et al* 2007[2]). A Nup in one column contains a counterpart of similar size and in a similar position in an adjacent column (Alber *et al* 2007[2]). These are Nup pairs and are often homologues or duplicate copies, making each spoke bipartite (Alber *et al* 2007[2]). Spokes (Figure 1.1 D) connect together forming several coaxial rings (Figure 1.1 C); a cytoplasmic ring (CR), a lumenal spoke ring (also known as membrane ring) and a spoke ring (also known as the inner ring) complex and a nuclear ring (NR) shown in Figure 1.1 A, B, C, D. These rings are distinct, but connected, structures as shown by cryo-electron tomography (Beck *et al* 2007). The spoke ring complex attaches to and coats the pore membrane (Alber *et al* 2007[2]). An inner luminal connector element connects the membrane contacts of the nuclear and cytoplasmic rings, spanning the lumen between the inner nuclear membrane (INM) and outer nuclear membrane (ONM) (Beck *et al* 2007). It is suggested in Beck *et al* (2007) that this may stabilise the whole NPC. The core scaffold consists of Nups with either an α-solenoid, a β-propeller or both (an amino-terminal β-propeller followed by a C-terminal α-solenoid domain) (Alber *et al* 2007[2]; Devos *et al* 2004). α-solenoid domains are numerous pairs of anti-parallel α-helices stacked to form a solenoid (Devos *et al* 2004). α-solenoids are thought to be flexible (Conti *et al* 2006). This may explain how the NPC has the required degree of flexibility for transport of many cargoes, and to keep the NE's structural properties (Alber *et al* 2007[2]). A β-propeller is several 'blades' arranged around a central axis in a 'propeller' arrangement. Each of the propeller blades is made of four-stranded anti-parallel β-sheets (Devos *et al* 2004; Andrade *et al* 2001). These core scaffold Nup fold types share similarities with vesicle coating complexes, and are thought to coat and curve the NE membranes. The similarities of the scaffold Nups with vesicle coating complexes hints at the NPC's origins (Devos *et al* 2004; Alber *et al* 2007[2]). Most of the interactions of Nups are heterotypic, often forming NPC substructures (Alber *et al* 2007[2]).

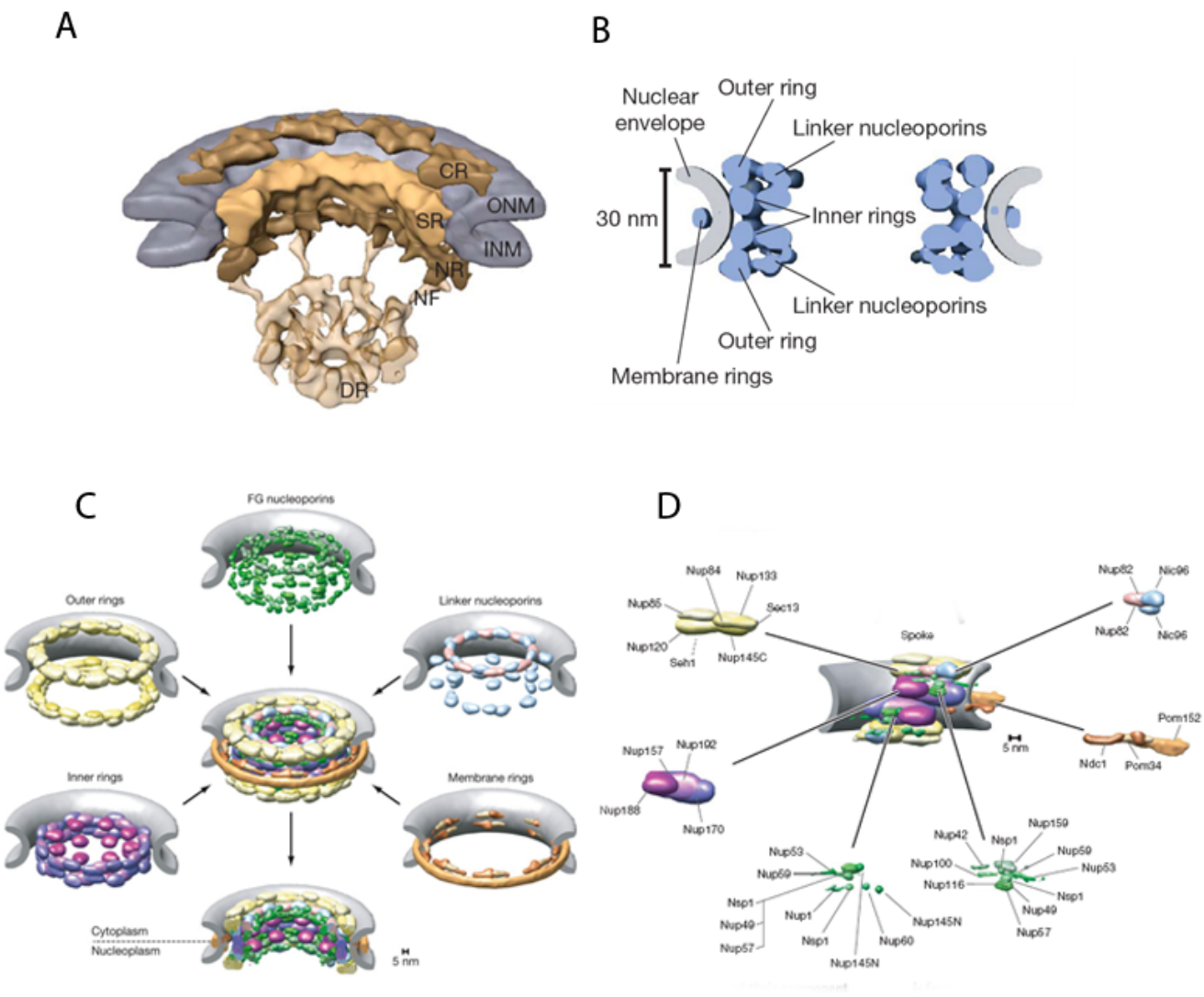

Figure 1.1 The predicted composition of NPC coaxial rings. (A) From Beck *et al* (2007). An NPC perforating the NE, ONM; outer nuclear membrane; INM, inner nuclear membrane; CR, cytoplasmic ring; SR, spoke ring; NR, nucleoplasmic ring; NF nucleoplasmic filament; DR, distal ring. (B) From Alber *et al* (2007[2]). The core scaffold consisting of the outer (cytoplasmic and nucleoplasmic rings), inner rings (spoke rings) and the membrane rings (luminal spoke ring) in the lumen of NE. (C) From Alber *et al* (2007[2]), depicts how the rings form the NPC. (D) From Alber *et al* (2007[2]), depicts the Nups forming a spoke, the spokes form the rings of the NPC.

Cytoplasmic Ring

Structural detail about the cytoplasmic ring has been obtained using field emission in-lens scanning electron microscopy (FESEM) in *Xenopus* by Goldberg and Allen (1996). This shows the

cytoplasmic ring to consist of 8 bipartite subunits with cytoplasmic filaments attached (Goldberg and Allen 1996). Removing the cytoplasmic ring removes cytoplasmic internal filaments, so these are likely to be attached to the cytoplasmic ring (Goldberg and Allen 1996). The cytoplasmic ring sits on top of the star ring structure (Goldberg *et al* 1996). The star ring consists of 8 triangular shaped subunits (Goldberg and Allen 1996). The cytoplasmic ring is also observed by cryo-electron tomography this shows the cytoplasmic ring to be seemingly only weakly connected to the spoke ring (Beck *et al* 2007).

Luminal spoke ring (Membrane rings) and Inner spoke ring

Each luminal spoke is thought to penetrate the NE and link with the radial arms forming a luminal ring (Akey *et al* 1995). Every spoke has a clamp shape attaching to the NE at two specific sites, the spokes fuse to form a ring. This spoke ring stabilises the membrane curvature (Beck 2007). The inner spoke ring of the Yeast NPC contains three pore membrane proteins (Pom) Pom152, Pom34 and ndc1 (Ylr018p) (Rout *et al* 2000; Alber *et al* 2007[2]). Pom152 homo-oligomerizes at its C-terminal forming the bulk of the luminal ring within the NE lumen (Figure 1 C and D) (Alber *et al* 2007[2]). Pom152 is predicted to have a cadherin fold. This forms homophillic binding interfaces and possibly makes the luminal ring (Alber *et al* 2007[2]; Devos *et al* 2006). Cadherin domains have been shown to connect two membranes, as in desmosomes (Devos *et al* 2006). It is therefore suggested by Devos *et al* (2006) that the cadherin domain of Pom152 may have a similar role in stabilising the interaction between the INM and ONM (Devos *et al* 2006). The luminal spoke rings point towards the NPC centre and may be able to bend, hinting that major rearrangements in the spokes might be involved in translocation of cargo (Beck *et al* 2004). This rearrangement has previously been observed where the NPC's spokes have been shown to have structural plasticity in response to detergent extraction and osmotic swelling (Akey *et al* 1995).

Nuclear ring

The NR is made of triangular subunits as shown in Figure 1.2. The NR is thinner than the cytoplasmic ring (Goldberg *et al* 1996). The NR is strongly connected to the spoke ring complex (Beck *et al* 2007). There is evidence for nucleoplasmic rings in yeast (Kiseleva *et al* 2004), attached to these are 8 fibres which extend into the nucleoplasm where they attach to a basket ring (Goldberg 1992).

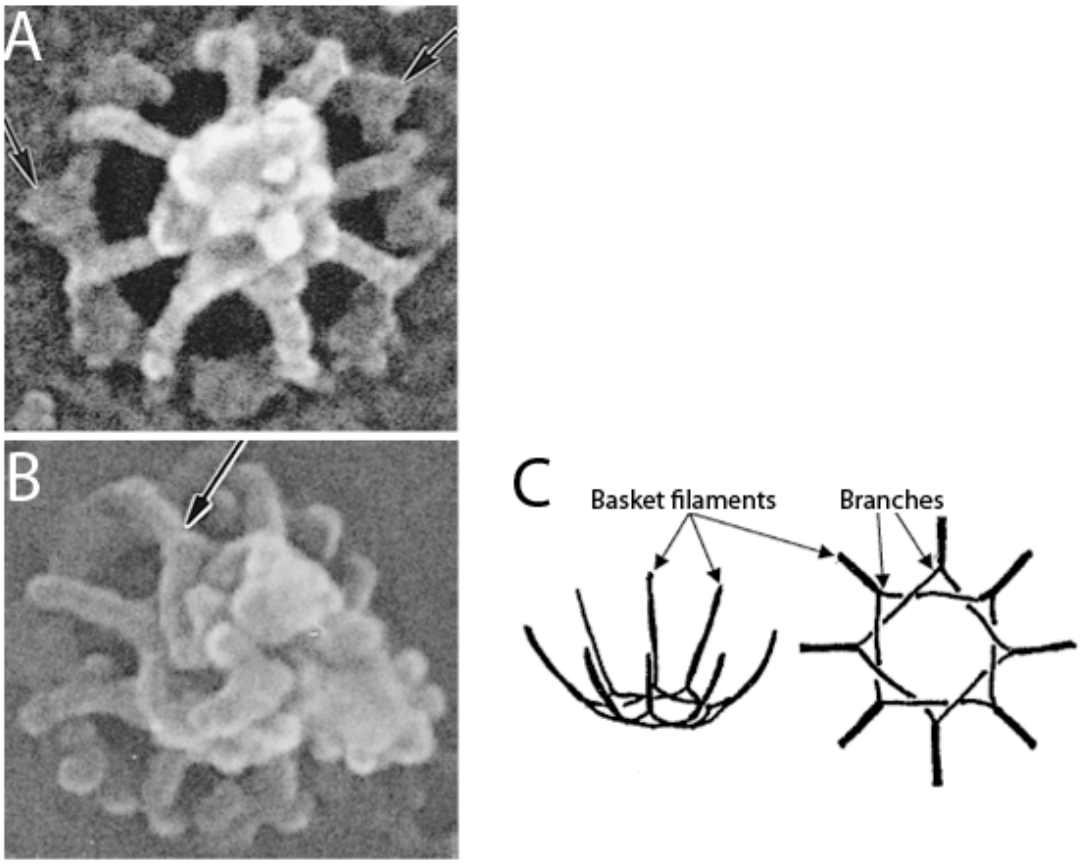

Figure 1.2 The nuclear basket. From Goldberg and Allen (1996). (A) The proteolysed nucleoplasmic face of the NE, arrow points to a triangular subunit of nucleoplasmic ring. (B) Arrow points to the distal end of basket filament where it appears to branch. Both A and B are Field Emission In-lens Scanning Electron Microscopy micrographs. (C) Shows how the basket filaments may be weaved making the distal basket.

Nucleoplasmic filaments and distal basket ring (DBR)

The DBR is composed of eight nucleoplasmic filaments attached to the periphery of the nucleoplasmic ring between each bipartite subunit. These filaments connect together at the basket as shown in Figure 1.2 (Goldberg and Allen 1996). Nup153 has been shown to be located to the base of the basket (Walther *et al* 2002). In Walther *et al* (2002) Nup153 depletion reduced importin-α/β mediated import to 15-20%. It also showed Nup98 and Nup93 (which are components of the basket) and Tpr (Translocated promoter region) (which interacts with Nup98) (Strambio-de-Castillia 1999) were not localised correctly. This indicates Nup153 has a role in basket formation. Basket formation is also important in anchoring the NPC in the NE (Walther *et al* 2002). In *Chironomus* the basket extends into the nucleoplasm 20-40 nm, the filaments are around 10nm in diameter and 20-40nm in length (Kiseleva *et al* 1996). The basket appears to undergo cyclic rearrangement when there is translocation of a specific messenger. Messenger RNA leaves

the nucleus in the form of messenger ribonucleoprotein (mRNP). mRNP can be large in size 35-40kb, for example the Balbiani Ring RNP is ~50nm in diameter. Kiseleva *et al* (1996), uses FESEM and suggests 5 main configurations of the basket, which change in relation to how far the Balbiani Ring has penetrated. The basket is also suggested to have the function of anchoring the mRNP particle to the NPC, ensuring it is in the correct orientation and position to begin translocation of the NPC. The basket has to rearrange for translocation of such a large transport cargo. The basket ceases to be closed and inactive in order to allow the RNP particle to translocate. The basket begins to open, forming the basket ring and the mRNP docks. The basket opens further as the particle enters the channel and finally the basket closes. It is uncertain whether it is the binding of the RNP particle that opens the basket or the opening basket which allows the RNP particle to bind (Kiseleva *et al* 1996). Atomic force microscopy (AFM) shows the nuclear basket opening ($+Ca^{2+}$) and closing ($-Ca^{2+}$) via the distal ring in a calcium dependant manner and is likened to "an iris diaphragm" (Stoffler *et al* 1999).

The distal basket ring can be visualised by 3-D electron tomography. However, this technique uses averages and so the opening and closing of the basket shown by Kiseleva *et al* (1996) will be averaged out and not be shown (Stoffler *et al* 2003). The distal basket ring has however been shown to change in relation to the position of the transporter or possible translocation event (Beck *et al* 2004). This was made possible using tomography by classifying conformationally different NPCs and averaged within the classes (Beck *et al* 2004).

The nuclear basket has been observed in diverse organisms including; yeast (*Saccharomyces cerevisiae*) (Kiseleva *et al* 2004), plant (Fiserova *et al* 2009), *Chironomus thummi* (Kiseleva *et al* 1998) and *Dictyostelium discoideum* viewed by cryo-electron tomography (Beck *et al* 2007).

Structures connected to the NPC

The nuclear interior is connected to the NPC interior via two myosin-like proteins, Mlp1p and Mlp2p (Strambio-de-Castillia 1999). They are similar to the homologous vertebrate and Drosophila Tpr. Mlp1p has a nuclear localization signal (NLS) within the C-terminal domain (Strambio-de-Castillia 1999). Therefore Mlp1p can be imported into the nucleus. Mlp1p has a predicted coiled-coil NH2 terminal to form extended structures which may organize filaments. It is suggested in Strambio-de-Castillia (1999) that the Mlp1p filaments could give chromatin free conduits. This is evidenced from over-expression of Mlp1p forming 'spheroidal fibrillogranular structures'. These structures seemingly displace chromatin as they grow. One function of these filaments could be

the guiding of macromolecules between nucleoplasm to the NPC (Strambio-de-Castillia 1999). Also attached to the basket is a fibrous lattice termed the nuclear envelope lattice, this has been observed by Goldberg *et al* (1992). Trypsin digestion and detergent extraction reveals lamina connections to the spoke ring complex (Goldberg and Allen 1996).

Cytoplasmic filaments

There are eight cytoplasmic filaments ~ 35nm around the central channel. They extend from the cytoplasmic ring towards the centre of the NPC (Beck *et al* 2004). Some averaging techniques such as in Stoffler *et al* (2003) only observe the filaments as small stubs. This is likely to be due to their large flexibility or dynamic structure. When averaged out the only part observed will be the area near the anchorage point, as is likely to have the least range of movement. Studies by Beck *et al* (2004) partially overcome this by averaging different NPC conformations based on the transporter which could represent potential cargo. This showed cytoplasmic filaments sometimes having thin connections to transporter structures (Beck *et al* 2004). Cytoplasmic filaments in individual bird NPCs can sometimes be seen extending towards the NPC centre (Goldberg *et al* 1997). RanGTP has been shown to be involved in the extension of the cytoplasmic filaments indicating that the conformational change to the cytoplasmic filaments may be part of the translocation process (Goldberg *et al* 2000). The extension into the NPC centre could correlate to the changes in the cytoplasmic filaments observed in relation to cargo or central transporter (Beck *et al* 2004).

Located to the cytoplasmic filament is RanBP2/Nup358 (no yeast homologue) (Walther *et al* 2002). This contains four RanGTP binding domains very similar to RanBP1. RanBP1 and the homologous domains in RanBP2 co-activate RanGTPase, assisting in the disassociation of RanGTP from importins and export cargo complexes (Walter *et al* 2002). RanBP2/Nup358 also acts as a binding site for SUMO1-modified form of RanGAP1, which is a RanGTPase activating protein. RanBP2/Nup358-deficient nuclei lack cytoplasmic filaments (however this does not significantly affect import) and are dispensable for NLS or M9 mediated import (Walther *et al* 2002). In contrast, Nup153 of the nuclear basket has been shown to have effects on some import (Walther *et al* 2001).

RanBP2/Nup358 contains FG repeat motifs. Electron microscopy (EM) work on purified RanBP2/Nup358 from rat liver NEs shows it to be a flexible filamentous molecule with a length of ˜36nm (Delphin *et al* 1997) and adopts a tight coiled spiral conformation. This structural information correlates to the structure of the cytoplasmic filaments (Jarnik *et al* 1991). In its coiled

conformation RanBP2/Nup358 resembles the granules seen on the NPC and may be a compacted/collapsed form of the cytoplasmic filaments. RanGTP targets importin-β to RanBP2/Nup358 and importin-β may support the binding of a transport factor (TF)-cargo complex (Delphin *et al* 1997). In yeast, Nup116, a glycine-leucine-phenylalanine-glycine (GLFG) Nup has been labelled (using immunogold labelling) and viewed using FESEM. This showed Nup116 to be peripheral and possibly associated with the cytoplasmic filaments (Kiseleva *et al* 2004). Shuttling nuclear transport factors interact with the N-terminal and GLFG domains of Nup116. Nup116 has specific roles in nuclear export (Lovine *et al* 1997) and has multiple interacting partners in multiple locations within the NPC, one being Nup82 on the cytoplasmic side of the NPC (Ho *et al* 2000).

Cytoplasmic filaments have been observed in diverse organisms including yeast (Kiseleva *et al* 2004), plants (Fiserova *et al* 2009) and *Xenopus* (Goldberg and Allen 1996).

Internal Filaments

Internal Filaments are attached to the inner rim of each subunit of the cytoplasmic ring, they extend towards the centre of the NPC where they join (Figure 1.3 in Goldberg and Allen 1996). The filaments are often disordered, so are not seen in reconstructions such as in Alber *et al* (2007[2]). The internal filaments attach to the underside of the cytoplasmic ring and appear one filament to one cytoplasmic ring subunit (Goldberg and Allen 1996). The internal cytoplasmic filaments extend towards the centre of the NPC where the internal filaments appear to join at a central structure, which is possibly made from branches of these filaments. This central structure could be the transporter. One suggestion in Goldberg and Allen (1996) is that if these filaments contract then they could open the transporter. It is also suggested that these filaments may form part of the central transporter structure (Goldberg and Allen 1996). There is some evidence for internal filaments in yeast (Kiseleva *et al* 2004) and plant (Fiserova *et al* 2009) but they are not as clear as the internal filaments in *Xenopus*. There is also evidence for nucleoplasmic internal filaments, these are attached to the inner nucleoplasmic rim attached to each subunit (Goldberg and Allen 1996).

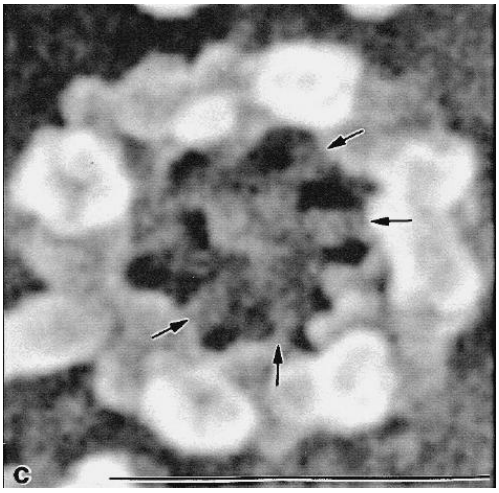

Figure 1.3 The NPC's cytoplasmic internal filaments. From Goldberg (1996). The cytoplasmic face of the NE. Arrows indicate the internal filament attachment site at the cytoplasmic ring. Scale bar represents 100nm.

Central Transporter (also known as the central plug) (CT/P)

The central transporter has been described as "a poorly structured mass in the centre of the pore with a high degree of variation of overall size" (Stoffler *et al* 2003). The main argument against the presence of the central transporter is that it is simply cargo mid-translocation. When nucleocytoplasmic transport is arrested at 4°C, AFM shows 45% of NPCs to be plugged (Stoffler *et al* 2003). When the temperature is raised to 25˚C (a more optimal transport temperature) 12% are plugged (Stoffler *et al* 2003). Therefore arresting transport is possibly plugging the NPC with cargo. This means that averaged data of the NPC will include data from cargos in translocation and this is possibly what has been interpreted as a transporter or plug (Stoffler *et al* 2003). Evidence for a transporter structure can be seen in three-dimensional cryo-electron microscopy (Figure 1.4) the transporter has central positioning and is suggested to be a tripartite, "hollow" and partially occluded by endogenous material (Akey and Radermacher 1993). These properties are the reasoning behind believing it to be a macromolecular transporter (Akey and Radermacher 1993). The cytoplasmic and nucleoplasmic faces appear solid with no clear entrance (Akey and Radermacher 1993). The transporter is also apparent in yeast NPCs (Yang *et al* 1998). The CT/P was found in 'almost all NPCs that were examined' (Beck *et al* 2004). A central particle has been observed in scanning electron microscopy (SEM) of plants and described as particles of various shapes, sizes and positions within the central channel, this was absent in some pores (Fiserova *et al* 2009).

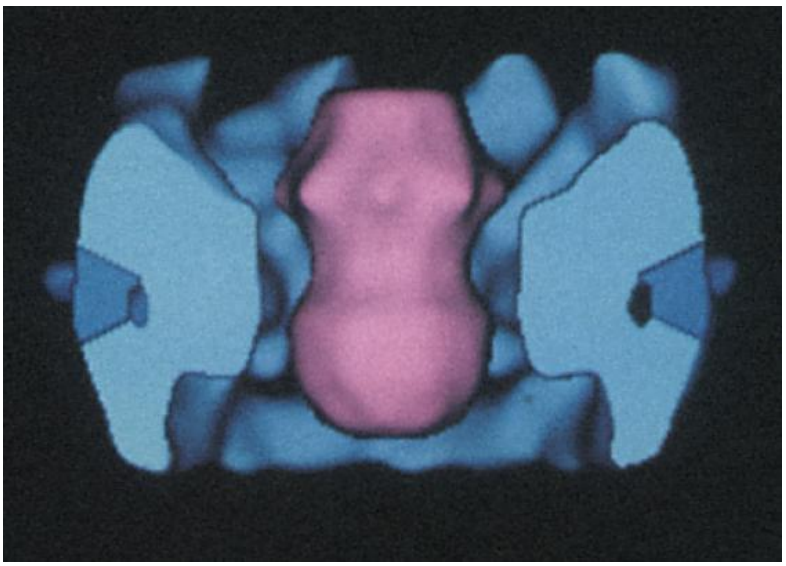

Figure 1.4 The 'suspended' central transporter structure. From Akey and Radermacher (1993). Shows the transporter structure (pink) in the centre of the NPC (blue) in *Xenopus*. Produced using three-dimensional cryo-electron microscopy.

As the shape and position of the transporter varied, Beck *et al* (2004) made two classes for two preferred centres of gravity of the transporter structure shown by Figure 1.5. These classes were defined as the cytoplasmic filament (CF) class and luminal spoke ring (LR) class shown in Figure 1.5. When in the CF class the cytoplasmic filaments are connected to the transporter by an elongated density (Beck *et al* 2004). In the LR class only the base of the cytoplasmic filament is shown, possibly indicating a higher freedom of cytoplasmic filament movement. This may cause the higher variability and result in the inability to average it. There are also differences in the distal basket and its ring. The basket filaments seem to be more bent in the CF class (Beck *et al* 2004). The distal ring has an opening in the CF class, and in the LR class. The distal ring is much larger, possibly indicating that there is mass bound to it (Beck *et al* 2004). The electron density of the transporter correlation is similar to that of cargo, adding to the evidence that the transporter is merely cargo (Beck *et al* 2007). Therefore, the changes in Beck *et al* (2004) could be structural changes to the NPC as translocation occurs. The transporter could also be contributed to by internal filaments as these are not resolved in averaging such as in Beck *et al* (2004) or Akey and Radermacher (1993). A recent study by Yamada *et al* (2010) also suggest that the transporter structure may be made from phenylalanine-glycine (FG) containing collapsed cohesive coils of some FG Nups (Yamada *et al* 2010).

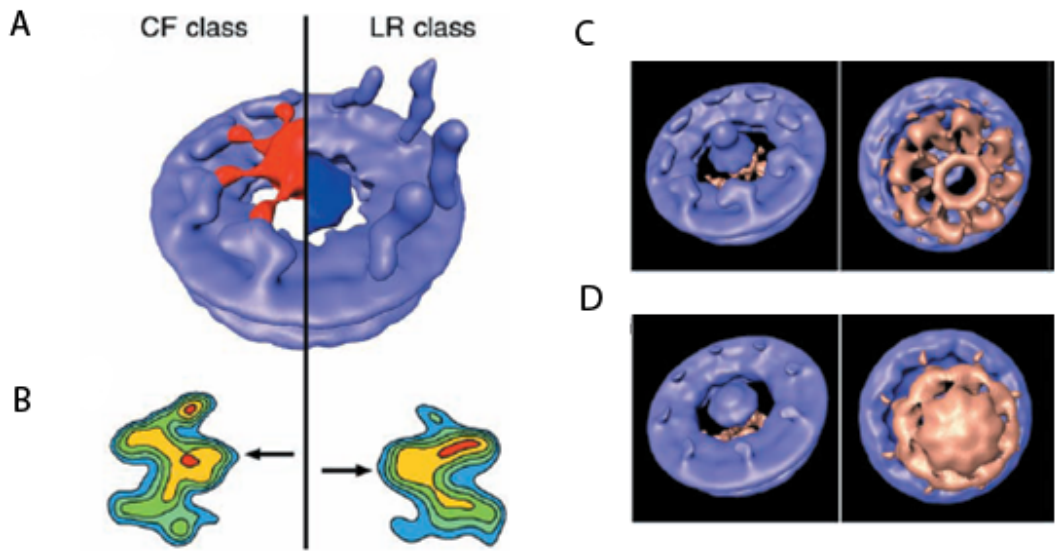

Figure 1.5 NPC Structural changes in relation to the central particle/transporter. From Beck *et al* (2004). Image developed by averaging classes of NPC based on Transporter position. (A) Depicts the changes to the cytoplasmic filaments. In the LR class the cytoplasmic transporters are not bound to the cytoplasmic filaments and so are thought to be variable in shape. Arbitrary shapes therefore represent cytoplasmic filaments here. In the CF class the cytoplasmic filaments are bound to the transporter as they appear as stubs, shown by D (left). (B) The constriction of the central channel in relation to the transporter. (C) The CF class cytoplasmic (left) and nucleoplasmic (right), the basket ring here has an opening. (D) The LR class cytoplasmic (left) and nucleoplasmic (right) showing the major differences between the classes.

Phenylalanine-glycine (FG) Nups (including Nup116)

Nups with repetitive stretches of FG repeats separated by polar spaces are termed FG Nups. These FG Nups mediate nucleocytoplasmic transport; the FG repeats within the FG Nups provide the docking sites for TF-cargo complexes. The FG repeats are represented by a 'cloud' filling the central channel shown in Figure 1.6 (Alber *et al* 2007[2]). The averaging in Figure 1.6 shows that the location of the FG repeats is within and surrounding the central channel and also protruding into the cytoplasm and nucleoplasm. This 'cloud' is seen to get thinner towards the centre of the 8-fold rotational axis (Alber *et al* 2007[2]). However, this is merely the predicted location and does not show individual NPC conformations. Some FG repeat domains of Nups have been shown to change their localisation within the NPC during translocation (Paulillo *et al* 2005), and potentially collapse during a potential translocation event (Lim *et al* 2007). This freedom of movement of the FG domains of Nups within the pore is likely to be due to the flexible and natively unfolded nature and their apparent ability to 'collapse' in response to Kap-β1 binding (Denning *et al* 2003; Lim *et al* 2007). There are many models of how these FG Nups are involved in translocation including

selective phase (Ribbeck and Gorlich 2001), FG-Hydrogels (Frey *et al* 2007), virtual gating (Rout *et al* 2000, Rout *et al* 2003), oily spaghetti (Macara *et al* 2001), reversible collapse (Paulillo *et al* 2005; Lim *et al* 2007) and forest (Yamada *et al* 2010). These translocation models are discussed later in Section 1.3. The models contain similarities in the role of FG Nups; it is thought that they do not facilitate the translocation of large proteins which are not complexed to a Kap. The FG Nups may even hinder this process.

The FG regions of FG Nups are natively unfolded and so lack ordered secondary structure. This means that FG regions are likely to be flexible and are highly dynamic, occupying a relatively large conformational space (Denning *et al* 2003; Krishnan *et al* 2008). If FG regions are unstructured they may be extended. For example, If extended, it is suggested that the FG Nup214 may be able to extend up to ~275nm (Paulillo *et al* 2005).

Structure of GLFG, in particular Nup116

The structure of the FG domains of Nup116 has been studied by Krishnan *et al* (2008). To study the role of phenylalanine in FG repeats (which are mostly GLFG repeats), a 111 amino acid (AA) region (AA 348-458) of Nup116 containing 10 FG repeats was compared to a mutant version (Krishnan *et al* 2008). The Nup116 mutant was generated by site directed mutagenesis replacing the phenylalanine in the 10 FG regions with alanine (F>A mutant) (Krishnan *et al* 2008). The study shows the FG region of WT Nup116 average end-to-end distance to be 20.84Å. However, simulations have showed that this can be increased by increasing the temperature, this is likely to be due to thermal melting (Krishnan *et al* 2008). In the 111 AA region of WT Nup116, the intermolecular distances between the FG repeats are smaller than that of an F>A mutant (Krishnan *et al* 2008). This causes the protein to be more compact in WT demonstrating that F plays a key role in the FG Nup's structure. It was also shown that FG domains in WT cluster, which did not occur in an F>A mutant (Krishnan *et al* 2008). The FG domains are thought to be responsible for the less disordered state. Nup116 interacts intermolecularly via phenylalanine repeats, which cluster by possible hydrophobic interactions; stacking, zippering or clustering of the aromatic ring of phenylalanine side chains (Krishnan *et al* 2008). It could be suggested that intramolecular competition from Kaps and other FG Nups accounts for the structural dynamics of the FG regions of the FG Nups. The FG domains are proposed to give Nup116 its pre-molten globular conformation. The F>A mutant is predicted to have a native coil conformation (Krishnan *et al* 2008). Based on the FG region of Nup116's mass, and adopting a pre-molten globule structure, Nup116's FG region is predicted to occupy a 12nm diameter sphere (Krishnan *et al* 2008). If this

prediction is correct then FG regions could interact with other FG regions from adjacent spokes, whilst being unable to span the NPC to opposite spokes (Krishnan *et al* 2008). GLFG domains contain few hydrophobic AAs, making the GLFG domain "stand out" (Patel *et al* 2007) because of its hydrophbicity (Patel *et al* 2007). GLFG Nup interactions were observed using bead immobilised GST-FG Nups. To these, soluble fluorescent CFP-FG Nups were added to see if they bound or not. Results from this showed GLFG Nups to interact via hydrophobic attraction between phenylalanine residues, however this was not the case for FxFG (phenylalanine any amino acid phenylalanine glycine) Nups (Patel *et al* 2007). L>A and F>A mutants did not bind to the GFLG domains of Nup57, Nup100 and Nup116 indicating that it is the LF motifs seem to be necessary for GLFG domain interactions (Patel *et al* 2007). Changing the AA sequence of Nup116 by individual F>Y and F>W mutations, maintaining the overall hydrophobicity, it was found that these bound to CFP-GLFG Nups just as well as WT. This means that hydrophobicity of phenylalanine is important for GLFG domain interactions (Patel *et al* 2007).

FG Nups binding Non-FG Nups

The GLFG domains of Nup116 have been shown to bind to non-FG Nup85 (Allen *et al* 2002). Also, Nup84 binds to Nup49 and the FG domains of Nup116, mediated by Nup85. Nup84 and Nup85 are possibly components of the outer rings (Alber *et al* 2007[2]). Mutants in Nup84 and Nup85 show NE structural abnormalities and have defects in mRNA export (Allen *et al* 2002). Nup116 has specific roles in nuclear export (Lovine *et al* 1997). NE structural abnormalities are also observed in Nup116 deletion mutants (Wente and Blobel 1993). This may suggest the requirement of Nup116 GLFG-Nup84, Nup85 interaction for the functionality in mRNA export and possibly a role in NE structure. A suggestion in Allen *et al* (2002) is that FG domain interaction with non-FG Nups may be involved in creating an effective seal.

The non-FG regions of the FG Nups are also involved in interactions which anchor them to the NPC, these are predicted to be via coiled-coil, β propeller or unique β sandwich structures. It is thought the non-FG regions may assemble on the scaffolds anchoring the FG Nup (Tran and Wente 2006). For example the Nsp1 C-terminal has four predicted coiled-coil regions which are responsible for Nsp1 forming into sub-complexes, with other Nups consequently linking it to the NPC scaffold (Bailer *et al* 2001). The FG Nups are anchored to either the inner rings or linker Nups. Most of the FG Nups anchor at NIC96 and Nup82, these anchoring sites face into the central channel (Alber *et al* 2007[2]).

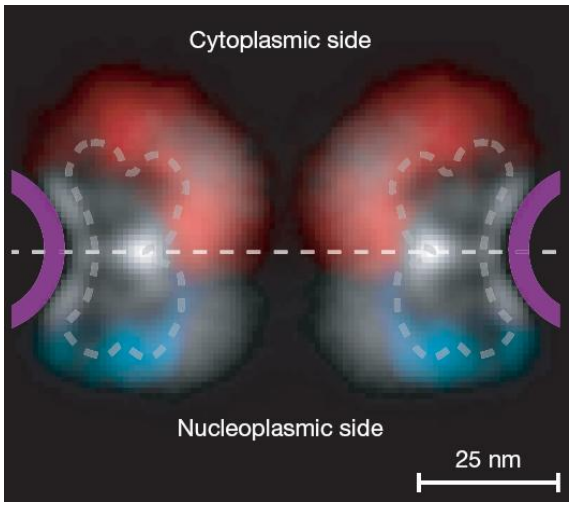

Figure 1.6 Predicted locations of the FG Nups. From Alber *et al* (2007[2]). A density plot of localisation probabilities of the FG Nups. Red represents cytoplasmically disposed, blue represents those nucleoplasmic and white represents those found on both sides. The white line represents the equatorial plane of the NPC and the NE in purple.

Localisation of FG Nups to the midplane (plane of the NE)

Nups in yeast can be categorised into their localization. Most are symmetric, however immuno-gold localisation in yeast has shown that four have a biased localization, three of which are towards the cytoplasmic face (Rout *et al* 2000). Two of these are FG containing; Nup100 and Nup116 showed a cytoplasmic bias, however the C-terminal fragment was symmetric (Rout *et al* 2000). The NH2 fragment of the GLFG Nup145 showed a bias towards the nucleoplasmic face (Rout *et al* 2000). Nup1 and Nup60 are FG Nups and are exclusively nucleoplasmic (Rout *et al* 2000). It is proposed by Rout *et al* (2000) that these constitute the nuclear basket. Nups159 and 42, two FG Nups, are cytoplasmic and could be part of the cytoplasmic filaments, as is Nup82, however this is a non-FG Nup (Rout *et al* 2000). Nsp1, an FG Nup, is found in complex with Nup82 (Ho *et al* 2000). The distribution of Nups is shown in Figure 1.7. It has been shown that Nup116C is localised on both cytoplasmic and nucleoplasmic sides with an asymmetric majority 54% on the cytoplasmic side, 18% at the midplane and 27% on the nucleoplasmic side (Ho *et al* 2000). Nup82 is associated with the C-terminal of Nup116 on the cytoplasmic side, however it is suggested in Ho *et al* (2000) that there may be more interacting partners for Nup116, for example RNA on the nuclear face.

In *Xenopus*, FG regions of Nups153 and 214 are thought to be flexible on the cytoplasmic and nucleoplasmic faces of the NPC, dependant on the transport state of the NPC. NPCs in an export state were obtained by microinjecting poly(A+) RNA into the nucleus, which was then exported. There is evidence that as this export event occurs there is a shift in the FG region localisation with

an initial increase of Nup214's FG region on the nucleoplasmic side. There is then an increase of Nups153 and 214 on the cytoplasmic side, followed by a return to the steady state once the translocation events are finished. It is suggested this shows that the FG regions guide the cargo through the pore (Paulillo *et al* 2005). Arresting nucleocytoplasmic transport at 4°C shows labelling of Nup153 from the cytoplasmic face is lost and becomes only nucleoplasmic. Nup214 now exclusively localizes to the cytoplasmic side of the NPC. Therefore, when transport is arrested the labelling for the flexible FG domains of Nups153 and 214 are found near their anchorage sites (Paulillo *et al* 2005).

It has been shown that Nup153 can collapse induced by Kap-β1 by the interaction of Kap-β1-FG. This collapse into a more compact form can be reversed by RanGTP addition. This is proposed to be intra-FG interactions within the same domain, causing Nup153 to bind to itself (Lim *et al* 2006, 2007).

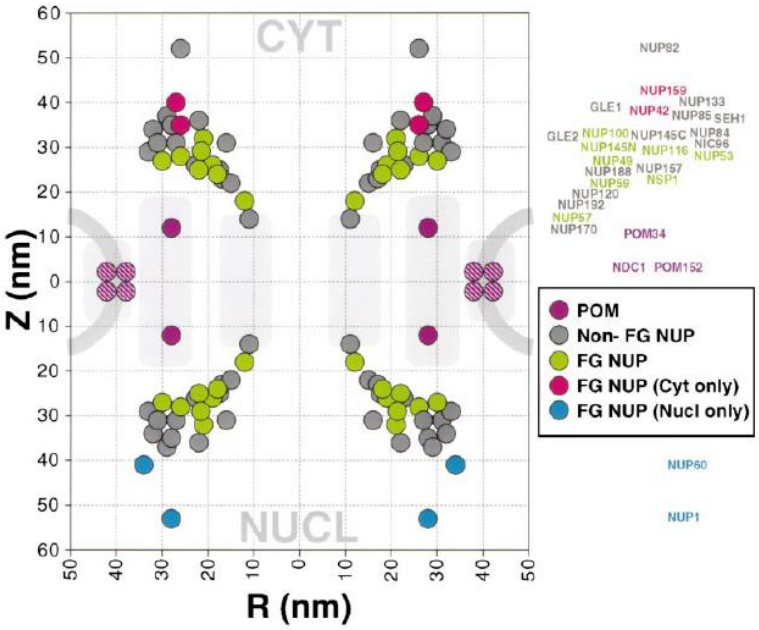

Figure 1.7 Localisation of Nups determined by immunogold TEM. From Rout *et al* (2000). A plot of the position of nucleoporins in yeast from collated immuno-gold labelling results, 20 images for each Nup were used.

Nup98 is the only known GLFG member of vertebrates. Nups100, 116 and 145 are the most similar yeast homologues. Nup98's GLFG domains target Nup98 to intranuclear bodies. Blocking Nup98 via antibodies has no effect on import, but blocks most RNA export. Nup98 binds Tpr. Nup98 is shown to move between the nuclear interior and the NPC. There also appears to be movement within the NPC from the nucleoplasmic side to the cytoplasmic side and Nup98 mobility is coupled to the transcription of RNA (Griffis *et al* 2002). Only the GLFG domains of Nup98 were transfected

to GFP and these localised to the intranuclear bodies (Griffis *et al* 2002). The mobility of Nup98 is sensitive to inhibitors of transcription (Griffis *et al* 2002) and functions in nucleocytoplasmic transport (NCT) of macromolecules (for example Crm1). It is mostly found on the nucleoplasmic side however a fraction is found on the cytoplasmic side of the NPC. Nup98 interacts through its N-terminal FG repeat domain, this interaction is RanGTP dependant (Oka *et al* 2010). Nup98 is a site for GDP/GTP exchange on Ran and termination of karyopherin β2-mediated nuclear import (Fontoura *et al* 2000). Nup98 has also been shown to be involved in HIV type 1 Rev export. Rev has been shown to recruit Nup98 and Nup214 (another FG Nup) into the nucleus (Zolotukhin and Felber 1999).

1.2 Ran's Role in Translocation

Transport factors

Most transport factors (TFs) (also known as transport receptors) are homologous proteins known as importins and exportins. These are collectively known as karyopherins (Kaps). There are 14 known Kaps in yeast and at least 22 in humans. Each Kap recognises a specific nuclear localisation signal (NLS) or nuclear export signal (NES) or interacts indirectly via adapter molecules (Reviewed in Conti and Lzaurralde 2001 and Stuart *et al* 2007).

Creation of a Ran gradient and its role in nucleocytoplasmic transport

The uptake and release of cargo is controlled by the interaction of a TF with Ran (a ras related nucleo-protein (Gorlich[1] *et al* 1996)) GTPase called Gsp1 in yeast (Fried and Kutay 2003). Ran functions as a molecular switch and is found in two states: either GTP-bound 'on' or GDP-bound 'off' (Scheffzek *et al* 1995). RanGDP can be converted to RanGTP by Ran guanine exchange factor (RanGEF) (Conti and Lzaurralde 2001), also known as RCC1 (regulator of chromosome assembly) in metazoans and Prp20 in yeast (Seki *et al* 1996; Fried and Kutay 2003). In Ran the hydrolysis of GTP to GDP is controlled by GTPase activating protein (RanGAP1 or Rna1 in yeast) (Fried and Kutay 2003). Hydrolysis of GTP by Ran inputs energy into transport to allow movement against energy potentials. GTP hydrolysis is co-stimulated by proteins which share a homologous RanGTP binding domain (BD). An example of this in vertebrates is Ran binding protein 1 (RanBP1) which binds RanGTP and accelerates nucleotide hydrolysis mediated by RanGAP (Conti and Lzaurralde 2001;

Dasso 2002). Using immunogold transmission electron microscopy (TEM), RanBP2/Nup358 has been shown to be associated with the cytoplasmic filaments in isolated rat liver nuclei (Yokoyama *et al* 1995). RanBP2 has four Ran binding domains which are highly homologous to RanBP1. The Ran binding domains of RanBP2 are flanked by FxFGs (Seki *et al* 1996). RanGAP, RanBP1 and RanBP2 are found on the cytoplasmic side of the NE. RanGEF is found in the nucleus bound to chromatin through histones H2A and H2B (Dasso 2002). This results in a Ran gradient with the RanGTP form in the nucleoplasm and the RanGDP form on the cytoplasmic side of the NE (Conti and Lzaurralde 2001).

Import receptors bind their cargo in absence of RanGTP (outside the nucleus) and then disassociate from them when in the presence of RanGTP (inside the nucleus). Export receptors bind cargo in presence of RanGTP. GTP is hydrolysed to GDP in the cytoplasm causing the disassociation of the exportin-cargo complex in the cytoplasm. Import is towards high RanGTP and export is away from it (reviewed in Goldberg 2004). Examples of import and export translocation events are shown in Figure 1.8.

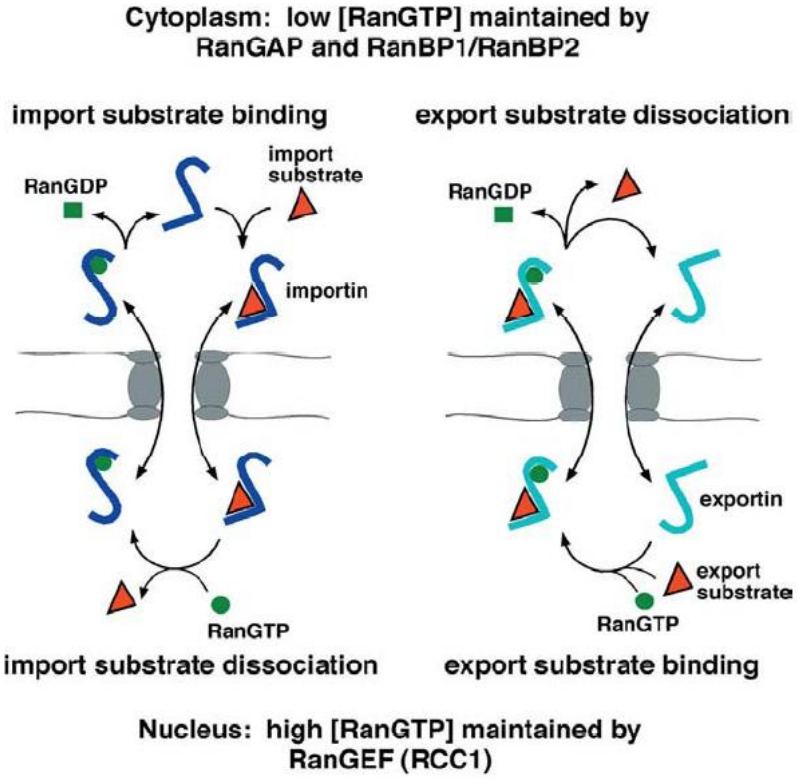

Figure 1.8 Ran in import and export events. From Fried and Kutay (2003): Figure depicts the facilitated import and export of cargoes. Import receptors often bind their cargo in absence of RanGTP (outside the nucleus) and then disassociate from them when in the presence of RanGTP (inside the nucleus). Export receptors bind cargo in presence of RanGTP (in the nucleus). GTP is hydrolysed to GDP in the cytoplasm, causing the disassociation of the exportin-cargo complex in the cytoplasm.

The facilitated nuclear import of a protein with an NLS

i) Protein with an NLS binding to importin-α: An NLS contains one or two clusters of basic residues. The NLS is recognised by an importin directly, or via an adaptor, for example importin-α. Importin-α is made from a tandem series of armadillo (ARM) repeats that generate a 'banana shaped molecule' (Stewart 2007). NLS-importin binding has been shown using crystallography (Conti *et al* 1998). In the presence of a protein with an NLS (for example SV40 T antigen), the NLS binds in an extended conformation to importin-α's concave face of the armadillo repeats (Conti *et al* 1998). This interaction is mediated by hydrophobic pockets formed by several tryptophans on the concave face of importin-α where side chains of the NLS are buried (Conti and Lzaurralde 2001).

ii) Protein with an NLS complexed with importin-α binding importin-β: Importin-α has an importin-β binding domain (IBB). The IBB domain was found by testing different fragments of importin-α and establishing their ability to bind importin-β by SDS-PAGE (Gorlich[1] *et al* 1996). The IBB domain consists of ~40% basic residues, similar to that of an NLS, and as such can bind to NLS binding sites (Gorlich[2] *et al* 1996). The IBB domain is shown to be necessary to bind importin-β (Gorlich[2] *et al* 1996[2]).The crystal structure of importin-α shows an auto-inhibitory function of the IBB domain (Kobe 1999). When there is no importin-β, the C-terminal end of the IBB domain can bind to the NLS binding pocket of the same importin-α molecule. This provides an auto-inhibitory function by competing with NLS for the NLS binding pocket (Conti and Lzaurralde 2001). The IBB domain of importin-α can bind to importin-β, making contacts with the acidic loop (Cingolani *et al* 1999). The rest of the IBB domain folds into a helix when bound to importin-β. This helix is enclosed in the complimentary negatively charged terminal arch of importin-β (Cingolani *et al* 1999; Conti and Lzaurralde 2001). When the IBB domain is bound to importin-β it cannot compete with NLSs for importin-α NLS binding site (Cingolani *et al* 1999). There is now a protein with an NLS-Importin-α-Importin-β complex. Importin-β docks at the NPC via FG repeats using its outer surface for docking and translocates through the NPC, taking the rest of the complex with it. There are many models of how complexes are translocated through the NPC, these are discussed in Section 1.3.

Disassociation of the import complex on the nucleoplasmic side

The crystal structure of yeast Kap95 (importin-β) complexed with residues 1-176 of RanGTP has been studied (Lee *et al* 2005). RanGTP binds to three sites on importin-β resulting in conformational changes to importin-β (Lee *et al* 2005). It is suggested by Lee *et al* (2005) that conformational changes to importin-β cause the IBB domain of importin-α to no longer effectively

interact with importin-β. This is possibly due to a structural change affecting the helicoidal pitch of importin-β causing the assumed α-helix of the IBB domain to no longer match (Lee *et al* 2005). This results in importin-α and the NLS-containing protein disassociating from importin-β. Experimental evidence showing the role of RanGTP in cargo disassociation is presented in (Gorlich[1] *et al* 1996). In this experiment the RanGTP binding site in importin- β was inactivated, resulting in the import complex arresting in the nuclear basket. This demonstrates the role of RanGTP in disassociation of the import cargo complex. The disassociation of the import cargo complex results in no importin-β in complex with the IBB domain. The IBB domain will therefore be 'free' and able to aid in the disassociation of the NLS containing protein-importin-α complex. The IBB domain facilitates this by competing for the NLS binding site and the displacement of the NLS containing import protein (Kobe *et al* 1999). The result of translocation is a protein with an NLS, importin-α, and importin-β with RanGTP bound and on nucleoplasmic side (Conti and Lzaurralde 2001; Stewart 2007).

Recycling receptors and regeneration of Ran Gradient

It is important that the factors facilitating translocation are moved back to their appropriate positions to initiate a new translocation event. For example importin-β with RanGTP bound docks with the NPC and translocates back to the cytoplasm. This is disassociated by RanGAP mediated hydrolysis of GTP. This is helped by the RanBD of RanBP1 and 2, without these Ran is resistant to RanGAP mediated GTP hydrolysis when bound to importins. The result is RanGDP on the cytoplasmic side of the NPC. RanGDP is transported into the nucleus, this is facilitated by nuclear transport factor 2 (NTF2) (Conti and Lzaurralde 2001). Once RanGDP is in the nucleus, RanGEF promotes RanGDP conversion to RanGTP and consequently maintains the Ran gradient (Conti and Lzaurralde 2001). Importin-α is exported in a complex with β-karyopherin CAS and RanGTP (Stewart 2007; Conti and Lzaurralde 2001).

Other roles of Ran

Ran has other cellular roles including NE formation, regulation of cell cycle progression and mitotic spindle assembly (Dasso 2002). There is also evidence for Ran having involvements in NPC assembly (Ryan *et al* 2003). Yeast cells, unlike vertebrate cells, have a closed mitosis, meaning the NE stays intact throughout mitosis, and all of the cell cycle stages, with NPC numbers increasing throughout the cell cycle and peaking at S-phase (Winey *et al* 1997). Yeast temperature sensitive mutants in the Ran GTPase cycle were studied by Ryan *et al* (2003). This included mutations in

Ran(Gsp1), Ran's regulators RanGEF (RCC1/PRP20) and Ran GAP, as well as mutations in the RanGDP import factor, NTF2. These mutants when grown at 34°C had the exhibited the following:

i. a decrease in nuclear rim staining of GFP-NIC96 and GFP-Nup170
ii. an increase in diffuse cytoplasmic GFP-Nup fluorescence
iii. clustering of GFP-Nups.

These observations indicate that there is a mislocalisation of Nups. This was further confirmed using TEM, showing Nup associated vesicle accumulation (Ryan *et al* 2003). Pre-existing NPCs stay stable for at least 6 hrs at non permissive temperature (Ryan *et al* 2003). This suggests Nup containing vesicles are intended for new NPC assembly. The number of NPCs per nucleus also declined with every round of cell division (Ryan *et al* 2003). Therefore evidence in Ryan *et al* (2003) indicates that the Ran GTPase cycle is likely to be involved in NPC assembly. It is speculated that Ran is possibly involved in transporting Nups to the nucleoplasmic side of the NE. Also, Nups in vesicles may be trafficked in vesicles to the NE, they may fuse and high Nup concentration may cause pore formation. In Ran GTPase cycle mutants there are NE perturbations, leading to the suggestion in Ryan *et al* (2003) that Ran may have a role in NE growth and maintenance (Ryan *et al* 2003). Kap95 mutants have similar observations as Ran cycle mutants indicating a mislocalisation of Nups (Ryan *et al* 2007). Based on the observations in Ryan *et al* (2003, 2007) a model is proposed whereby Kap95 normally inhibits the fusion of vesicles until a high RanGTP concentration at the NE is met (Ryan *et al* 2007).

1.3 Translocation Models

Models of transport through the NPC

A key feature of the NPC is the ability to allow the diffusion of small molecules and at the same time inhibit the transport of macromolecules. It also allows the fast translocation of cargos which possess specific signals. These signals interact with the nuclear transport receptors allowing the passage of the complex through the pore (Fried and Kutay 2003).

The translocation capacity of a NPC is high, a single NPC allows a mass flow of nearly 100MDa/s and around 10^3 translocation events per second (Ribbeck and Gorlich 2001). These translocation rates are confirmed using permeabilised cells and investigating the maximum nuclear accumulation rate of NLS-2xGFP (Yang *et al* 2004). These figures are best estimates as it is experimentally very difficult to measure translocation rates of individual NPCs. Problems may

include rates varying from NPC to NPC or cell to cell. Errors may be caused by not measuring all the transport factors, however this can be reduced by largely depleting the endogenous transport factors. The problems encountered when measuring rates using fluorescence may include the fluorescent label photobleaching and fluorescent labelling perturbing cell function. This could be overcome by multiphoton microscopy detecting the resonant four-wave mixing of gold nanoparticles (attached to NLSs) (Masia *et al* 2009). Other difficulties faced are rate limiting factors e.g. binging of Ran GTP to importin-β (Ribbeck and Gorlich 2001). The models of transport through the pore are discussed below, in these models FG-repeats always play a key role.

Oily spaghetti model: This model proposes the NPC centre is filled with FG repeats (Figure 1.9). It is suggested by Macara (2001) that the FG repeat region of the FG Nups form chains that fill the pore like loose oily spaghetti. This spaghetti forms a layer around central pore. Macromolecules (>10nm) are unable to bind to FG repeats and are thought to be hindered by the 'spaghetti' (Macara 2001). TF-Cargo complex can push them aside (Macara 2001).

This model suggests that the binding of TF-cargo complexes does not limit translocation rates and that it could be the disassociation rate from a FG repeat which determines the rate of translocations. There could therefore be multiple transient interactions between TF-cargo-FG repeat (Macara 2001).

TF-Cargo complexes are proposed to be able to bind and move relatively unhindered through the NPC by random transient associations with the FG repeats. These FG-TF-cargo associations within the NPC are suggested to be weak to allow rapid translocation. Outside these weak affinities is suggested to be stronger affinities for FG-TF-cargo complex for cargo unloading. This could be tested at 37°C by observing a cargo and seeing if it arrests at external docking sites at lower temperatures. Cargo may be found to be arrested in the NPC lumen as FG repeats termed 'spaghetti' would have reduced conformational motion and so is not as easily pushed aside (Macara 2001).

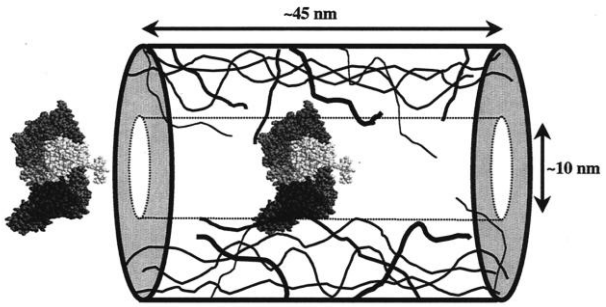

Figure 1.9 Oily Spaghetti model. From Macara (2001). The FG repeats form loose chains around the central pore like oily spaghetti. The TR-cargo complex is translocating through the pore via transient interactions with FG repeats (Macara 2001).

Selective phase model: Gel filtration experiments were performed with NTF2 (29kDa) and GFP (28 kDa). Results from this showed GFP would diffuse in an aqueous medium faster than NTF2. Rates of NTF2 import were then measured. Fluorescently labelled NTF2 was added to permeabilised cells and nuclear import was measured. Results from this experiment show NTF2 passing through the NPC 120 times faster GFP (Ribbeck and Gorlich 2001). This higher rate of translocation of NTF2 than GFP indicated NTF2 translocation is facilitated. The rate of translocation is ~4 times slower than through a hypothetical pore where the centre consists of an unrestricted aqueous medium (Ribbeck and Gorlich 2001). This suggests no mechanism propelling the translocation species from one side to the other. The model proposed by Ribbeck and Gorlich (2001) is that translocation occurs through a homogeneous medium. This medium restricts the free flow of some molecules more strongly than others, suggesting there are some molecules with translocating-promoting properties which are likely to have an affinity for specific NPC components. The homogenous medium is likened to the lipid bilayer in Ribbeck and Gorlich (2001). The lipid bilayer is more permeable to lipophillic molecules than charged ones as it is energetically more favourable. Size is another criterion for translocation across the lipid bilayer. The central plug may work like the lipid bilayer; consisting of a semi-liquid phase which transport receptors can break into. The transport receptor's role would be to increase the cargo's solubility in the semi-liquid phase environment of the NPC centre. The selective phase model suggests that a mutual attraction between the hydrophobic phe-rich clusters forms a permeability barrier in the central channel of the NPC (Figure 1.10 A). This is hypothesised to give a meshwork that could restrict the flow of molecules that cannot break into the meshwork. Translocation is thought to be permitted due to affinity between the translocating species and the phe-rich clusters. The structural basis for this interaction between FxFG and importin-β has been shown (Bayliss *et al* 2000). The passage of large molecules requires breaking into this mesh locally. Entry into the meshwork could be done by competing for the phe-rich interactions by directly binding to the repeats, allowing it to become part of the meshwork (Ribbeck and Gorlich 2001) (Figure 1.10 C). Interactions between phe-repeats are thought to be very weak, allowing easy rearrangement during transport. Only weak interactions between transport factors and phe-repeats are required to compete for the mutual attraction between the phe-rich repeats. The central plug filled with phe-rich repeats would create an energetically unfavourable environment for hydrated molecules so creating a barrier for hydrophilic molecules, whilst allowing transport receptors with hydrophobic surfaces to pass (Ribbeck and Gorlich 2001).

This model does not explain the peripheral translocation of specific cargos observed in Fiserova *et al* (2010). The selective phase model is extended by Frey *et al* (2007) with the hydrogel model.

FG-Hydrogels: It is proposed that a hydrogel would form a 3D sieve with meshes forming through hydrophobic interactions between the FG domains of the FG Nups (Frey *et al* 2006). The barrier is predicted to allow small molecules to pass but restrict large inert molecules to enter. TFs bind hydrophobic clusters between FG domains disengaging them and allowing entry and translocation through the hydrogel. Large inert molecules enter the hydrogel slowly. Transport receptors, however, enter much (25000 fold) faster.

FxFG-Hydrogels have been constructed from the N-terminal repeat domain of yeast Nsp1. Nsp1 contains 18 regular FSFG repeats and 16 less regular FG repeats (Frey *et al* 2006). A 2 µl hydrogel was made using 0.27mM of the N-terminal domain of Nsp1. The period allowed for gelation to complete was 48hrs. The rate of influx was measured using confocal laser scanning microscopy. Results presented in Frey *et al* (2007) show these gels have similar permeability properties to that of an NPC. It is the saturated hydrogels which have the permeability properties most similar to that of the NPC (Figure 1.11). Here importin-β and other transport receptors have been shown to enter 1000X faster than a similarly sized inert molecule (acRedStar protein). Importin-β went ~50µm into the gel in 30min. This is evidence for intragel diffusion of the importin-β-cargo complex. This supports the selective phase model (Frey *et al* 2007) as the concentration of the N-terminal repeat domain of Nsp1 was increased, the barrier to acRedStar protein was improved. GLFG hydrogels have also been made from Nup49 and Nup57 (Frey and Gorlich 2009). The experimental conditions of hydrogels greatly differ from the conditions of an NPC. One such difference is that the hydrogel does not contain the many different FG Nups. Also, these FG domains are not anchored. However, it provides a model for how TF interact with individual FG repeat domains of FG Nups. NPC structural studies have shown the presence of a central transporter (also known as the central plug or particle), some examples include Akey *et al* (1993), Yang (1998), Beck (2004) and Fiserova *et al* (2009). This may be the FG regions of FG Nups joining in the NPC centre to form a hydrogel-like structure. If the FG Nups associate or form the internal filaments then there is evidence in Goldberg *et al* (1996) that they join in the centre of the NPC. The central transporter structure is also shown to not fill all of the NPC (i.e. not filling the periphery of the pores, only the centre). Therefore, if this central transporter structure does correlate to a hydrogel then it is possible that not all cargoes pass through the hydrogel. The presence of a central transporter structure is debated; one argument against it is that it may be

cargo caught in transit (Beck *et al* 2007). NPCs with minimal numbers of FG domains were created in Strawn *et al* (2004). Over half of the mass of the FG domains can be deleted without the loss of viability of the yeast. NPC permeability is not affected by FG domain loss which would not be expected if FGs form the permeability barrier in a hydrogel-like way. Deleting some FG domains has been shown to have implications on some transport factors and not others, this hints at multiple transport pathways. Multiple transport pathways could be feasible only if the hydrogel were more ordered (Strawn *et al* 2004).

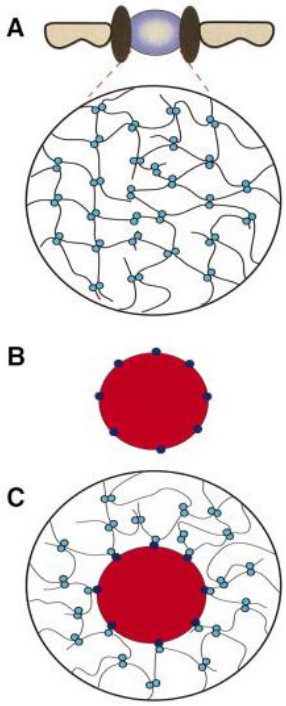

Figure 1.10 Diagrammatic explanation of the selective phase model. From Ribbeck and Gorlich (2001). (A) Phe-rich clusters in the central plug. (B) Weak hydrophobic attraction between the phe-rich clusters. The transport receptor with hydrophobic patches on the surface. (C) The transport factor can compete for the phe-rich cluster attraction, causing local rearrangement of the meshwork and allowing the TF entry into the central plug.

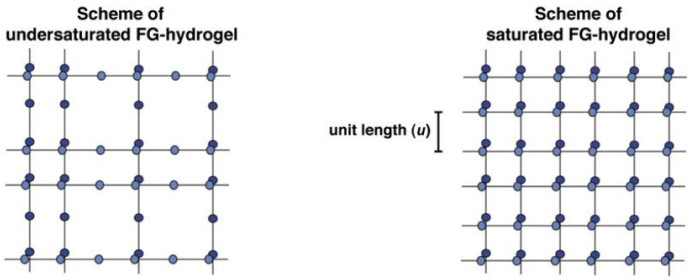

Figure 1.11 Interactions in a saturated and unsaturated hydrogel. From Frey *et al* (2007). A saturated hydrogel (right): all the hydrophobic clusters are engaged in hydrophobic contacts. An unsaturated hydrogel (left): not all the hydrophobic clusters are engaged in hydrophobic contacts due to distances between some potential partners causing larger meshes and inter repeat partners (Frey *et al* 2007).

Virtual gate: This model, proposed in Rout (2000, 2003), is based on the following observations:

- The NPC lacks proteins associated with mechanical transport
- The Transport path is surrounded by a large number of closely packed FG Nups
- Most (8 of 12) of these FG Nups are on both cytoplasmic and nucleoplasmic sides of the NPC
- Asymmetry of other FG Nups is suggested to be involved in termination of import and export events.

The virtual gate model, like others, suggests that the probability of a molecule passing through the NPC decreases as the size increases. Due to the size restriction of the NPC, translocation probability of cargoes above 40 nm is negligible. The FG Nups add to the entropy unfavourability by limiting the diameter. Some specifically binding molecules (transport factors) have an affinity to bind to the NPC's FG Nups. Therefore these macromolecules have access to a transition state for translocation and will be more likely to pass through the NPC (Figure 1.12 (B)). Also, the apparent size of the diffusion channel would be larger for these FG binding macromolecules. Macromolecules which have a lower affinity for binding with FG Nups have a lower probability of entering the transition state for translocation so will cross the NE less frequently (Figure 1.12 (A)). Diffusion energy alone is not thought to be enough to allow translocation, but by including binding energy the energy gradient is favourable enough to allow translocation. This binding must not be too strong otherwise leaving the pore would be energetically unfavourable, leading to an accumulation of transport receptors in the pore. Ideally the barrier and binding energy should be balanced as such to not exclude transport factors, preventing accumulation and allowing passage with minimal resistance. In virtual gating it is thought FG Nups help form the barrier and are binding sites for transport factors. They provide hundreds of different binding sites across which transport factors can step between to translocate the pore. The locations of these FG Nups are mapped using TEM (Rout *et al* 2000). Rout *et al* (2000) proposed that the cargo complex would have the highest binding affinity on the one sided FG Nups. Therefore the import complexes would have the highest binding affinity for nucleoplasmic FG Nups, and export complexes for cytoplasmic FG Nups. This idea of virtual gating is questioned by the results of Paulillo *et al* (2005). These results show that the translocation state of the NPC is coupled with a shift in the FG domain localisation in *Xenopus*. Hence, FG Nups are suggested to guide the cargo through the NPC, suggesting a larger role than just gating the NPC.

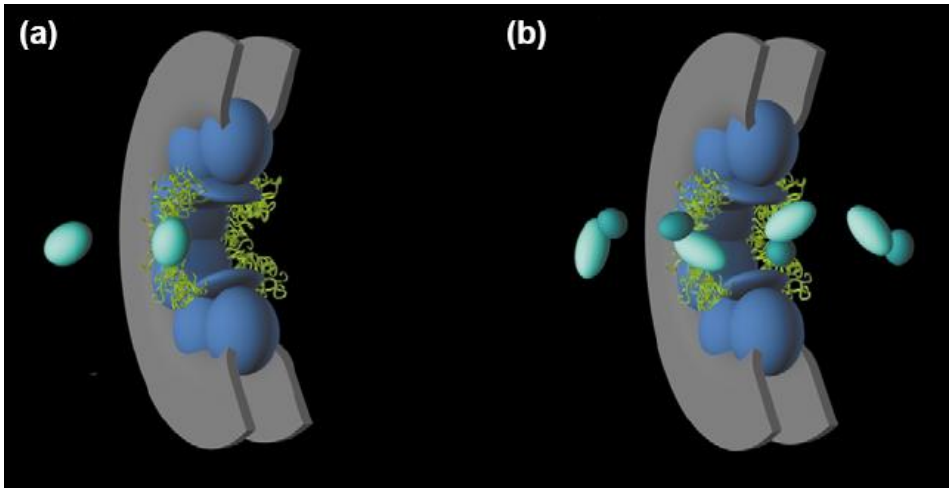

Figure 1.12 Virtual Gate model. From Rout (2003). (A) A macromolecule with low binding affinity for the NPC so lowering the probability of getting through the virtual gate and entering the transition state for translocation. This meaning a much lower chance of translocation. (B) Macromolecules with a higher affinity for the NPC have a much higher chance of entering the transition state for translocation so have a higher probability of translocation.

Reversible collapse model: This model predicts a random flux of collapsing and distending FG domains regulated by the binding and unbinding of the transport receptors (Figure 1.13) (Lim *et al* 2009). Immunogold TEM studies show Nup153-C diffuses around the nuclear basket, when Kap-β1 is added. Nup153-C is then found to be at the distal ring, which is its anchorage site (Lim *et al* 2007). This proposes the idea of Nup153 having collapsed to its anchorage site when Kap-β1 is bound. Further evidence is shown by arresting nucleocytoplasmic transport by reducing the temperature to 4°C. Under normal conditions there is some (13%) Nup153 FG region labelling which is cytoplasmic. Arresting transport causes loss of Nup153 FG region labelling from the cytoplasmic face and is now only nucleoplasmic near its N-terminal anchorage site, possibly at the nuclear ring (Paulillo *et al* 2005). Under the same arrest conditions Nup214's FG region also locates closer to its N-terminal anchor at the cytoplasmic side, possibly the cytoplasmic ring (Paulillo *et al* 2005). Nup153 and Nup214 are both found in different proportions on the cytoplasmic and nucleoplasmic faces of the NPC, dependant on the transport state of the NPC (Paulillo *et al* 2005). Import conditions were established using an import competent mixture with excess nucleoplasmin. This caused Nup153 to be localised on both sides of the NPC at 5mins. Then, relatively, the cytoplasmic labelling increases after 15mins and after 30mins. It is located exclusively to the nucleoplasmic face (Paulillo *et al* 2005). Under the same import conditions FG domains of Nup214 also show increased nucleoplasmic localisation, this again increases at 15 and

30 minutes (Paulillo *et al* 2005). NPCs in an export state were obtained by microinjecting poly(A+) RNA into the nucleus, which will be exported. There is evidence that as this export event occurs there is a shift in the FG region localisation of Nup153 (anchored at the nucleoplasmic face). Initially the FG regions of Nup153 are mostly located to the nucleoplasmic face (Paulillo *et al* 2005). Then subsequently the FG regions are found to be more (63% of labelling) cytoplasmic (Paulillo *et al* 2005). Nup214's (anchored at cytoplasmic face) FG regions under the same export conditions became more nucleoplasmic (up to 89% of labelling Nup214 nuclear labelling was nucleoplasmic) (Paulillo *et al* 2005).

This evidence is suggested by Paulillo *et al* (2005) to be the FG regions guiding the cargo through the NPC shown by Figure 1.14. This flexibility of Nup153 and Nup214 could also be explained by collapse and extension events. Experiments presented in Lim *et al* (2006, 2007), use AFM with Nup153 attached to a nanodot. This experiment shows changes in brush Nup153 height collapsing into compact molecular structures when Kap-β1 binds. As levels of Kap-β1 are increased so Nup153 takes a more compact shape (up to a point). The collapse is described by Lim *et al* (2007) as "reeling" the Kap-cargo complex into the centre of the NPC. The addition of RanGTP reverses this collapse (Lim *et al* 2007).

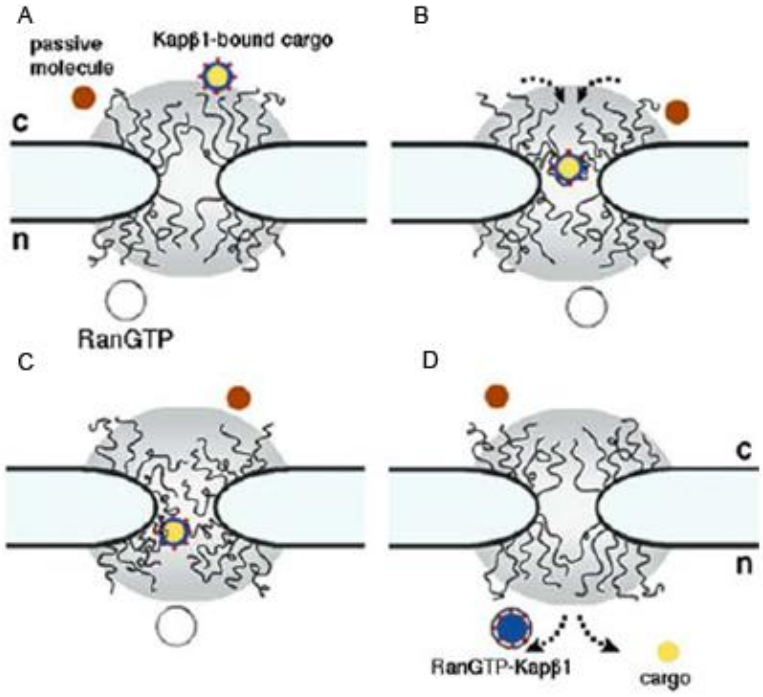

Figure 1.13 Reversible collapse model. From Lim *et al* (2009). Grey area represents the entropic barrier in the absence of a transport factor. (B) The hypothesised localised collapse of FG domains caused by the binding of Kap-β1. This collapse pulls the transport receptor-cargo complex into the centre of the pore. (C) The stochastic translocation of the transport receptor-cargo complex towards the nucleus this movement is caused by the collapse of the FG domains it is bound to be followed by a distension of these domains. (D) RanGTP in the nucleus which in this example sequesters Kap causing the disassociation of cargo (Lim *et al* 2007).

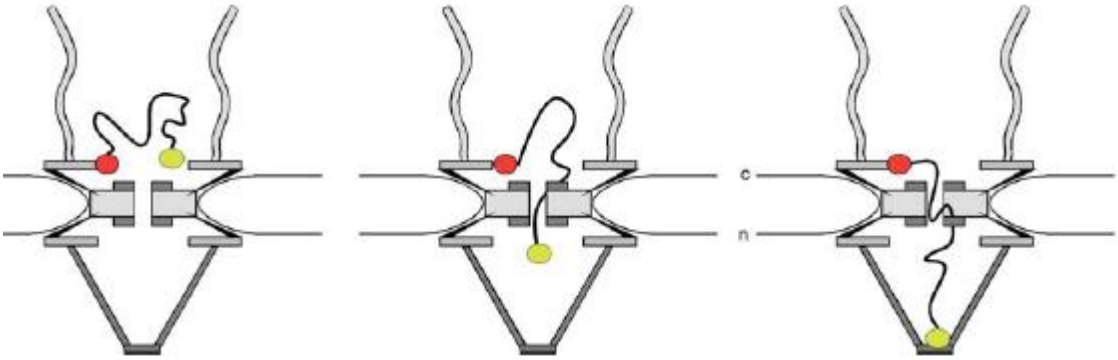

Figure 1.14 The flexible FG domain Nup214. From Paulillo *et al* (2005). Nup214 is shown by thin section TEM to be anchored at the cytoplasmic ring by its N-terminal domain and central domain (red dot). The C-terminal FG repeat domain (yellow dot) is possibly flexible as it is observed at from the cytoplasmic face to the distal basket ring region.

Forest Model: The 11 yeast FG Nups were studied in Yamada *et al* (2010) by purifying them and observing how compact a configuration they take. This was done by measuring their Stokes radii and their NMR diffusion coefficient and comparing it with proteins of equal mass in different hypothetical structural configurations (Yamada *et al* 2010). Results in Yamada *et al* (2010) suggest that the structural configuration of an FG Nup domain is influenced by the content of charged AAs and the ratio of charged to hydrophobic AAs.

The FG domain interactions are shown in Yamada *et al* (2010) to be determined by two rules:

i) FG domains with low (<4%) content of charged AAs can bind to each other, those with high >18 cannot. Evidence for this was obtained by adding charged AAs to the cohesive Nup116, making it noncohesive.

ii) FG motifs are required for cohesion of FG Nups.

This suggests two categories of FG Nup domains (see Figure1.15) (Yamada *et al* 2010):

i. The collapsed coil FG domains, which are able to bind to each other (shrubs).

ii. The relaxed or extended coil domains, which repel FG domains (trees) these may also have cohesive collapsed coil ends.

These two categories of FG form the basis of the forest model. Some Nups are suggested to have a 'stalk' region between the FG repeat region and the anchor. For example Nup116 and Nup100 have a 200 AA 'stalk' region these lack FG domains and have a high charge content. Models of

transport and gating have different views on whether the FG domains interact or not. The idea that there are two categories of disordered structures in FG Nups leads to the idea that multiple gating models could exist within a NPC (Yamada *et al* 2010). It is therefore thought that two gating models (forest model) could exist in a single pore; one as a FG hydrogel (like in Frey *et al* 2006 and Frey and Gorlich 2007; 2009) and the other as an entropic brush (reversible collapse model) (similar to Lim *et al* 2007; Yamada *et al* 2010). Brushes are proposed in Yamada *et al* (2010) to be formed by 'trees' FG Nups crowding in the NPC. This crowding is suggested to make some 'tree' FG Nups extend out like brushes (Yamada *et al* 2010). FG Gels are proposed in the forest model to be created by the lateral interacting shrub FG Nups and where the tree FG Nups collapsed coils regions possibly meet in the centre of the NPC (Yamada *et al* 2010).

Averaging studies (Beck *et al* 2004; Akey *et al* 1993) have shown an object known as the central transporter in the middle of the pore. This object or central transporter has also been observed in individual NPCs (Fiserova *et al* 2009). Other translocation models do not offer a role of this observed central transporter, possibly as there is evidence that it is actually cargo in transit (Beck *et al* 2007). The forest model predicts a low density protein ring (corresponding to the transporter) in the NPC centre made from disordered collapsed coil FG domains (Figure 1.16) (Yamada *et al* 2010). This protein ring made of FG domains is suggested to be connected to the inner spoke ring via the low density cables, which are the relaxed or extended coils of FG Nups (Yamada *et al* 2010). These relaxed and extended coils are low density and flexible, this is why they are not detected by averaging techniques such as used by Akey *et al* (1993). Internal filaments in individual NPCs are seen by SEM to join at the NPC centre in Goldberg *et al* (1996). It could be suggested that these observed internal filaments are FG Nups with relaxed or extended coils. Where the internal filaments join could be the cohesive collapsed coil end of FG Nups. The filaments extending from the spoke ring to the centre of the NPC are the relaxed or extended coil regions of the FG Nups. The FG domains of Nup116 and Nup100 and cohesive tips of Nsp1 and Nup1 are suggested to form the transporter region (Yamada *et al* 2010). Immunogold labelling nuclei of these Nups for use with SEM may help clarify if they are constituents of the transporter structure.

The forest model also suggests two zones within the NPC for transport of macromolecules of transport. It has been experimentally shown that different molecules take different spatial routes through the NPC (Fiserova *et al* 2010).

Zone one in the region of the central transporter is proposed to be hydrophobic due to FG repeats and the lack of charged AAs in the FG regions forming. This hydrophobic property means

negatively charged macromolecules with hydrophobic surfaces like Kaps. It could allow for the entry of Kap-cargo if the transporter could deform and expand the channel. Alternatively translocation here may be similar to through a hydrogel (Yamada *et al* 2010).

Zone two is proposed to be at the NPC periphery and is a region containing stalks of the tree Nups (extended coil regions of Nsp1 and Nup1, and the relaxed coil stalk regions of Nup116 and Nup100). In these tree stalks, the Nups have high numbers of charged AAs, creating a hydrophilic zone between the transporter and the inner wall lined by the 'shrubs'. It is proposed that a Kap could make the extended coil FG domains collapse, retracting the globular FG domains from zone one and widening the tunnel (Yamada *et al* 2010). Kaps with small cargoes and small Kaps are suggested by Yamada *et al* (2010) to translocate in zone two in a reversible collapse manner. For example Kap121 binds Nup53 at AA 461-475 which is near (<10nm) to where it is potentially inserted or tightly associated with the membrane (Patel and Rexachl 2008) by AA461-475 (Yamada *et al* 2010).

Passive diffusion could occur in the forest model by zone one having a diffusion channel. In zone two eight diffusion channels could exist between the stalk regions of the Tree Nups. The size of each of channel would be determined by the distance between the shrub Nups and the transporter (collapsed coil cohesive ends of the tree Nups) (Yamada *et al* 2010).

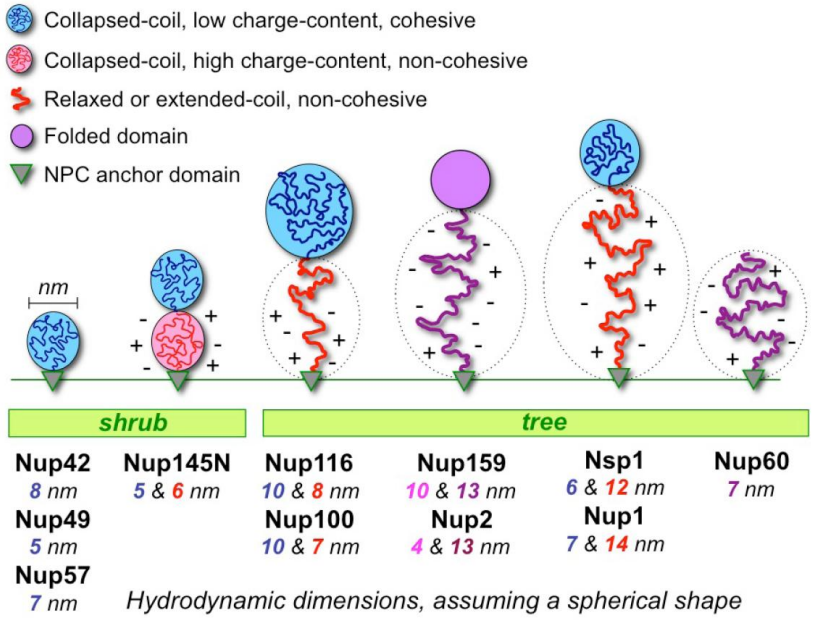

Figure 1.15 FG Nup predicted structures. From Yamada (2010). A diagram of the hydrodynamic dimensions and topology of intrinsically-disordered domains FG Nups categorising the FG Nups as shrub or tree like.

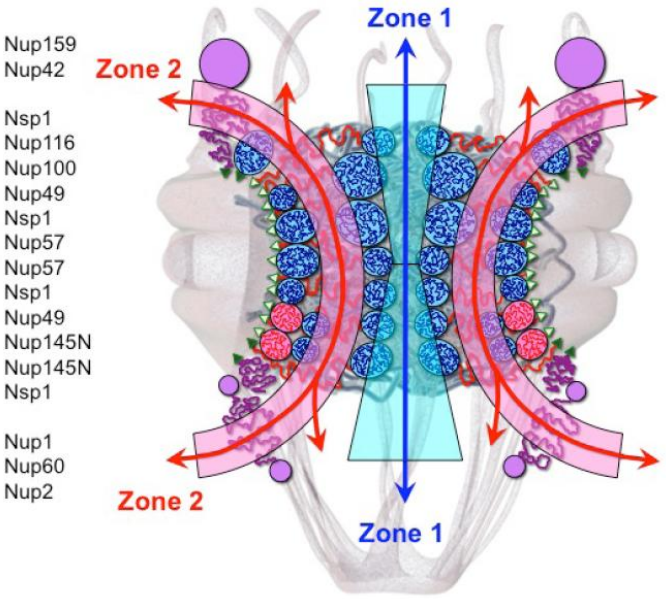

Figure 1.16 Forest Model. From Yamada *et al* (2010). A diagram of the two zones proposed by the Forest model. Zone 1 is composed of the central transporter structure and is hydrophobic. Zone 2 is composed of elongated domains connected to the central transporter creating hydrophilic areas.

Clearly FG repeats play a vital role in nucleocytoplasmic transport. They have an inherent ability in creating an entropy barrier, which can be overcome by transport factors. The different models have different views on how the FG Nups interact with each other.

Chapter 2 Materials and Methods

Materials

All reagents were purchased from Sigma unless stated

YPD medium: distilled water, 2% bacto-pepton , 1% Yeast extract, 2% glucose (taken from 20% stock). Add glucose separately as more prone to contamination once glucose is added. Autoclave YPD once made and use in sterile conditions, before use check for contamination.

YPD plates: YPD medium with 2% agar is autoclaved. When needed YPD medium is heated in a water bath in a microwave and poured into plates in sterile conditions, preferably in a fume hood, giving sample protection. Allow plates to cool in the fume hood without a lid to prevent build up of condensation, which poses a risk of cross contamination if multiple strains are in one agar plate.

Fixative for freeze substitution: 0.2% uranyl acetate, 0.2% gluteraldehyde, 0.01% osmium tetroxide, 5% H_20 in acetone.

Yeast cells are kept at -70°C before plating.

Yeast FG deletion mutants made by Strawn *et al* (2004) the method they used is given below.

A disruption cassette was used with S.pombe $His5^+$ gene flanked on both sides by loxP sites. PCR was used to create DNA fragments consisting of a disruption cassette flanked by the sequence homologous to the FG regions to be deleted. These were then transformed into diploid yeast cells. Homologous recombination resulted in the replacement of the sequence encoding the FG region to be deleted with the disruption cassette. The $His5^+$ gene was removed using Cre recombinase resulting in an inframe epitope tag and a loxP site in place of the FG repeat region. To check the mutant FG Nup protein expression antibodies against the epitope tag were used. Haploid cells containing the FG deleted region of the Nup were created by sporulation and tetrad analysis. Then haploids of opposite mating type were crossed creating a heterozygous diploid, which was used as the starting strain on which the same process was repeated to delete another FG region. Alternatively, the haploids of cells containing different FG deletions were crossed making a heterozygous diploid which was sporulated giving multiple deletion mutants.

2.1 TEM Procedure

Method taken from Fiserova and Goldberg (2010)

1) Transfer yeast cells to YPD plate to grow at room temperature (RT) for 48hrs allowing the formation of colonies, then stored at 4°C.
2) Transfer a single colony of yeast cells to 10ml of liquid YPD. Shake on a horizontal shaker for 6hrs at RT. Check the optical density (OD) and calculate how much to dilute the culture to inoculate 50ml of media so that overnight will grow to an OD of 0.5-1 assuming doubling time around 2 hr for WT, mutant strains can vary and are often slower.
3) Inoculate 50ml of media with calculated volume of yeast culture. Shake overnight in horizontal shaker at 24°C, and check that the OD is 0.5-1 in the morning.

High pressure freezing

1) Set up the high pressure freezer, and prepare specimen carrier and all other materials needed for high pressure freezing.

The following steps should be completed quickly to maintain the yeast in best conditions.

2) Filter the 50ml yeast culture gently through syringe filter and place the yeast on a damp filter paper in a plate. Use wooden toothpicks to transfer a small amount of concentrated yeast culture to the specimen carrier, ensuring it covers the middle part. Excess above the specimen carrier should be scraped off leaving only yeast in the specimen carrier. It is important that there are no areas without yeast culture in the specimen carrier.
3) Transfer the planchet (now containing the yeast sample) to the specimen pod and tighten with the torque wrench. Attach the loading device, the sample is now ready to load and freeze in the Leica EM PACT high-pressure freezing unit. The sample can be stored in LN_2 indefinitely.

Freeze substitution and resin embedding

1) The Leica EM AFS freeze substitution unit needs to be programmed for sample fixation and acetone washes. The programmed steps should be at T1:-90°C for 49hrs, S1 5°C increment per hour to -25°C, T2: -25°C 12hrs, S2 0°C 0hrs, T3: -25°C 50hrs. Before adding samples pre-chill for 1hr.

2) Place FT capsules into cryovials, half fill with fixative and freeze in LN_2. While in LN_2 add the specimen carriers on top of the frozen fixative in the FT capsules and place in pre-chilled Leica Em AFS freeze substitution chamber and run the program.
3) When T2 of the program is complete place FT capsules onto FT chamber filled with acetone chilled to -25°C keep at -25 for 15mins (repeat wash step twice).
4) Remove specimen carriers from FT capsules, ensuring the specimen has come away from the carrier. If not, scrape out using fine tweezers. Add Lowicryl HM20 (Polysciences, Eppelheim, Germany) to the FT chamber with 50% Lowicryl HM20 for 1h, 66% for 1hr and 100% for 1hr and 100% overnight all at -25°C. Ensure bubbles in the Lowicryl HM20 are not made.
5) Load G chamber with gelatin capsules and place in the substitution chamber. Fill the gelatin capsules with 100% Lowicryl HM20 and chill to -25°C. Put the FT-capsules into the gelatin capsules and top up to fill with Lowicryl HM20 if needed. Put the spider cover on the gelatin capsules tightly and remove from the G chamber then place on the stem holder. Use the resin embedding program with T1: -25°C 24hrs; S1 5°C increase/h to 25°C, T2: 25°C, 100hrs (done with the UV lamp).
6) The blocks of resin with sample are now finished. Remove the resin blocks by taking off the spider cover with the attached gelatin capsules label them accordingly. Remove the blocks from the capsules using a razor blade.
7) Trim the blocks using a razorblade to make the best shape for sectioning. Take sections using an ultramicrotome; using a glass knife for sections 50-70nm or a vibrating diamond knife (Diatome Sonic) for 25nm sections. For serial sections it is required that ribbons of sections are being produced. The sections should be picked up as quickly as possible from the water bath on formvar-coated nickel grids.

Immunogold labelling procedure

1) Soon after sectioning (same or next day) rinse with PBS with 0.1% glycine four times for 1 min. This removes any unreacted aldehyde groups.
2) Block in PBS with 1% BSA for 3mins to help prevent nonspecific interactions.
3) Incubate with primary antibody dilution (7µl per grid) on parafilm in a wet chamber at RT for 90mins. When the grid is first put on the antibody drop agitate it.
4) The dilutions used for primary antibodies are: 1 in 10 anti GLFG

1 in 50 anti GFP (Abcam mouse monoclonal to GFP (ab1218))

5) **Note:** if doing double labelling both primary antibodies are in the same solution
6) Wash in PBS four times for 2mins.
7) Incubate with secondary antibodies dilution (7µl per grid) on parafilm in a wet chamber at RT for 60mins. When first put the grid on the antibody drop agitate it.
8) Dilutions used for secondary antibodies: 1 in 20 (Goat anti-rabbit with 5nm gold conjugate (British Biocell International EM.GAR5) for labelling GLFG only). (For double labelling (Goat anti-mouse with 10nm gold conjugate (British Biocell International EM.GAM10) for labelling anti GFP primary and Nanoprobes Goat anti Rabbit with 1.4nm gold conjugate for labelling anti-GLFG primary).
9) **Note:** if doing double labelling both secondary antibodies are in the same solution.
10) Rinse in PBS three times for 5s.
11) Wash in PBS four times for 2mins.
12) Stabilise with 4% gluteraldehyde in PBS.
13) Wash in distilled water 10 times for 1 min.
14) Use gold enhancing (nanoprobes) on the double labelled sections to enhance the 1.4nm nanogold indirectly labelling the GLFG domains, and the 10nm gold particle indirectly labelling the NLS. Store gold enhance mixture on ice and perform enhancing on ice. 8-12s to provides best results.
15) If the contrast is not high enough on the sections then post staining is required, this can help define membranes. Post staining cannot be carried out on grids which have already been viewed using TEM as the resin will have sealed.
16) Post stain with aqueous Uranyl acetate for 10mins.
17) Repeatedly dip into distilled water for 30s.
18) Float grid on lead citrate for 10mins.
19) Repeatedly dip into distilled water for 30s.
20) Place grids on filter paper and wait 5mins before looking at on TEM.
21) Carry out TEM observations on a Hitachi H-7600 at 100KV.

2.2 SEM Procedure

Method developed By J. Fiserova

Materials

Buffer 1: 0.1M Tris-HCL, 10mM DTT, in distilled water pH 7.4.

Buffer 2: 1.2M Sorbitol, 20mM potassium phosphate, 0.5 mM $MgCl_2$ in distilled water pH 7.4.

Buffer 3: 150µl Lyticase, 0.1% PEPA, 0.1% PMSF in 5ml buffer 2.

Fixative 1: 4% Paraformaldehyde, 0.5 mM $MgCl_2$, 0.2M sucrose, in 20mM potassium phosphate pH 6.5.

Fixative 2: 2% Gluteraldehyde, 0.2% tannic acid, 0.5 mM $MgCl_2$, in 20mM potassium phosphate pH 6.5.

Potassium phosphate buffer 500ml pH 7.4.

YPD.

1) Transfer yeast cells to YPD to grow at RT for 48hrs to allow the formation of colonies, then store at 4°C. Grow 50 ml of yeast culture in liquid to 0.5-1 OD at 24°C.
2) Centrifuge 50ml yeast culture at 3000g for 3mins at RT.
3) Quickly pour off YPD and gently re-suspend pellet by pipetting in 20ml distilled water.
4) Centrifuge at 3000g for 3mins at RT.
5) Quickly pour off the distilled water and gently re-suspend pellet in 30ml of buffer 1 for 35mins at 24°C with moderate shaking.
6) Centrifuge at 3000g for 3mins at RT.
7) Quickly pour off the buffer 1 and gently re-suspend pellet in 30ml of buffer 2.
8) Centrifuge at 3000g for 3mins at RT.
9) Quickly pour off the buffer 2 and gently re-suspend pellet in 5ml of buffer 3 for 35mins at 24°C with moderate shaking. Check every 15mins for 70-80% spheroplasts (check lysis in 0.5mM $MgCl_2$).
10) When 70-80% spheroplasts, centrifuge at 3000g for 3mins at RT.

11) Quickly pour off the buffer 3 and gently re-suspend pellet in 5ml of buffer 2.
12) Centrifuge at 3000g for 3mins at RT.
13) Quickly pour off the buffer 2 and gently re-suspend pellet in 5ml of buffer 2. The spheroplasts can be stored for two hours at 4°C.

The following steps should be carried out on ice.

14) Gently re-suspend the pellet in its current solution (buffer 2).
15) To 200µl pre-chilled 0.5mM $MgCl_2$ at 4°C in an eppendorph tube add 200µl spheroplast containing solution. Different ratios should be tested to the given 1:1 above as a lysis which is frequent enough to see but not too severe as to disrupt the structures is required. It is good practice to do a couple of trial runs of different ratios and observe lysis under a light microscope at 40x.
16) Immediately after lysis transfer 4-40µl of sample by pipetting gently onto top of fixative 1 in previously prepared 1.5 microtube chambers. Centrifuge the chambers at 3000g for 10mins at 4°C. *if immunogold labelling now perform steps A-I.
17) Wash chips in fixative 1 without sucrose for 10mins at 4°C.
18) Incubate chips with fixative 2 for 10mins. Samples can be stored in fixative 2 for 48hrs in a covered petridish.
19) Wash in cacodylate buffer for 10s.
20) **Note:** Ensure sure chips are out of ethanol for a minimum possible time.
21) Dehydrate in a series of ethanol washes each for 2mins: one 50%, one 70%, two 95%, three 100% washes.
22) Quickly place chips in Critical point dryer (Bal-Tec CPD 030) using 100% ethanol as the intermediate reagent.
23) Chips can be stored in a vacuum for a few months or in a sealed petridish for up to a week.
24) Coat the chips using 3nM Chromium of thickness 1.5-2nm (Cressington coating system 328).
25) View samples using Hitachi S-5200

Note: The temperature sensitive mutants are grown at 37°C for 4hrs once the culture has reached ~0.5 OD as it is still possible for them to grow.

For the **immunogold labeling** experiments follow the normal procedure up to and including step 14.

A. Transfer the chips with samples on to PBS and incubate for 60mins.
B. Wash twice in PBS for 5mins.
C. Transfer chips to 0.1M Glycine in PBS for 10mins.
D. Transfer chips to 1% BSA in PBS.
E. Incubate with primary antibody in PBS dilution on parafilm in a wet chamber at RT for 90mins. Dilutions used for primary antibody anti GLFG 1 in 10 PBS.
F. Wash in PBS twice for 10mins.
G. Incubate with secondary antibodies in PBS dilution in wet chamber on parafilm at RT for 60mins. Dilutions used for secondary antibody: goat anti-rabbit with 5nm gold conjugate (British Biocell International EM.GAR5) in a 1 in 20 ratio in PBS.
H. Wash three times in PBS for 10mins in PBS.
I. Go to step 17.

Chapter 3 Results

3.1 Mapping GLFG Repeats

Mapping the NPCs GLFG repeats of WT and comparing to FG deleting mutants and temperature sensitive mutants

The aim of this work was to investigate the location of the GLFG repeats of the nuclear pore in yeast wild type (WT). WT GLFG distribution could then be compared to that of FG deletion mutants (SWY2971 and SWY3064). The FG deletion mutants used in this study were made by Strawn *et al* (2004). SWY2971 has all the asymmetrically localised to the NE FG repeats removed. SWY3064 had all asymmetric FG repeat domains removed and Nsp1 a symmetric FxFG and FG Nup. Comparison of WT to FG deletion mutants experiment was done:

(i) To see if removing a large proportion of the FG mass (~40%) has an effect on GLFG distribution. If a difference is noticed it indicates interactions between FG and GLFG repeats, possibly due to GLFG Nups no longer being able to reach as far or to a loss of mass of FG repeats.

(ii) To see if removing a larger proportion of the FG mass (>50%), including a symmetric FG Nup (Nsp1), has an effect on GLFG distribution.

Yeast cells were prepared using high pressure freezing, low temperature fixation and embedding Lowicryl HM20. This method developed in Fiserova and Goldberg (2010) is able to give information from labelling in intact whole cells. This cryofixation process is fast, as is nuclear transport, so we are more likely to capture NPCs and their GLFGs in a more native conformation than by long chemical fixation periods. Some example sectioned NPCs from wild type (WT) are shown in Figure 3.1.1. Data showing the positions of the labelling for GLFG repeats in the NPCs was gathered using transmission electron microscopy (TEM). The yeast strains used were:

- wild type
- SWY2971: Nup42ΔFG, Nup159ΔFG, Nup60ΔFxF, Nup1ΔFxFG and Nup2ΔFxFG (source Strawn *et al* (2004)).

- SWY3064: Nup42ΔFG, Nup159ΔFG, Nup60ΔFxF, Nup1ΔFxFG, Nup2ΔFxFG and Nsp1ΔFGΔFxFG (source Strawn *et al* (2004)).

The deleted regions of the Nups were from the sequence encoding the first designated FG repeat to the amino acid of the last FG repeat in the corresponding Nups.

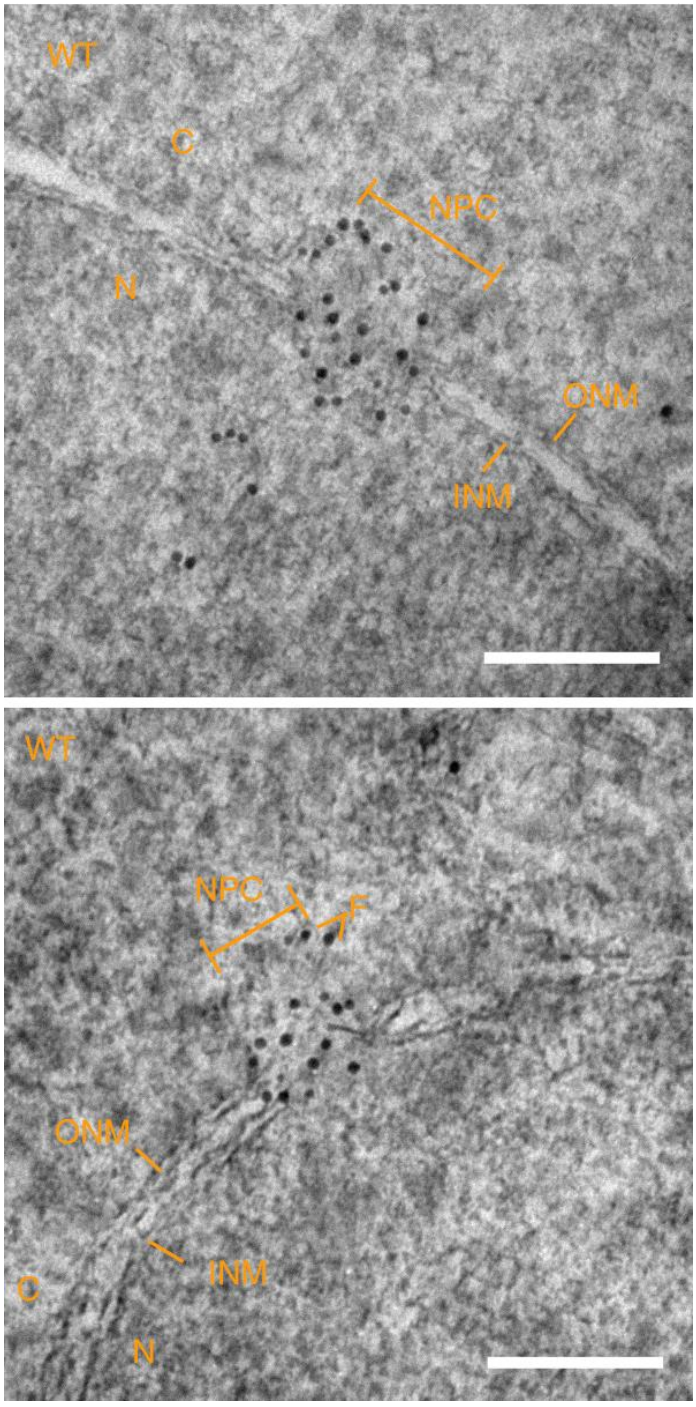

Figure 3.1.1 TEM micrographs of NPCs labelled for GLFG repeats. Labelling of GLFG repeat is done on high pressure frozen, freeze substituted WT yeast. ONM, outer nuclear membrane; INM, inner nuclear membrane; N, nucleus; C, cytoplasm; NPC, nuclear pore complex; F denotes (lower panel) potential filaments with GLFG labelling. In the top image the labelling for GLFG repeats extends into the nucleus, but it is unclear if all the labelling is associated with the NPC. This labelling would sometimes be seen and could correspond to the nuclear basket. Image taken at 100KV. Scale bars represent 100nm.

To show the GLFG repeats, sections were immunogold labelled with an anti-GLFG antibody. The antibody used was raised against the GLFG domain of Nup116, but also appears to recognise the GLFG domains of Nup57 and Nup49 on Western blots (S. Wente personal communication). GLFG labelling was mapped relative to the central plane of the pore (y) and its edges (x). Sectioning through the cell at random points, it is unknown how far the section itself was from the centre of the pore (see Figure 3.1.2). To find out the distance of the GLFG label from the pore edge the location of the gold particle within the pore must first be calculated. In order to do this the diameter of an average pore is used. Taking the distance between the edges of an individual sectioned pore (bars labelled NPC Figure 3.1.1 show this distance) it can be calculated how far the section is through the pore. This can then be used to calculate how far the labelling is away from the centre of the pore (x). This enables us to define where the labelling actually is within the pore in relation to the edge of the NE. The y-coordinate is measured from the x-axis and shows how cytoplasmic (positive value) or nucleoplasmic (negative value) the GLFG label is.

The accuracy that a gold particle labels an 15nm due to the indirect labelling method used. Each point depicts a gold particle used in indirect immunogold labelling specific for GLFG repeats.

Mapping the GLFG repeats represents the situation in an average NPC. However, such an averaged NPC could contain several of the different conformations of the GLFG repeats. The resolution of the labelling is up to ˜15nm, which means that the maximum inaccuracy will be 15nm in any direction. It is very unlikely that the labelling will be in line with either the x or y axis so the inaccuracy in the x and y-coordinates will usually be less than 15nm. Human error must also be taken into account when measuring the exact width of the pore and identifying the central plane. Due to this apparent variability and limited level of resolution for labelling it is problematic to identify trends.

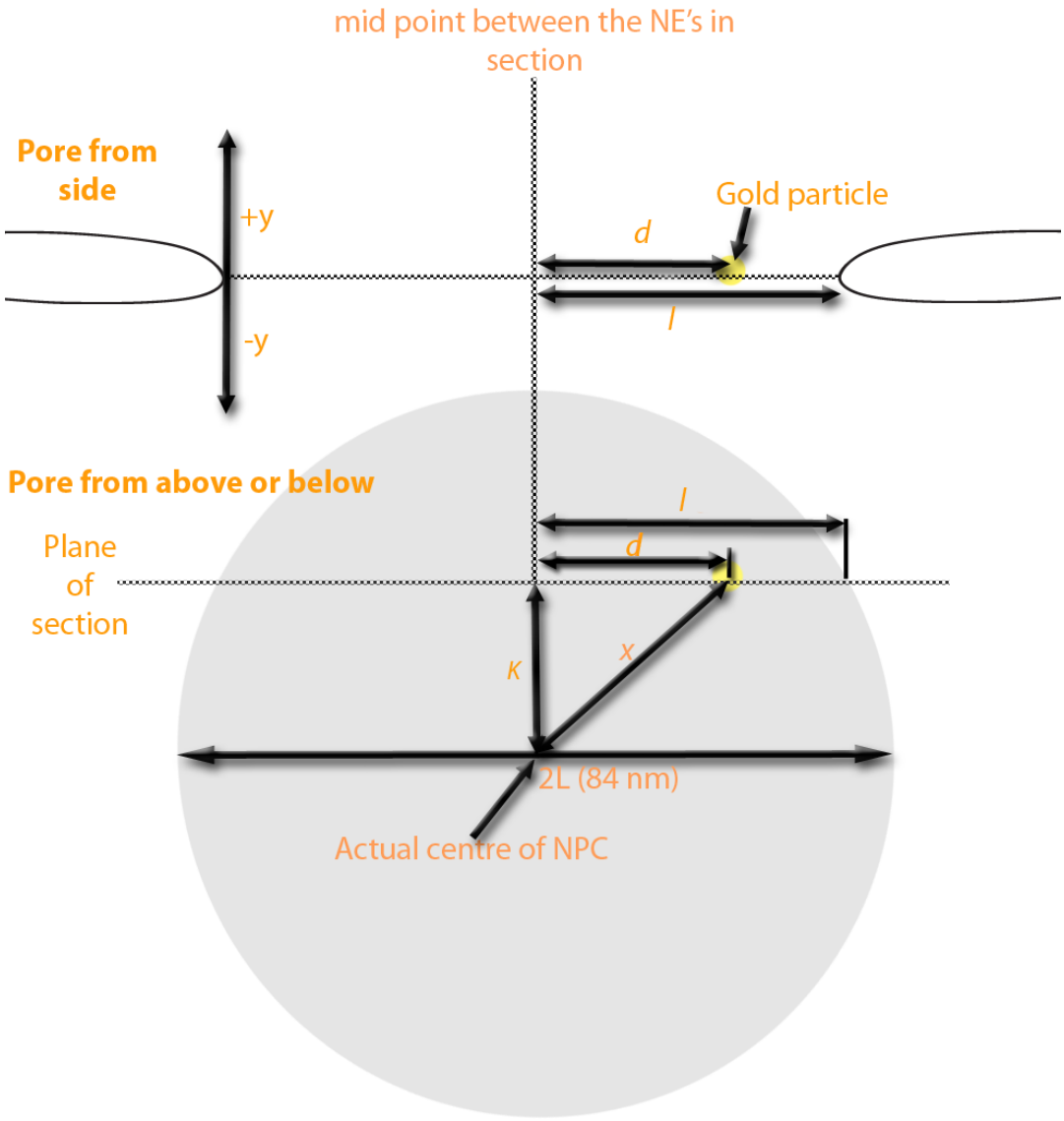

Figure 3.1.2 Illustrates how the gold labelling in the section mapped to give its position relative to the NPC edge. This shows how we get from the labelling in the TEM micrograph shown in Figure 3.1.1 to the standardised data. First the distance between the membranes of the NPC being analysed is measured (*l*). This tells us the distance (k) of the section through the pore to the actual centre of the pore (this can be calculated as 2L is known). Then, the distance of the labelling from the midpoint of the sectioned pore (d) is found. The distance of the GLFG label from the actual centre (centre of 8 fold rotational axis), *x*, is found via Pythagoras ($k^2+d^2=x^2$). The y-coordinate of the GLFG labelling gives the how cytoplasmic (+ve) or nucleoplasmic (-ve) the label is.

The largest pore diameter measured was in WT at 107nm. This is not too dissimilar from other studies such as Rout and Blobel (1993), where the NPC diameter is measured at 97nm with a standard deviation of ±5nm from 10 measurements in yeast nuclei. The calculated position of the

gold particle within the pore is based on the set diameter of the NPC, however the NPC appears to be variable in size. This variability means calculated distance from the edge of the pore may not be very accurate. In each strain, variation in NPC size would be expected, however it is unknown whether the average size differs between strains. The inaccuracies in measurement for each strain would be presumed to be the same and therefore it would be possible to compare the strains. Comparisons between strains is also useful as it shows the distance of the GLFG labels away from its hypothetical centre of the 8 fold rotational axis, which can be compared.

Due to variability in NPC size and the GLFG domains within, experiments which could reconstruct individual NPCs would be advantageous rather than averaging all NPCs. One solution to this could be serial sectioning an individual NPC many times and reconstructing. This may also reveal dynamic structures and better show individual conformations. This may also make it easier to identify trends.

Raw data used	WT	3064	2971
Pores analysed	114	113	121
Gold particles mapped	1376	1356	1364
Average number of gold particles per pore	12.070	12.000	11.273

Table 3.1.1 The number of pores analysed, total number of gold particles mapped and the average number of gold particles per pore for each strain of yeast.

The average number of labelling for GLFG repeats is similar between WT, 3064 and 2971 (Table 3.1.1). This result is due to deletions in SW2971 and SW3064 being in FG domains and not GLFG domains.

The results of the data collected are shown in Figures 3.1.3, 3.1.4 and 3.1.5.

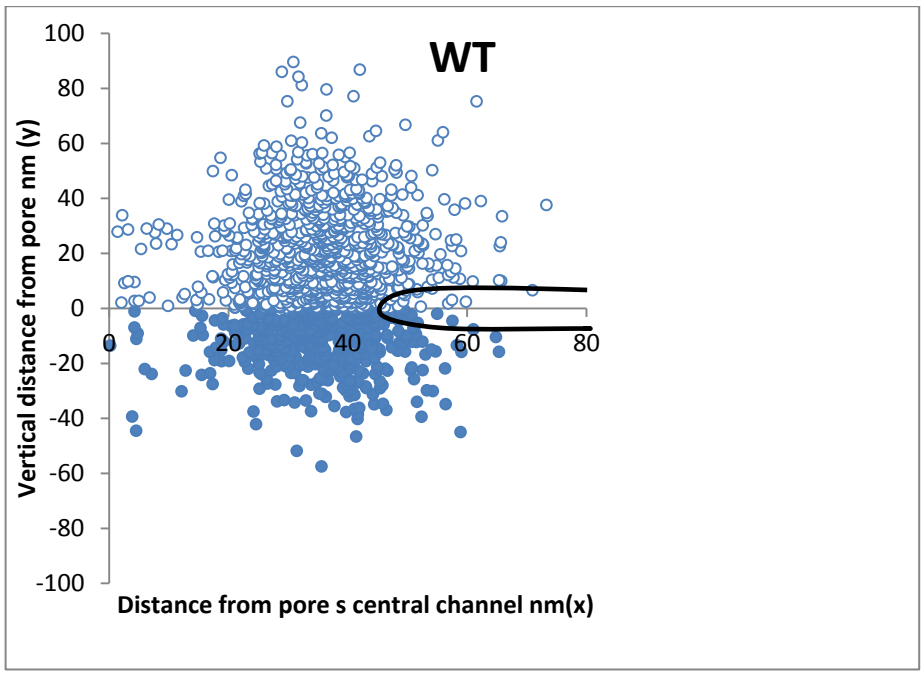

Figure 3.1.3 Mapping the GLFG labelling within an average WT NPC. Shows the distribution of GLFG repeats from the edge of the pore in WT.

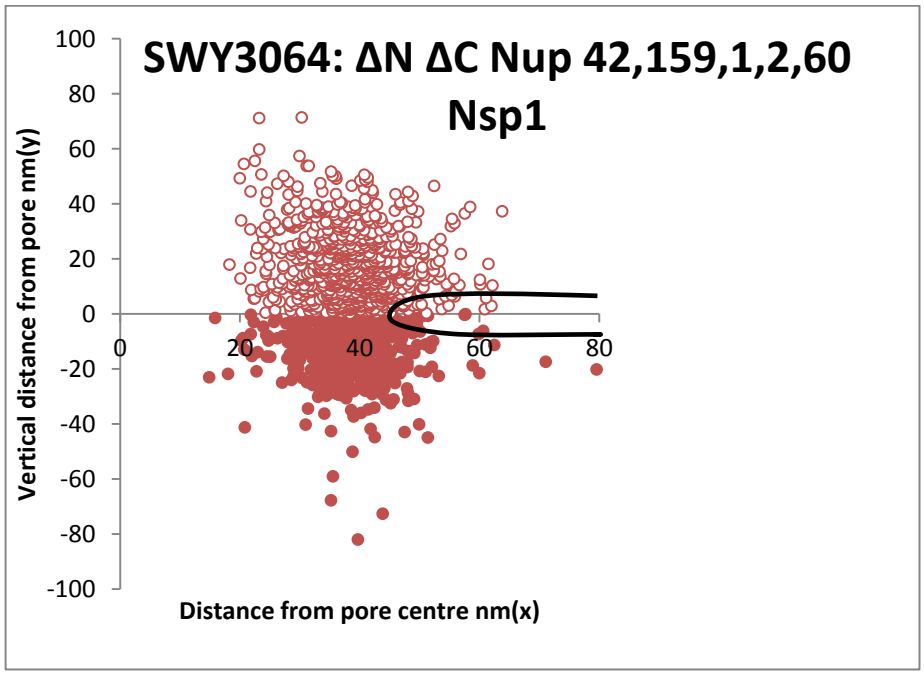

Figure 3.1.4 Mapping the GLFG labelling within an average 3064 NPC. Shows the distribution of GLFG repeats from the edge of the pore in 3064 which has Nup42ΔFG, Nup159ΔFG, Nup60ΔFxF, Nup1ΔFxFG, Nup2ΔFxFG and Nsp1ΔFGΔFxFG. The GLFG labelling appears to be close to the edges and low towards the centre of the averaged NPC.

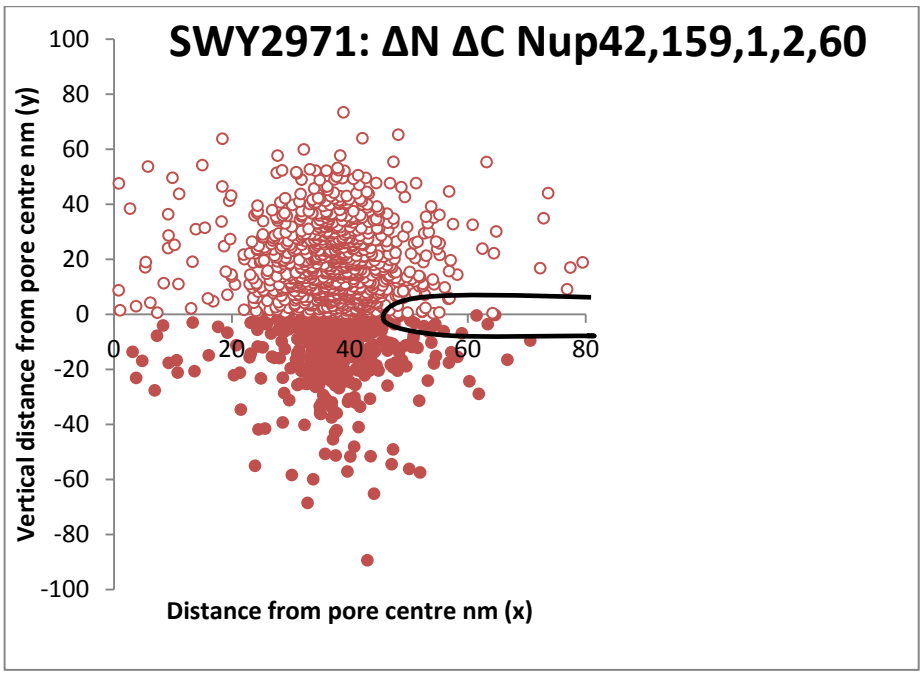

Figure 3.1.5 Mapping the GLFG labelling within an average 2971. Shows the distribution of GLFG repeats from the edge of the pore in 2971 which has Nup42ΔFG, Nup159ΔFG, Nup60ΔFxF, Nup1ΔFxFG and Nup2ΔFxFG.

In WT the GLFG domains can be seen extending into the cytoplasm and nucleoplasm much further than just being localised to the central plane of the pore. There is a reduced amount of data towards the centre of the NPC, this is because the probability of cutting through the NPC's central channel is much lower than cutting through the edge (every section of an NPC has to be cut through the edge but not the central channel). This creates a bias towards the edge. From looking at the scatter plots (Figures 3.1.3, 3.1.4 and 3.1.5) the mutants 2971 and 3064 appear to have lower levels of GLFG labelling far into the cytoplasm, and also into the central channel compared to WT. To confirm this histograms were made to look at the distribution through the x-axis and y-axis. The histograms of the x-axis (Charts 3.1, 3.2 and 3.3) show how close or far away GLFG labelling is from the actual centre of the pore and the nuclear pore edge at the NE.

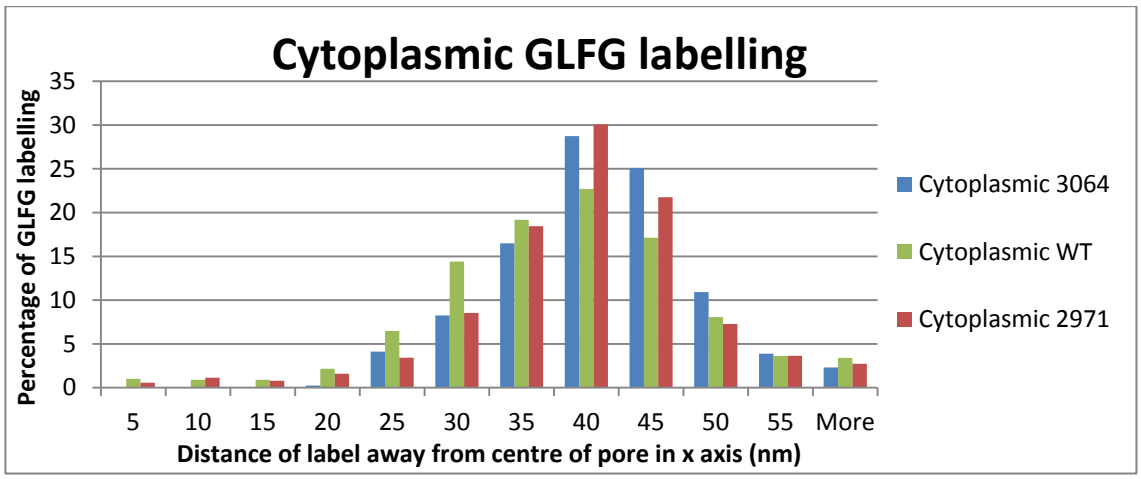

Chart 3.1.1 The distribution of cytoplasmic GLFG labelling towards the edge of the NPC. All three yeast strains have highest labelling at edges. FG deletion mutants have a higher percentage of GLFG labelling at the edge than WT. WT has slightly higher percentages of GLFG labelling towards the centre than FG deletion mutants.

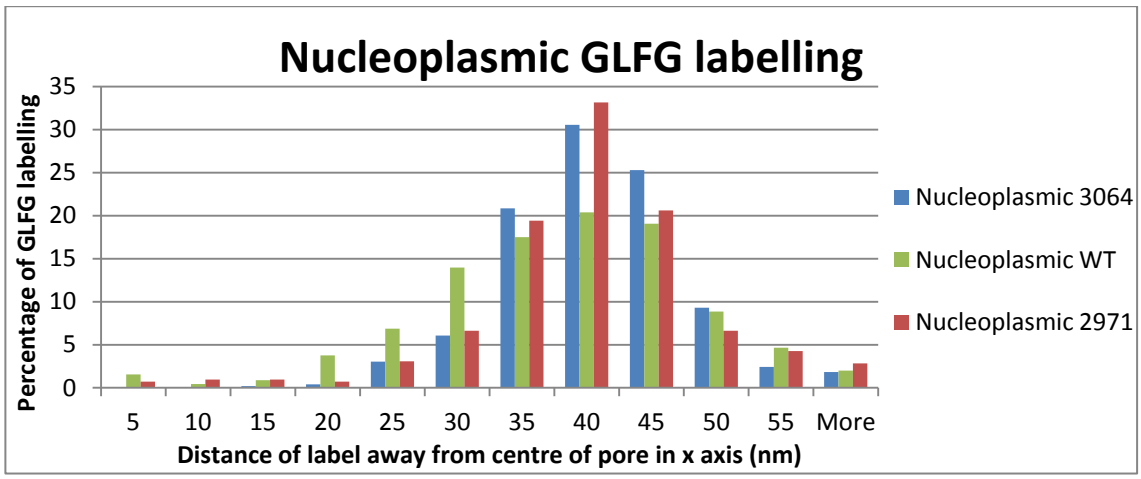

Chart 3.1.2 The distribution of Nucleoplasmic GLFG labelling towards the edge of the NPC. All three yeast strains have highest labelling at edges. FG deletion mutants have a higher percentage of GLFG labelling at the edge than WT, especially shown by the nucleoplasmic labelling. WT has higher percentages of GLFG labelling towards the centre than FG deletion mutants.

The distance along the x-axis from the centre of the 8 fold rotational axis was analysed. There are subtle differences between the WT and mutants. All strains have the greatest amount of labelling towards the edge of the pore. This is likely to be due to sectioning bias meaning more data was collected towards the edge of the NPC. This would be expected to be the same for all pores in all strains and so a direct comparison is still informative. 2971 and 3064 strains have a higher relative percentage of their labelling towards the edge of the pore compared to WT, especially when looking solely at the nucleoplasmic labelling. 3064 and 2971 have lower percentages of labelling

towards the centre of the pore than WT. There therefore appears to be a shift in the location of the GLFG domains away from the centre towards the periphery when certain FG domains are deleted.

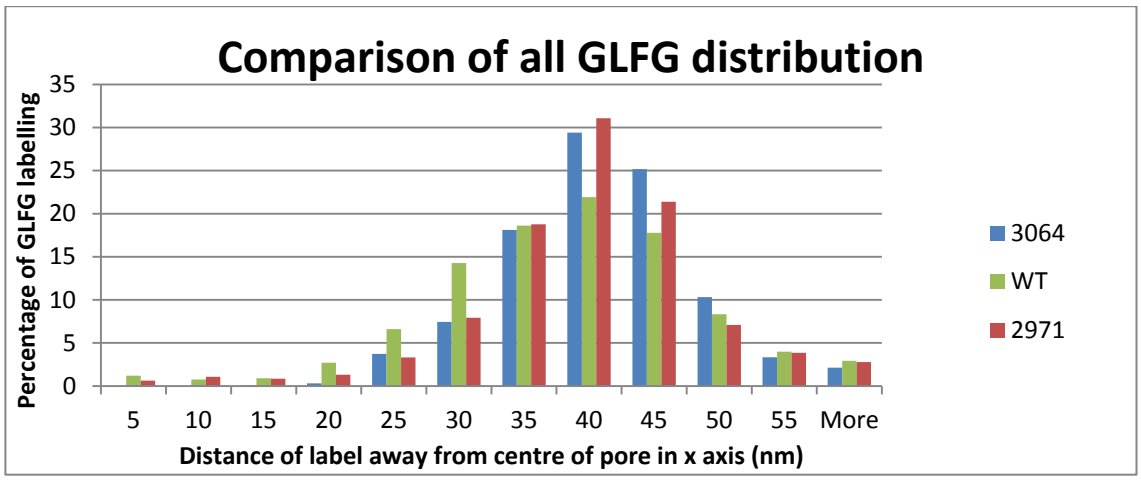

Chart 3.1.3 The distribution of GLFG labelling towards the edge of the NPC. All three strains have highest labelling at edges. FG deletion mutants have a higher percentage of GLFG labelling at the edge than WT, WT has higher percentages of GLFG labelling towards the centre than FG deletion mutants.

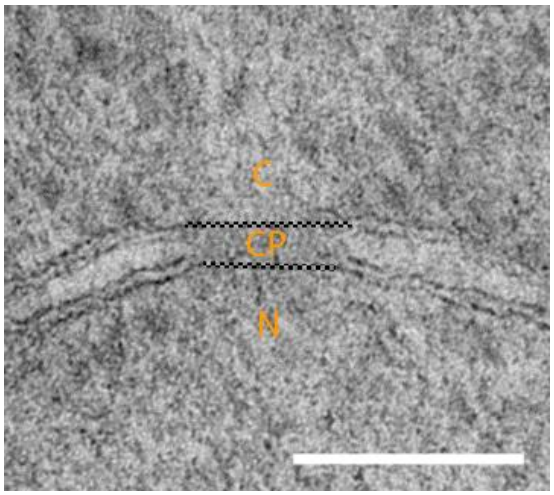

Figure 3.1.6 How the GLFG gold labelling will be categorised based on where it is found. N, nucleus; CP central plane; C, cytoplasm. The central plane follows the line of the NE, it is midway between the inner and outer membranes and separates the cytoplasm from the nucleoplasm. Taken at 100KV with a 30nm section. Scale bar represents 100nm.

To define this central plane the average thickness of the NE adjacent to the NPC was measured, an example is shown in Figure 3.1.6. This was measured from the inside of the inner nuclear membrane to the outside of the outer nuclear membrane (the largest distance). The membranes which appeared damaged (presumably during high pressure freezing, freeze substitution or sectioning) were not counted, as the damaged membranes appeared thicker than undamaged membranes, see for example Figure 3.1.2 Image 3. Previous studies measure the NE thickness of

the NE in yeast to be ˜25-30nm based on 31 measurements (Yang *et al* 1998), however, results in Table 3.1.2 show the NE thickness next to a NPC to be ~18.5nm. The difference observed could be caused by differences in sample preparation.

The central channel was defined to separate the NPC into areas which could be compared. The width of the central channel is greater than the maximum potential inaccuracy in the labelling, therefore there should be no nucleoplasmic labelling mis-scored as cytoplasmic and vice versa.

yeast	NE thickness next to pore (nm)	Number of measurements taken
WT	18.6±2.8	100
3064	18.5±3.1	50
2971	18.5±3.1	50

Table 3.1.2 Average thickness of the NE next to the NPC with the standard deviation and the total number of pores analysed for each strain.

	WT	2971	3064
Cytoplasmic GLFG labelling (%)	49.099	48.615	44.806
Central plane GLFG labelling (%)	30.405	32.692	32.827
Nucleoplasmic GLFG labelling (%)	20.495	18.692	22.365

Table 3.1.3 GLFG labelling distribution in WT, 2971 and 3064.

The labelling for GLFG repeats is found to extend further into the cytoplasm than the nucleoplasm in WT, 2971 and 3064. WT, 2971 and 3064, had <1% of labelling for GLFG repeats found past 25-30nm into the nucleoplasm. For 2971 and 3064 <0.98% of labelling is found 45-50 nm into the cytoplasmic side and for WT there is ~1% of labelling 55-60 nm into the cytoplasm. The peak of the GLFG labelling in WT, 2971 and 3064 is around 5-10nm into the cytoplasm. Also, WT especially has a level of symmetry around that peak.

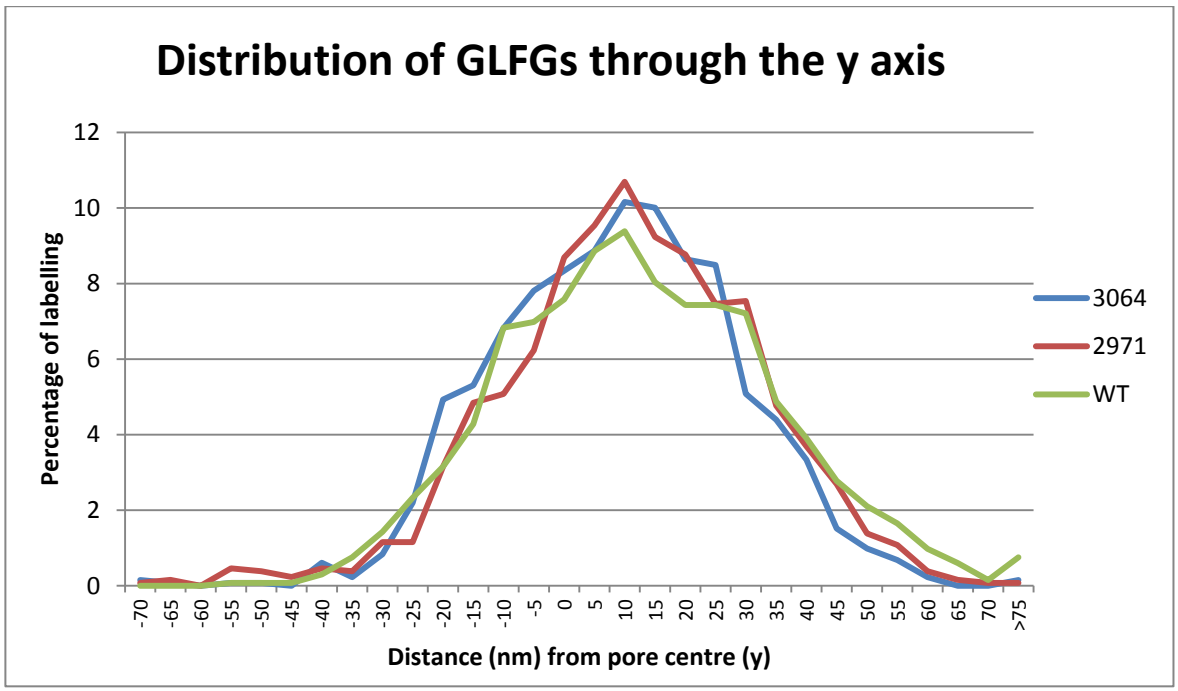

Chart 3.1.4 The distribution of the GLFGs through the y-axis. This is how far into the cytoplasm (+) or nucleoplasm (-) the GLFG labelling is in WT 2971 and 3064. Note 3064 has lower cytoplasmic labelling and higher nucleoplasmic labelling than WT. 3064 and 2971 both have higher peaks of labelling in the midplane than WT.

The results in Chart 3.1.4 and Table 3.1.3 show there to be a higher proportion (~49%) of GLFG labelling on the cytoplasmic side than the nucleoplasmic side in WT (20%) and 2971 (19%). This helped confirm the observation that the WT NPCs have most labelling on the cytoplasmic side. 3064 also has a majority (45%) of GLFG labelling on the cytoplasmic side compared to nucleoplasmic (22%), however this majority is lower than for WT and 2971.

2971 and 3064 have higher peaks of labelling in the midplane than WT. 2971 has a slightly higher cytoplasmic percentage of labelling from 0-30nm into the cytoplasm compared to WT. 3064 has higher levels of labelling just inside the nucleus and lower levels of labelling 25nm or greater into the cytoplasm when compared to WT and 2971. The difference between 2971 and 3064 is that 3064 has the symmetric Nsp1 FG Nup deletion. Therefore the increase in nucleoplasmic and decrease in cytoplasmic GLFG labelling is likely to be due to Nsp1 FG region deletion. The lower cytoplasmic labelling for 3064 compared to WT can also be seen in Chart 3.1.4.

Conclusions from mapping the NPCs GLFG repeats and comparing to FG deleting mutants.

The GLFG distribution in the asymmetric FG Nup Nup42ΔFG, Nup159ΔFG, Nup60ΔFxF, Nup1ΔFxFG, Nup2ΔFxFG 2971 mutant and the 3064 mutant, which has an additional symmetric FG domain deletion in Nsp1(Nsp1ΔFGΔFxFG deletion), is localised more to the NPC edge than in WT. WT has higher levels of GLFG labelling in the centre of the NPC. In WT, GLFG domains appear to extend further into the cytoplasm than in 2971 and 3064. WT, 2971 and 3064 all had a cytoplasmic labelling bias, for 3064 there is a slight shift in the GLFG labelling from the cytoplasm to the nucleoplasm compared to WT and 2971. It is interesting that there is a difference in GLFG labelling as the GLFG domains of Nups have not been removed, only FG domains of Nups have been deleted in 2971 and 3064. Therefore the FG repeats are influencing the GLFG repeats. This could be through crowding as suggested in Yamada *et al* (2010). This is suggested as these mutants have a large mass of FG domains deleted so FG domains would be less crowded in the NPC. The asymmetric FG Nups may therefore be interacting with GLFG regions of Nups in the x-axis. There may also be interactions of symmetric FG Nups and GLFG Nups on the y-axis.

This study could be furthered by analysing the distribution of only symmetric FG regions of FG Nups deletions and the effect this has on the GLFG repeats. This may give more evidence to an effect of symmetric FG Nups of GLFG labelling distribution.

Effect of Prp20 mutation on GLFG repeat distribution

The GLFG coordinates of WT NPCs were compared with observed temperature sensitive Prp20 mutants. Prp20 mutants are mutants in RanGEF. RanGEF regenerates RanGTP from RanGDP, so this mutation stops RanGTP regeneration. RanGTP disassociates cargo from the NPC (Gorlich *et al* 1996). Low levels of RanGTP should lower the rate of cargo disassociation and show the effect on GLFG distribution caused by an NPC that is likely to be stuck in late translocation. The mutation is a Gly to Ser change at AA 282 in Prp20 (*Prp20-G282S)*. The yeast cultures used were WT and temperature sensitive strains SWY3733 and SWY3742. The mutation phenotype is present at the non permissive temperature (37°C), and not present at the permissive temperature (24°C).

The yeast strains used and their mutations are shown in Table 3.1.4, strains 3742 and 3733 had the same *Prp20-G282S* mutation. However they had GFP conjugated to different Nups. In 3742, GFP was conjugated to Nup145, and 3733 had GFP conjugated to Nup1. The use of two strains containing the same mutation was a useful control. It is important to note that the other cellular

functions of Prp20 and Ran are in NE formation, cell cycle progression, mitotic spindle assembly (Dasso *et al* 2002) and new NPC formation (Ryan *et al* 2003; 2007).

Yeast sample	Genotype
WT	
3742 37˚C	G282S (npa14) Nup145-C GFP His 3 Trp 1-1 Met 15 Do Ura 3 Leu2
3742 24˚C	G282S (npa14) Nup145-C GFP His 3 Trp 1-1 Met 15 Do Ura 3 Leu2
3733 37˚C	G282S (npa14) Nup1-GFP His 3 Trp 1-1 Met 15 Do Ura 3 Leu2
3733 24˚C	G282S (npa14) Nup1-GFP His 3 Trp 1-1 Met 15 Do Ura 3 Leu2

Table 3.1.4 Yeast strains used for Prp20 experiments

To initially analyse changes to GLFG distribution a scoring method was used. This divided the NPCs into three categories dependant on the location of the GLFG labelling; mostly nucleoplasmic, mostly cytoplasmic or both sided. When observing serial sections it was found that if a NPC had a few gold particles on the cytoplasmic side and had many on the other side in the next section the few gold particles would become many. The serial section results (Section 3.2) were used to help obtain a better judgement of where most of the labelling would be. It was decided that the following categories would be used to score the NPCs:

- Mostly cytoplasmic: there could be gold particles in the central plane and extending into the cytoplasm. There could also be 1 or 2 gold particles a short distance (up to ~5nm) into the nucleoplasm
- Mostly nucleoplasmic: there could be gold particles in the central plane and gold particles extending into the nucleoplasm. There could also be 1 or 2 gold particles a short distance (up to ~5nm) into the cytoplasm
- Both sided: there could be particles in the central plane or there could be particles in the central plane and gold particles outside this central plane on both nucleoplasmic and cytoplasmic sides.

Some NPCs may have been cut at an angle and may be placed into the wrong category, but most should be in the correct category. With some NPCs it was not always clear which category it should be placed in, therefore the results may include some subjective evidence. Some examples of how the NPCs would be scored are shown in Figure 3.1.7.

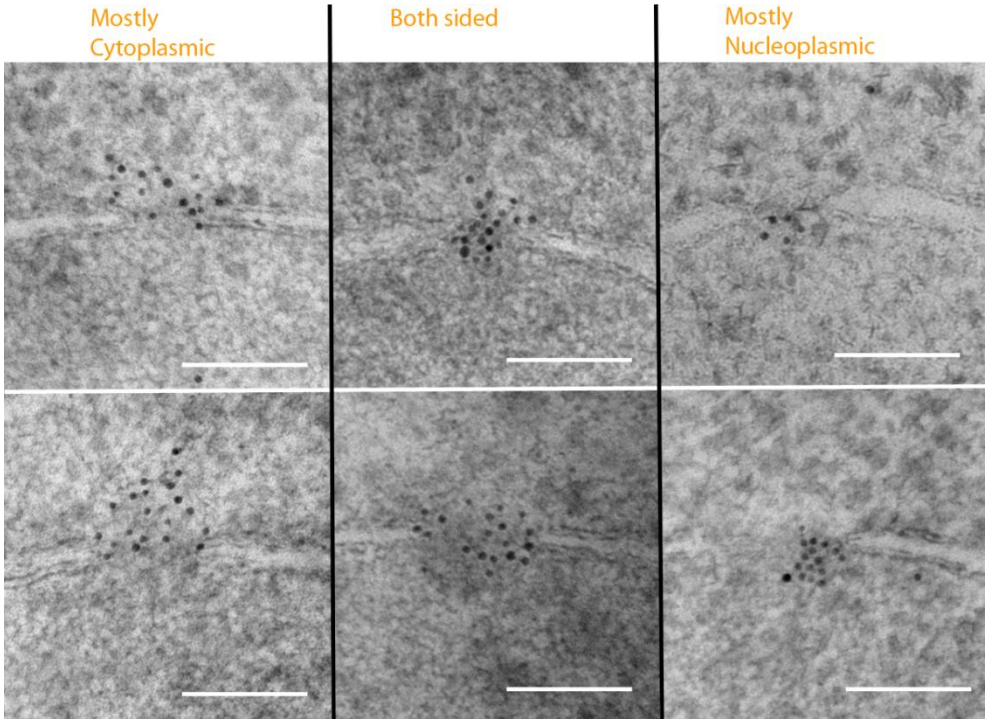

Figure 3.1.7 Examples of how each NPC would be scored. Sample is WT GLFG labelled. The NE is orientated so that cytoplasmic is at the top and nucleoplasmic at the bottom. Scale bar 100nm.

Yeast sample	Mostly nucleoplasmic (%)	Mostly cytoplasmic (%)	Both (%)	Total number of NPCs scored for each yeast sample
WT	7.9	55.3	36.8	152
3742 37	35.5	24.3	40.1	152
3742 RT	13.6	46.6	39.8	118
3733 37	37.7	22.3	40.0	130
3733 RT	15.2	39.2	45.6	125

Table 3.1.5 The percentages of NPCs scored into each category for each strain of yeast.

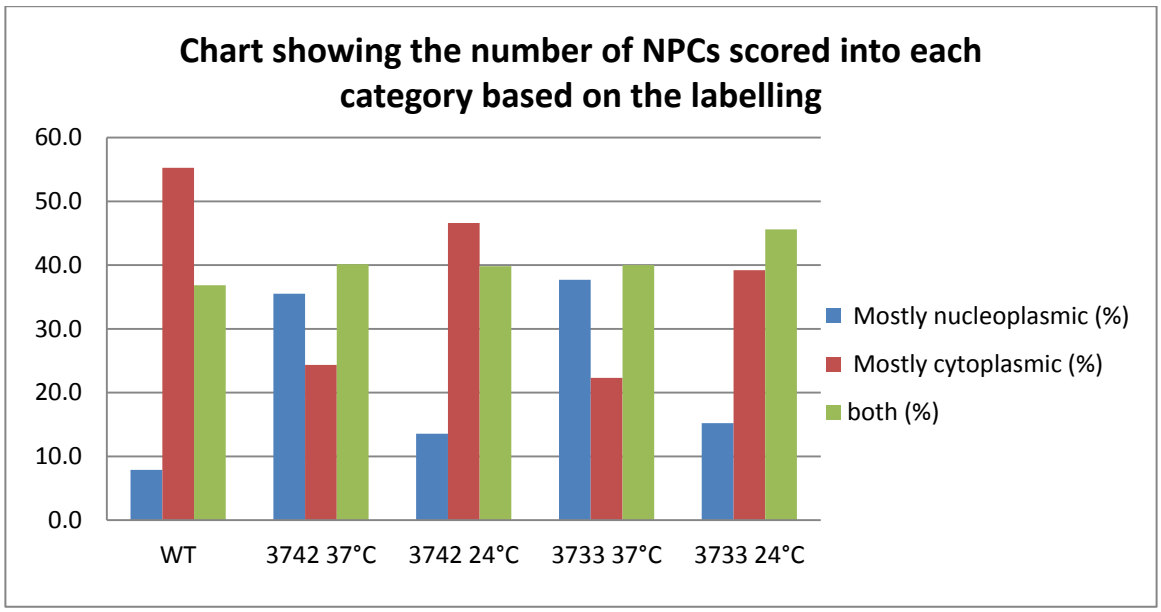

Chart 3.1.5 How the NPCs have been scored based of their GLFG distribution into the following categories: mostly nucleoplasmic, mostly cytoplasmic or both sided. WT and 3742 at 24°C have NPCs that are similar in their GLFG distribution. 3733 at 24°C is also similar as most NPCs are both sided or cytoplasmic, with only a minority mostly nucleoplasmic. When the mutants 3742 and 3733 are at the non permissive temperature of 37°C the NPCs observed a GLFG distribution which is more often nucleoplasmic than at the permissive temperature and WT. All strains of yeast have populations of NPCs about 40% with no clear asymmetry in GLFG labelling (both).

Table 3.1.5 and Chart 3.1.5 show that WT and the Prp20 temperature sensitive mutants at permissive temperatures, 24°C, have high percentages of mostly cytoplasmically GLFG labelled NPCs. These also had low percentages of mostly nucleoplasmic GLFG labelled NPCs. Prp20 temperature sensitive mutants were grown at the non-permissive temperature, 37°C. At 37°C the Prp20 temperature sensitive mutants have increased percentages of NPCs with mostly nucleoplasmic labelling, and a smaller percentage of cytoplasmically labelled NPCs compared to at the permissive temperature, 24°C. This showed that limiting RanGTP regeneration with the Prp20 mutants caused an increase of nucleoplasmic GLFG labelled NPCs, and a decrease in cytoplasmically labelled NPCs. The percentage of NPCs scored as both stayed fairly constant for all yeast samples.

This method of scoring NPCs however is partially subjective, so more objective evidence was sought for this apparent change in the distribution of the GLFG domains. For this, the individual coordinate positions of the GLFG gold labelling in relation to the central plane of the pore was measured. This gave the y position of the gold particle (+ve y is cytoplasmic; –ve y is nucleoplasmic shown in Figure 3.1.2). Due to the high amount of data to collect, only one Prp20 temperature

sensitive mutant (SWY3733) was selected to analyse. SWY3733 was grown at 24°C (permissive) and SWY3733 at 37°C (non-permissive), this could then be compared to the WT data previously obtained. SWY3733 was chosen as the samples were better prepared and images showed the membranes clearly (including the NE). A clear NE meant it was easier to analyse and likely to give more accurate GLFG labelling positioning in relation to the NE. Using the measurements of the NE (Table 3.1.2), the central plane of the NPC is defined as ~18.5 nm or 9.25 either side of the central plane of the pore. For a more complete experiment, WT at 37˚C should also be examined, however time limitations did not allow for this.

The y positions of gold particles corresponding to GLFG labelling for WT, 3733 at 24°C and 37°C were mapped. The y position tells us the particle's location in relation to the mid central plane axis of the pore. Therefore, ±9.25nm either side of 0 (middle of the central plane) is scored as the central plane, labelling outside the central plane in the nucleoplasm (y coordinate of <-9.5nm) is nucleoplasmic, likewise everything outside the central plane in the cytoplasm (>9.5nm) is cytoplasmic, shown by Figure 3.1.6.

	WT 24°C	3733 24°C	3733 37°C
NPCs analysed	114	102	101
Gold particles mapped	1332	1279	1288

Table 3.1.6 The number of NPCs analysed and the number of particles analysed for each yeast strain.

	WT 24°C	3733 24°C	3733 37°C
Nucleoplasmic	20.495	22.127	41.149
Central channel	30.405	31.274	32.298
Cytoplasmic	49.099	46.599	26.552

Table 3.1.7 How GLFG labelling was categorized for WT, 3733 (24°C) and 3733(37°C) into a percentage breakdown of where the labelling is located with central plane. The central channel was defined as 9.25nm either side of the central plane (midplane between each double membrane of the nuclear envelope), this is 18.5nm in total. The nucleoplasmic side is outside this central channel in the nucleoplasm, the cytoplasmic side is outside the central channel on the cytoplasmic side.

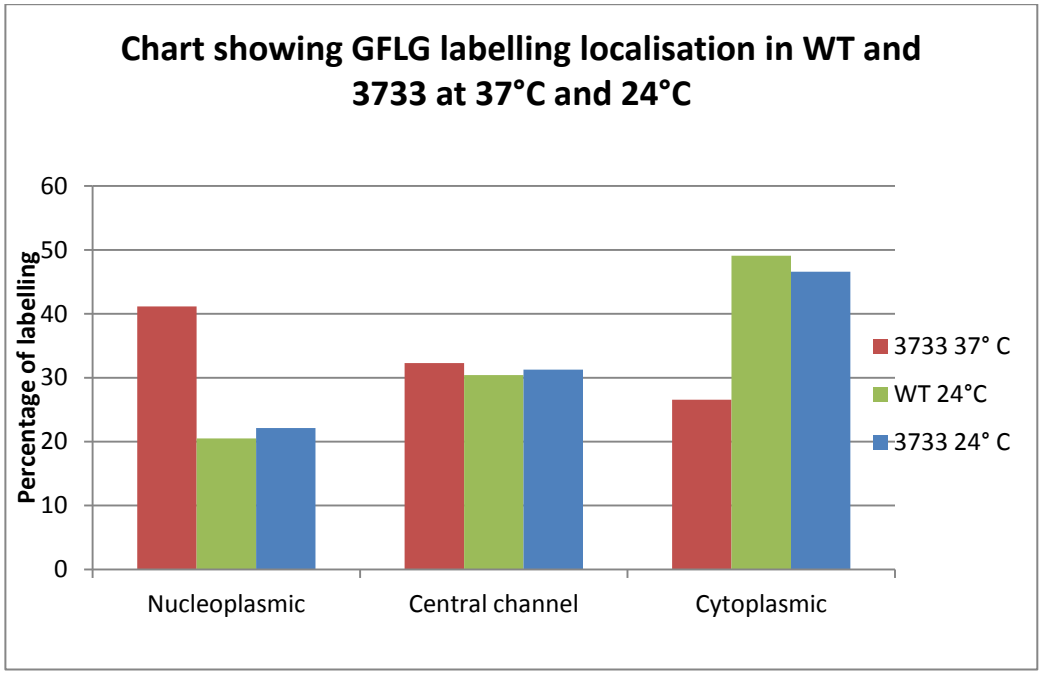

Chart 3.1.6 The percentage of labelling in each defined area (nucleoplasmic, cytoplasmic and central channel). The central channel is defined as ±9.25nm from the central plane of the NE, this is 18.5nm in total. Nucleoplasmic is labelling outside this, on the nucleoplasmic side and cytoplasmic is counted as everything outside the central channel, on the cytoplasmic side. The chart shows a doubling of nucleoplasmic labelling from WT and 3733 at 24˚C to 3733 at 37˚C.

Chart 3.1.6 helps confirm the observations made by the NPC scoring method shown by Chart 3.1.5. The results show a higher percentage of nucleoplasmic GLFG labelling in the 3733 mutant at 37°C compared to WT and 3733 at 24°C. 20.495% of WT labelling was in the nucleus and 22.127% in 3733 at 24°C, compared to 41.149% in 3733 at 37°C, which is over double that of WT. The levels of labelling in the central channel stayed at similar levels in the three yeast samples. Cytoplasmic levels of labelling are higher in WT at 49.099% and 3733 at 24°C at 46.599% than 3733 at 37°C with 26.553%, this is nearly half the percentage found for WT.

Conclusions from Prp20 temperature sensitive mutant results

The results in Table 3.1.7 and Chart 3.1.6, along with the NPC scoring method results in Table 3.1.5 and Chart 3.1.5 show that at the non permissive 37°C the Prp20 mutant yeast has an increased percentage of GLFG labelling in the nucleoplasm compared to WT and the Prp20 mutant at 24°C. Also, at the non permissive 37°C the Prp20 mutant yeast has lower percentages of GLFG labelling in the cytoplasm, compared to WT and the Prp20 mutant at 24°C. To confirm this change in GLFG distribution is not the effect of changing temperature to 37°C, WT at 37°C should be analysed. This shift in GLFG labelling occurs because the loss of Prp20 causes lower levels of RanGTP

regeneration. Lower levels of RanGTP may therefore be directly acting on the GLFGs, or it may be that there is limited disassociation of cargo, causing cargo to get stuck in the NPC and the GLFGs to stay structurally in a later stage of translocation.

Membrane structures associated with the NPC

Whilst studying the NPC in WT yeast it was noticed that GLFG repeat labelling can be seen occasionally extending from the NPC towards membrane vesicles. Due to the nature of EM it cannot be seen if these vesicles are moving towards or away from the nucleus. These membrane structures appear to have internal membranes (blue arrows in Figure 3.1.8). This hints that these vesicle structures are mitochondria and appear similar to some mitochondria observed in Garofalo *et al* (2007) and the isolated mitochondria in Fortsch *et al* (2011). However, this observation should be confirmed by immuno EM which was not permitted due to time limitations.

In the FG domain deletion mutant (SWY2971) yeast, similar structures (H) are seen to be still associated and sometimes continuous with the NE. There is no guarantee that these structures are related between the WT and 2971 mutant, however they are of similar size and are membrane bound. Structures similar to these herniations have been observed in temperature sensitive Nup116 null mutants (Wente and Blobel 1993). In Wente and Blobel (1993) they seem to be in clusters and are more common than observed in this study of SWY2971 and SWY3064. The reason for seeing something more frequently could be that it is happening more often, or simply that the step is taking longer hence being observed more. The herniations (H) in Figure 3.1.9 have labelling for GLFG domains in them.

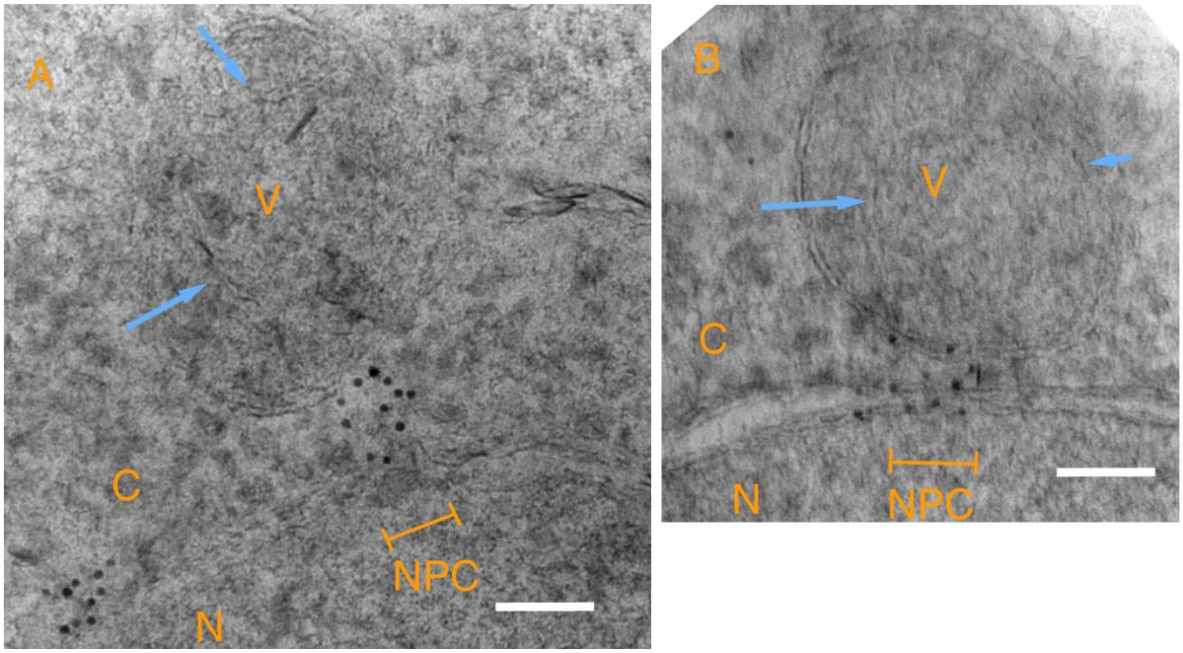

Figure 3.1.8 GLFG repeat labelling extending from NPCs towards vesicle-like membrane structure of high pressure frozen, freeze substituted GLFG indirect immunogold labelled WT yeast. Labelled with GLFG antibody and goat-anti-rabbit secondary gold conjugated antibody. V, double membrane vesicle (potential mitochondria); NPC, nuclear pore complex; C, cytoplasm; N, nucleus. Blue arrows point to possible internal membranes. Scale bars represent 100nm.

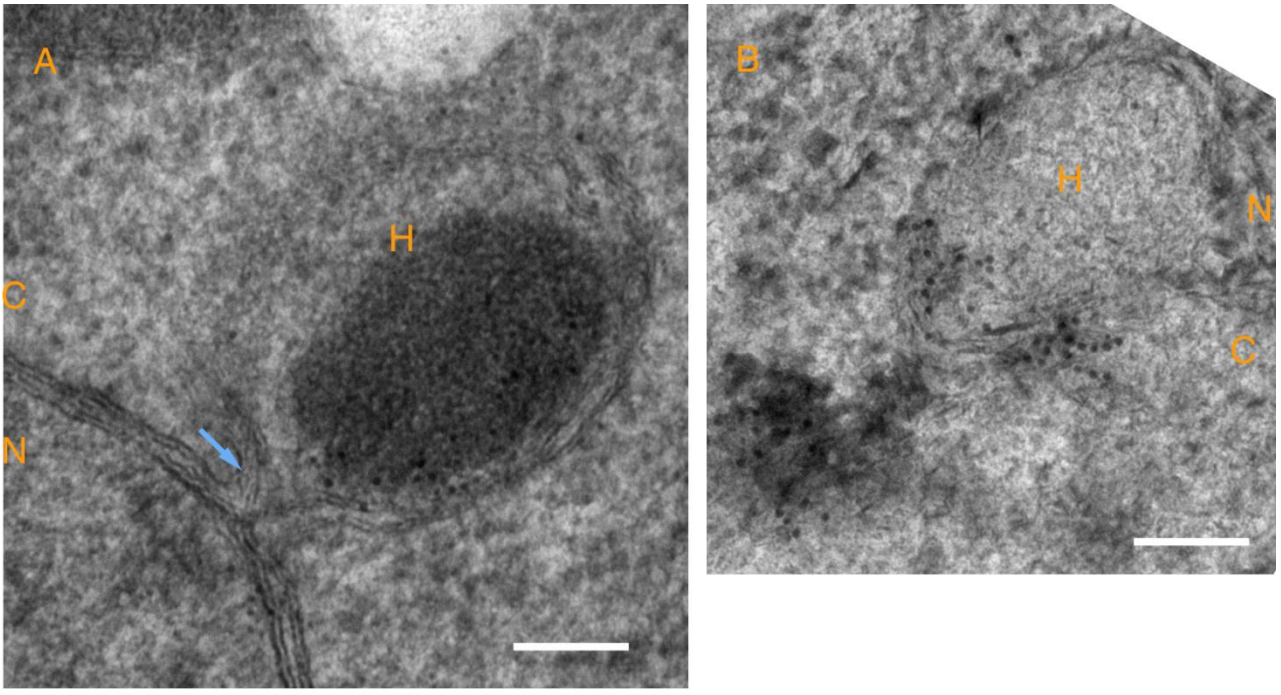

Figure 3.1.9 GLFG labelled herniated NE in 2971 yeast of high pressure frozen, freeze substituted GLFG indirect immunogold labelled 2971 yeast. Labelled with GLFG antibody and goat-anti-rabbit secondary gold conjugated antibody. The herniation in (A) is continuous with the NE. Both herniations (A) and (B) contain labelling for GLFG domains within them. H, herniation of the nuclear envelope; C, cytoplasm; N, nucleus. Blue arrow points to where there is continuous NE with the herniation. Scale bars represent 100nm.

3.2 Reconstructions of individual NPCs to examine the 3-D GLFG distribution

When looking at the GLFG domain labelling in the NPCs it was noticed that some appeared to be largely cytoplasmic, largely nucleoplasmic or fairly evenly distributed about the central plane. The largely cytoplasmic GLFG labelled NPCs appeared to be the most common. One possible interpretation was that the appearance of the GLFG repeats was asymmetrically distributed in some NPCs due to the angle at which the NPC is cut. The section may be cut at an angle such that there is more of the cytoplasmic side or nucleoplasmic side of the NPC, giving the appearance of the labelling mostly being on one side. Serial sectioning was used to test whether there is a genuine asymmetric distribution of GLFG domains in individual NPCs. By cutting through the same NPC multiple times it can be seen if the labelling is still one sided when the whole 3-D volume of an individual NPC is considered. It then shows that GLFG domains can be asymmetrically distributed in individual NPCs. To cut through an individual NPC multiple times very thin sectioning must be used. To achieve this a vibrating diamond knife was used and sections were labelled for GLFG domains.

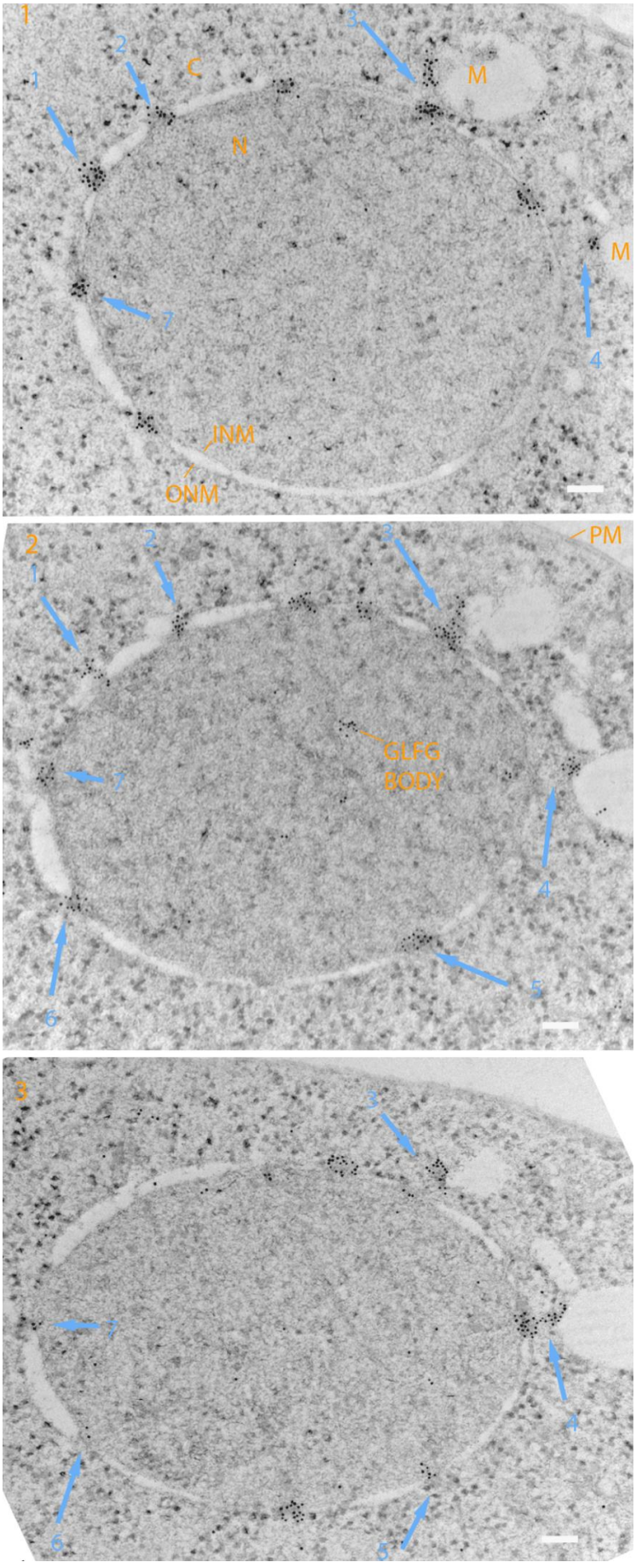

Figure 3.2.1 Sections through a nucleus with NPCs displaying various distributions of GLFG labelling. Serial sectioned, high pressure frozen, freeze substituted whole yeast nucleus and labelled for GLFG repeats. Blue arrows point to NPCs with numbers corresponding to that individual NPC in the different sections. In NPCs 1, 2, 3, 4 GLFG labelling appears to be mostly distributed on the cytoplasmic side of the NPCs, with the GLFG domains of NPCs 3 and 4 extending towards a membrane like structures (M), which could potentially join further into the sample. NPC 5 appears to have mostly nucleoplasmic distributed GLFG domains. NPCs 6 and 7 appear to have cytoplasmic and nucleoplasmic domains so are 'both sided' NPCs. The GLFG labelling in NPCs 6 and 7 does not appear to extend very far from the central plane. N, nucleus; C, cytoplasm; INM, inner nuclear membrane; ONM, outer nuclear membrane; PM, plasma membrane. Present in the second section is an area within the nucleus highly labelled for GLFG domains; this could be a GLFG body. Sections were ˜30nm thick. Scale bar representing 100nm.

Figure 3.2.1 shows how GLFG labelling distribution can vary greatly between NPCs within the same nucleus. The NPC labelled 5 in Figure 3.2.1 Image 2 can be seen to have largely nucleoplasmic GLFG labelling. This appears to be the least frequent GLFG labelling distribution as shown by WT in Charts 3.1.5 and 3.1.6. Other NPCs in Figure 3.2.1 have GLFG labelling which is largely cytoplasmic, for example NPCs labelled 1,2,3,4. The NPCs labelled 3 and 4 have GLFG labelling extending towards membrane structures (M), which may be only one structure. The NPCs labelled 6 and 7 in Figure 3.2.1 do not have GLFG labelling extending either cytoplasmically or nucleoplasmically.

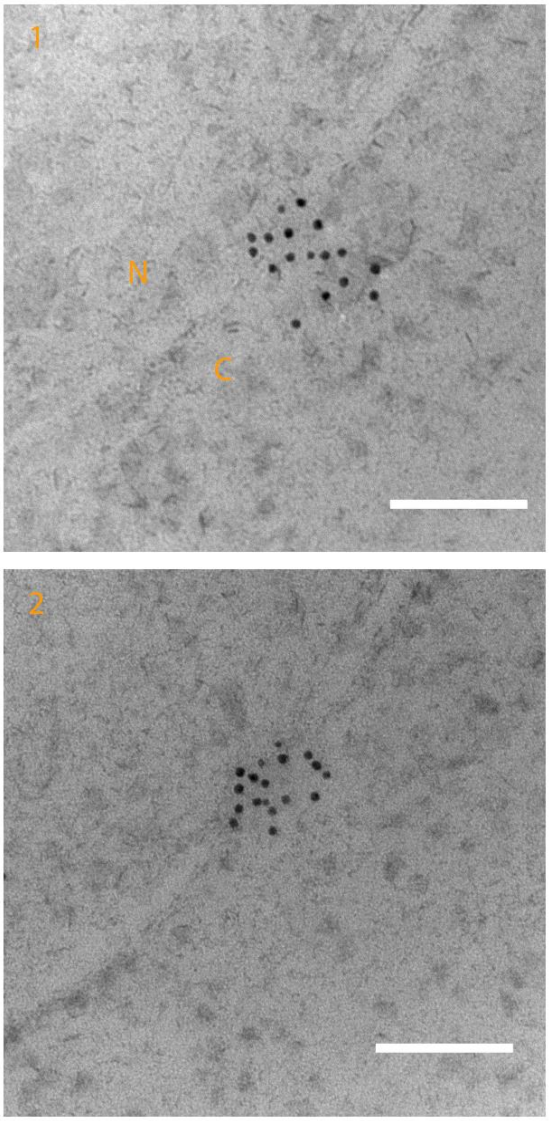

Figure 3.2.2 Serial sectioned NPC with mostly cytoplasmic GLFG labelling. Most of the labelling is on the cytoplasmic side. This is especially shown in the first section. The second section shows one gold particle just on the nucleoplasmic side, but still very close to the centre of the central plane. N, nucleus; C, cytoplasm. Sections taken at ~25nm Scale bar 100nm.

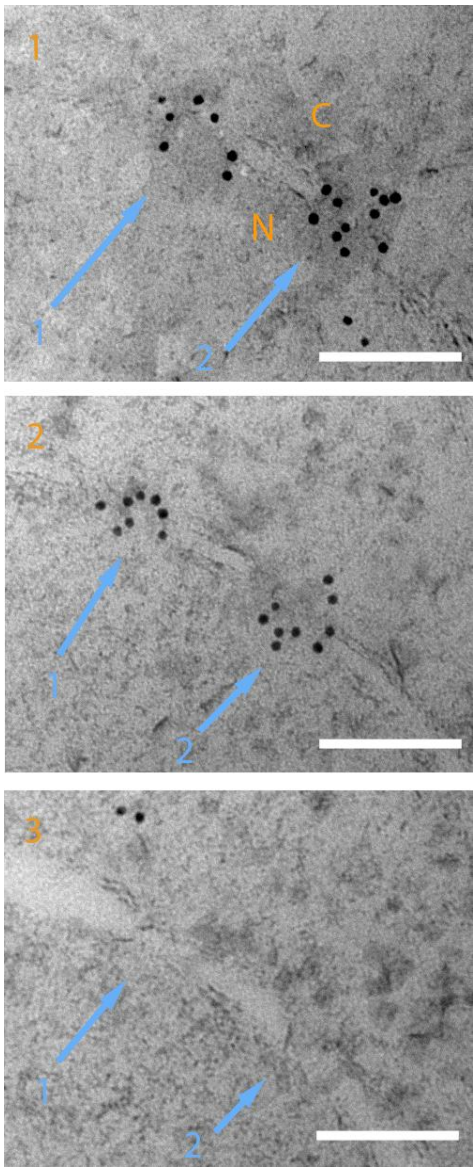

Figure 3.2.3 NPCs with GLFG labelling on both cytoplasmic and nucleoplasmic sides. N, nucleus; C, cytoplasm. NPCs 1 and 2 have labelling on both sides of the NPC, however for NPC 1 it is hard to tell whether the NE position is on one side of the NPC in section 1. Section 3 is at the very edge of the NPC and no GLFG labelling is present.

Averaging results in Section 3.1 indicated that more WT NPC GLFG labelling was biased towards cytoplasm rather than the nucleoplasm. This high level of cytoplasmic bias of GLFG labelling can be seen in individual NPCs as shown by Figure 3.2.2. The cytoplasmic bias is present in both sections through the pore. There are also examples of NPCs with a cytoplasmic GLFG labelling bias, shown in Figure 3.2.5. Some NPCs had no clear cut bias, as shown by the NPCs in Figure 3.2.3 and NPC in Figure 3.2.4. Figure 3.2.4 section 1 shows near the NPC periphery, which interestingly is not GLFG labelled. This could be due to being greatly peripheral on the NPC or it may suggest that GLFG labelling can also be biased within the plane of the nuclear envelope. Due to the lower prevalence of NPCs with a nucleoplasmic GLFG labelling bias it was more problematic to obtain good images.

However, NPCs with a nucleoplasmic GLFG labelling bias can be observed in Figure 3.2.1 (NPC arrowed 5) and Figure 3.2.7 (NPC arrowed 1).

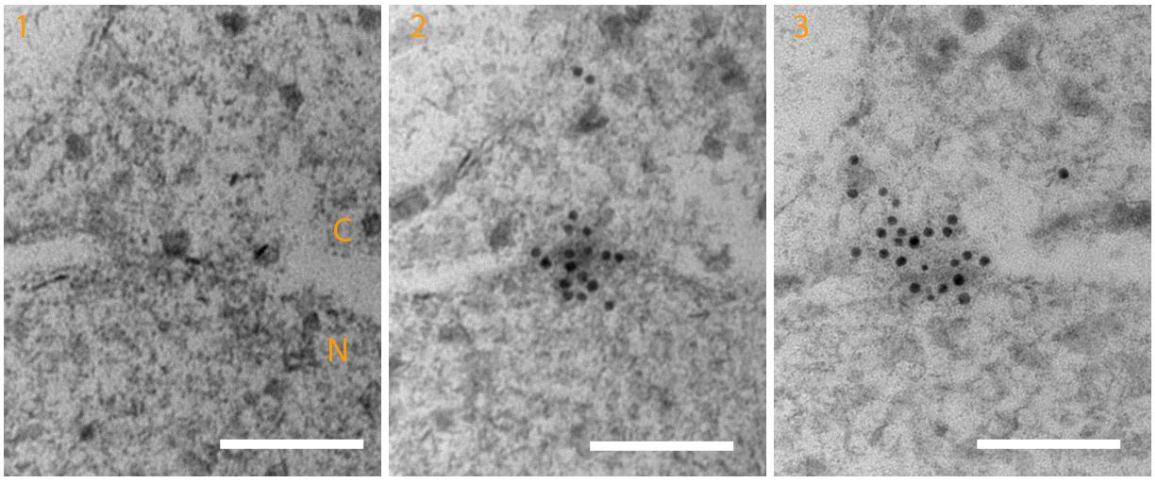

Figure 3.2.4 Three sections through a NPC with GLFG labelling on both cytoplasmic and nucleoplasmic sides. In section 1 there is no labelling possibly due to it being the NPCs periphery. Sections 2 and 3 through the NPC show that labelling can be on both sides. In section 3 the labelling is shown to extend towards a membrane structure in the cytoplasm. N, nucleus; C, cytoplasm. Scale bar represents 100nm. Taken at 200000X magnification.

The GLFG's labelling in some cases seems to be located together, such as the NPCs with biased GLFG distributions. This hints that sometimes GLFG's domains all move together, possibly affecting each other.

The NPCs sometimes have GLFG labelling which can be seen extending towards membrane structures (shown in Figure 3.2.6). Figure 3.2.6 C suggests that the GLFG extensions towards vesicles may be thin as the mid GLFG region (arrowed) can only be observed labelled in one section (C2). The structures the NPC's GLFG labelling extends towards may be different. This difference is suggested by the membrane structure (M) in A1, which seems to be vesicle-like. This differs from that in B1, which is vacuole-resembling, and C1, which appears to have internal membrane structures. This difference however may be due to sample preparation, which could be tested by labelling for different structures and GLFGs.

These images also indicate that GLFG domains are not just located to the central plane of the pore. They may therefore have other roles within the cell and seem to be variable and able to extend long distances from the NPC into the cytoplasm. There is also the presence of a 'GLFG body' within the nucleus.

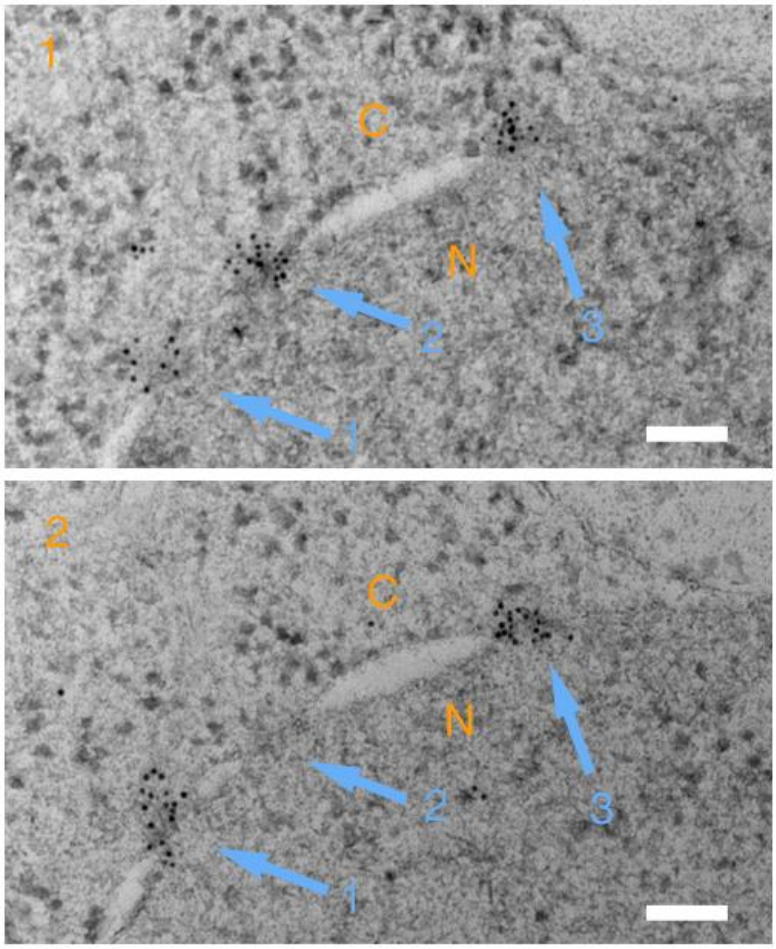

Figure 3.2.5 NPC with mostly cytoplasmic GLFG labelling. Serial sectioned high pressure frozen, freeze substituted yeast. NPCs 1 and 3 have most labelling on the cytoplasmic side. Labelling is not present for NPC 2 in the second section as it appears to be at very edge of the NPC. TEM micrographs taken at 200000X magnification. N, nucleus; C, cytoplasm. Sections taken at ~25nm. Scale bar represents 100nm.

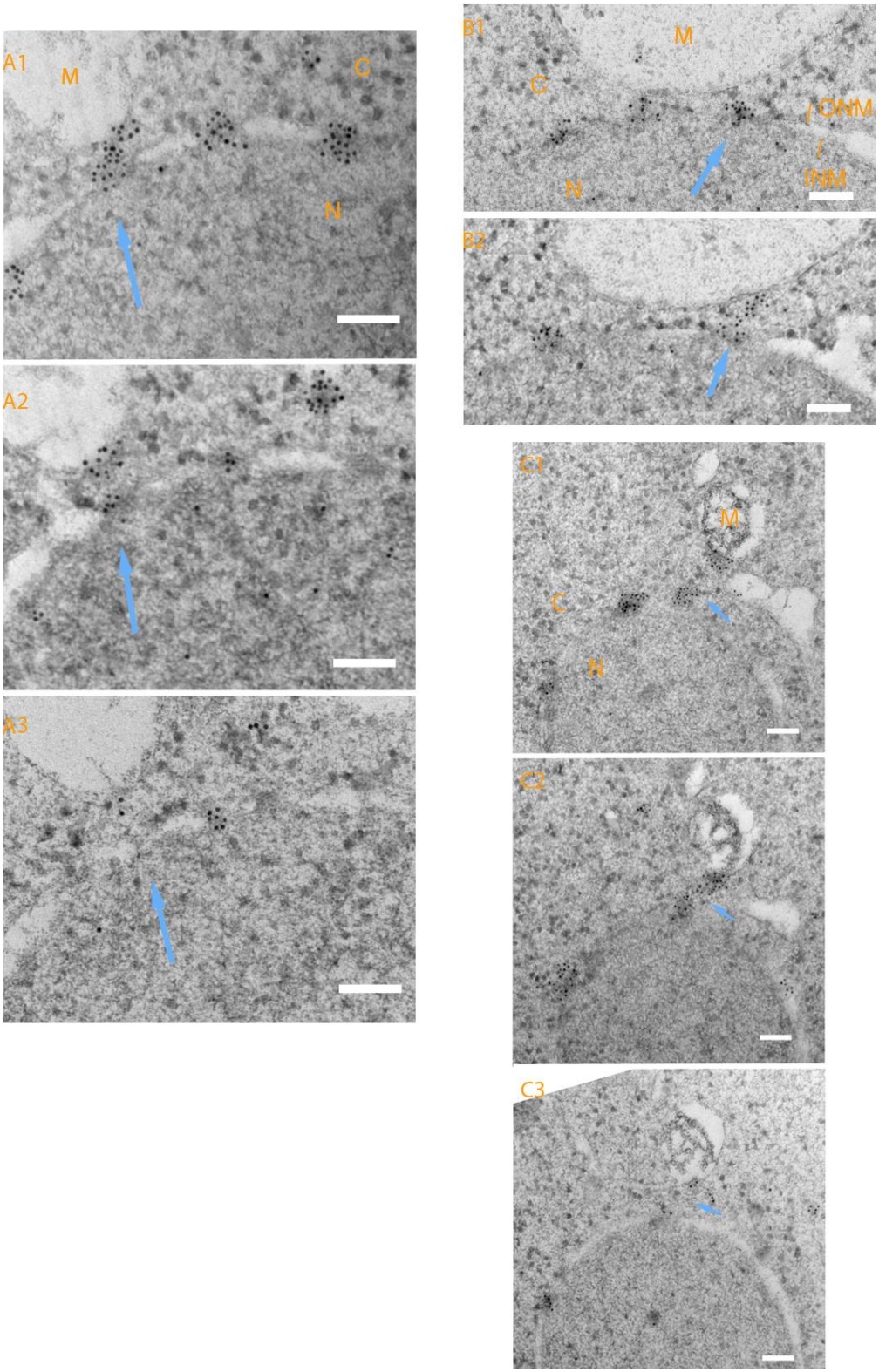

Figure 3.2.6 NPCs GLFG repeat labelling extending towards membrane structures in the cytoplasm. Serial sectioned high pressure frozen, freeze substituted yeast. N, nucleus; C, cytoplasm; INM, inner nuclear membrane; ONM, outer nuclear membrane; M membrane structure. A1, 2 and 3: the GLFG repeat labelling extends towards a vesicle-like structure. B1, 2 and 3: the GLFG repeat labelling extends towards a vacuole-like structure. C1, 2 and 3: NPC GLFG repeat labelling extending towards a membrane structure which seemingly possesses internal membranes. Scale bar 100nm.

NPCs (Figure 3.2.7 NPCs arrowed 3 and 4) can be seen either side of part of the NE which has a large gap (G) between the membranes. This was only occasionally observed so one possible explanation for is that the membrane is damaged by the fixation process. Alternately, it could be speculated that the GLFGs are pulling membrane in to fuse with the NE. This could be a method of NE growth. Figure 3.2.1 may show an earlier stage of this. In Figure 3.2.1 pores 3 and 4 have GLFG labelling which seems to join up to a membrane structure (M), which appears be one structure. Possible ways to test if GLFGs are involved could be to examine GLFG deletion mutants for defective NE growth. Alternately the role of NPCs in NE growth could be examined. This could be done by stopping new NPCs from forming (many Ran mutants do this, however this may have other consequences) and observing the effect on NE growth.

Also observed in Figure 3.2.7 were some interestingly GLFG labelled NPCs. An NPC (arrowed 6) has GLFG labelling extending ~70nm from the midplane of the NPC into both the cytoplasm and the nucleoplasm, this was not often observed. A NPC with nucleoplasmic biased GLFG labelling (NPC arrowed 1) is also seen.

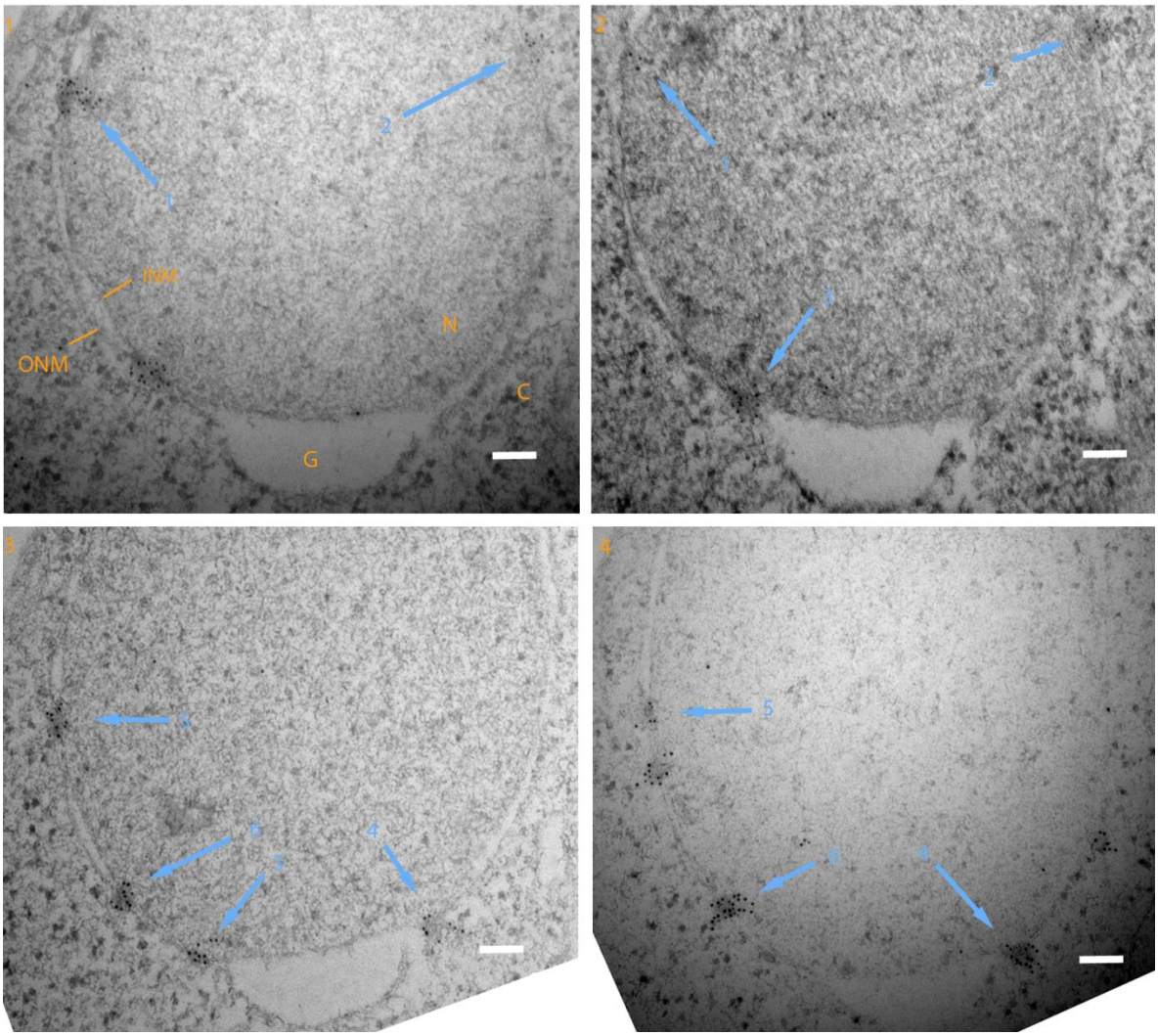

Figure 3.2.7 Serial sectioned nucleus with NPC with GLFG domains extending in both directions and pores at either side of thick NE. Pore 1 has most labelling for GLFG domains on the nucleoplasmic side, pores 2 and 4 the labelling is highest on the cytoplasmic side in both sections. Labelling on Pores 3, 5 and 6 is both sided, in pore 6 the GLFG labelling extends large distances in both cytoplasmic and nucleoplasmic directions in section 4. This was not a common observation. The NE has a wide separation of its membranes (G) with NPCs at either side. N, nucleus; C, cytoplasm; INM, inner nuclear membrane; ONM, outer nuclear membrane; G, Gap between NE membranes. Scale bar representing 100nm.

These three sections (Figure 3.2.8) show a yeast cell undergoing cell division. Structures resembling spindle pole bodies (SPB) can be seen and are identified as they have microtubules (MTs) emanating from them. Also, SPBs are larger than NPCs. To clarify if these structures are SPBs they should be labelled for, however it will be assumed here that they are. The SPBs are labelled for GLFG repeats, it is not clear which GLFG containing protein is being labelled in the SPB. The GLFG labelling from the SPB can be seen extending towards a vesicle-like structure (V) in section 2. The results suggest that GLFG repeats have a role in cell division. The extension of GLFGs towards

membrane structures such as vesicles is also observed from NPCs. This indicates a possible conserved function of GLFG repeats in SPBs and NPCs. The MTs can be seen stretching from one SPB across the nucleus to the other.

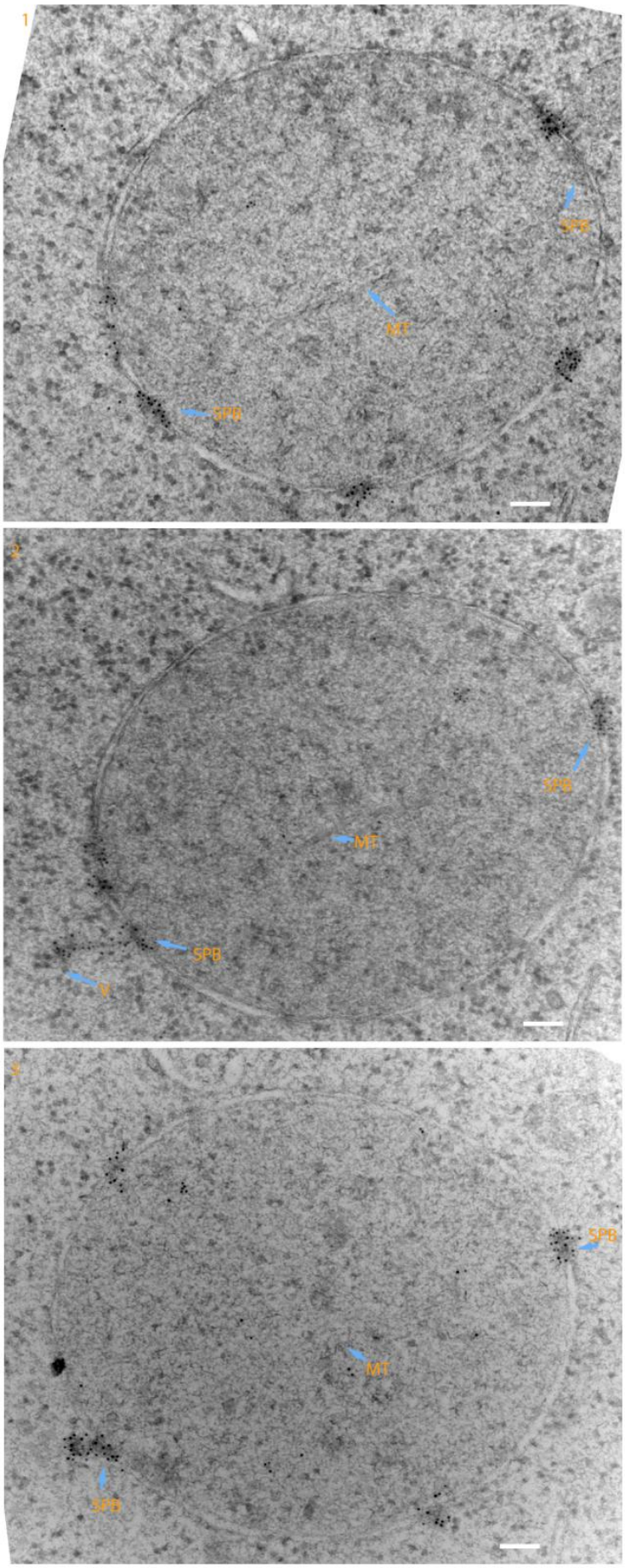

Figure 3.2.8 Nucleus undergoing cell division. Serial sectioned high pressure frozen, freeze substituted yeast. SPB, spindle pole body; MT, microtubule. The MT array can be seen and the SPBs can be seen at either end. Interestingly the interpreted SPBs have GLFG repeats labelled, these can be seen extending towards a vesicle-like structure (V) in section 2. Indicating GLFGs may have roles in cell division. The MTs can be seen from one SPB to the other. Sections ~25nm thick. Scale bar 100nm.

The results of the serial sectioning show that the distribution of GLFG domains appears to vary between individual NPCs. Some individual NPCs have mostly cytoplasmic GLFG labelling, some show mostly nucleoplasmic bias and some no strong bias. This is confirmed by the GLFG labelling bias towards cytoplasmic or nucleoplasmic sides of NPCs often staying the same in all sections through the NPC. The NPCs with labelling on both cytoplasmic and nucleoplasmic sides often stayed the same in all sections through that pore. There is also limited evidence (Figure 3.2.4) that the GLFG labelling could be biased in the plane of the nuclear envelope.

The results also hint at other roles of GLFG domains, for example extending to membrane structures. GLFG domains are present in interpreted SPBs, which also extend to membrane structures. This could be speculated that this tethers the membrane structure to the nucleus and the NPC. Alternately or additionally, GLFG domains of the NPC may be involved in NE growth.

3.3 Observing the effect of import of Kap121 on GLFGs

This experiment was designed to see if the asymmetry in labelling of the GLFG domains in some NPCs was due to a translocation event. A label for protein import route was used on wild type yeast, which had been transformed with Spo12-NLS-GFP, a marker for Kap121 import (Fiserova *et al* 2010; Chaves and Blobel 2001). Kap121 dependant cargo-GFP will be referred to as cargo-NLS. Sections were stained with anti-GFP antibody and anti-GLFG antibody as primaries, then with 10nm gold conjugate antibody for anti GFP and 1.4nm nanogold conjugate on a fab fragment antibody. These were then gold enhanced for 8-12 seconds. Gold enhance (nanoprobes) deposits gold around the gold immune probe increasing its size. This resulted in gold particles of ˜4nm indirectly labelling GLFG repeats and ˜14nm indirectly labelling Kap121. The sections were observed using TEM (Hitachi H7600).

This method can only show snapshots of what is going on and cannot show live translocation events. I have therefore grouped the images based on the distance of the Kap121 dependent import labelling from the central plane and attempted to recreate a time sequence of import translocation using data from many NPCs. Sectioning through pores will not give a full cross section of the NPC due to cutting at various angles (e.g. getting more of the cytoplasmic side of an NPC). Serial sectioning NPCs with labelled cargo could be performed. This could better determine

the distribution of GLFG 3D distribution in relation to individual cargos. It should be noted that like the other TEM indirect labelling experiments, the estimated maximum imprecision of the labelling is ±~15nm. The NPCs high translocation capacity suggests that these observed import events may not be the only translocation event that the NPC is undertaking. This could be tested further using isolated NEs so that NPCs could be controlled to import only one type of cargo. Serial sectioning could then be performed. This would provide a best estimate of the translocation events occurring and may show the FG repeats are changing with respect to the specific translocation event.

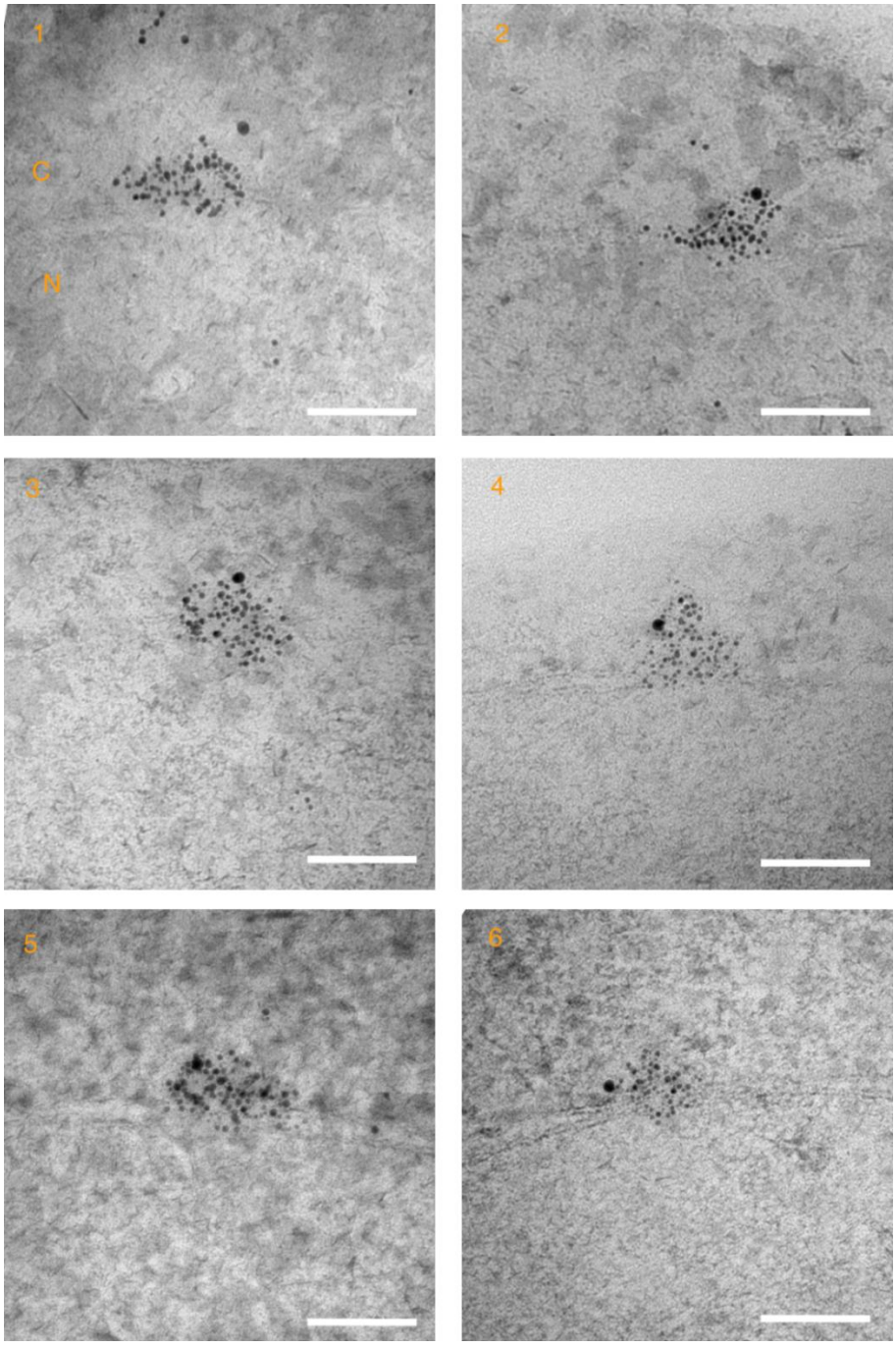

Figure 3.3.1 Start of translocation of Kap121 dependant cargo. High pressure frozen freeze substituted yeast were labelled for GLFG repeats with small gold particles and for Kap121 (Spo12-NLS-GFP) with the larger gold particles. Images are ordered by distance of cargo-NLS labelling from the NPC central plane. These images represent the probable start of translocation with GLFG repeat labelling extending into the cytoplasm, where the Kap121 dependent import labelling isalso present. C, cytoplasm; N, nucleus. Scale bar represents 100nm.

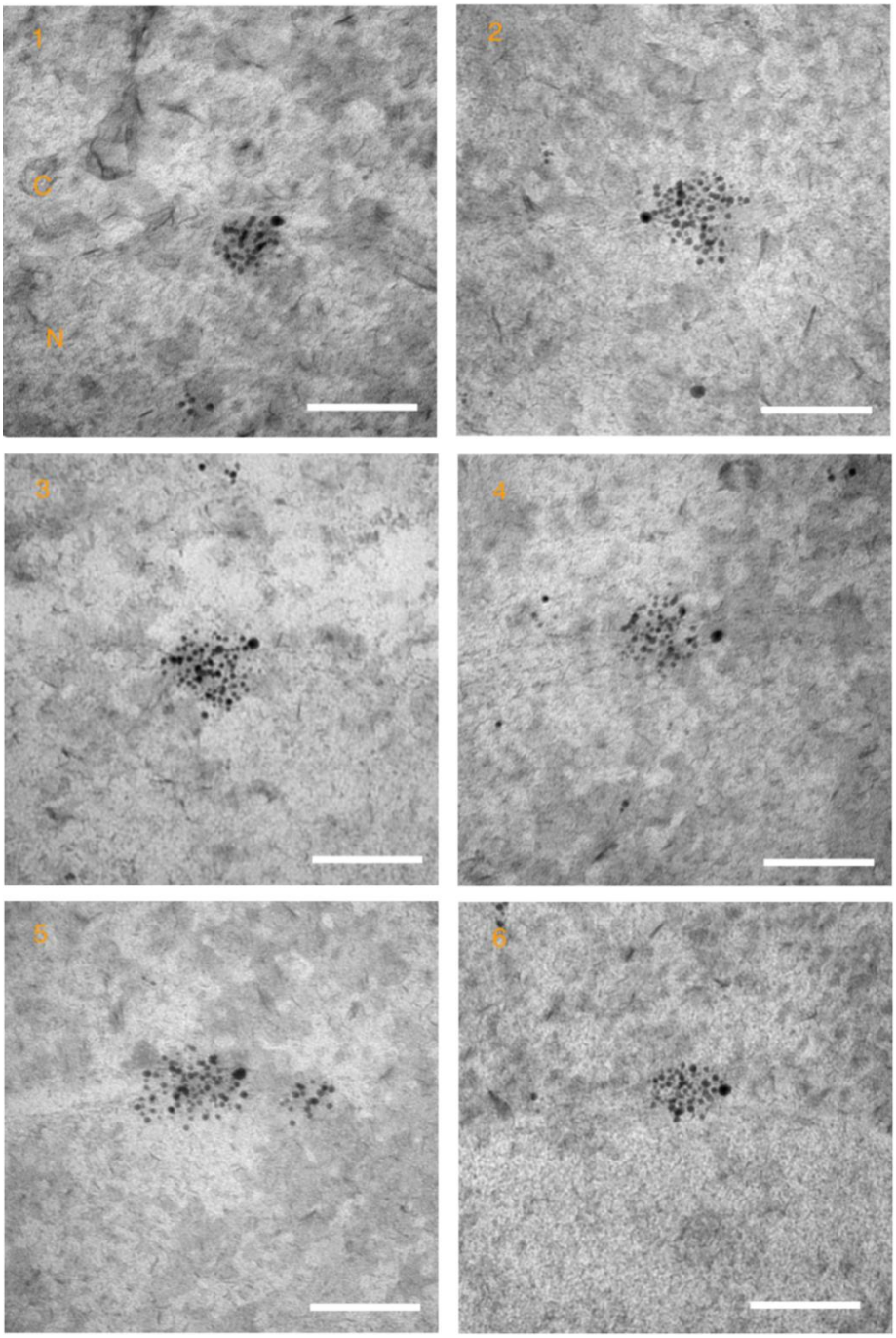

Figure 3.3.2 Mid translocation of Kap121 dependant cargo. High pressure frozen freeze substituted yeast is labelled for GLFG (small gold particles) and for Kap121 (Spo12-NLS-GFP) (larger gold particles). Images are ordered by distance of cargo-NLS labelling from the NPC central plane. Here, the cargo-NLS labelling is at the midplane of the pore. C, cytoplasm; N, nucleus. Scale bar represents 100nm.

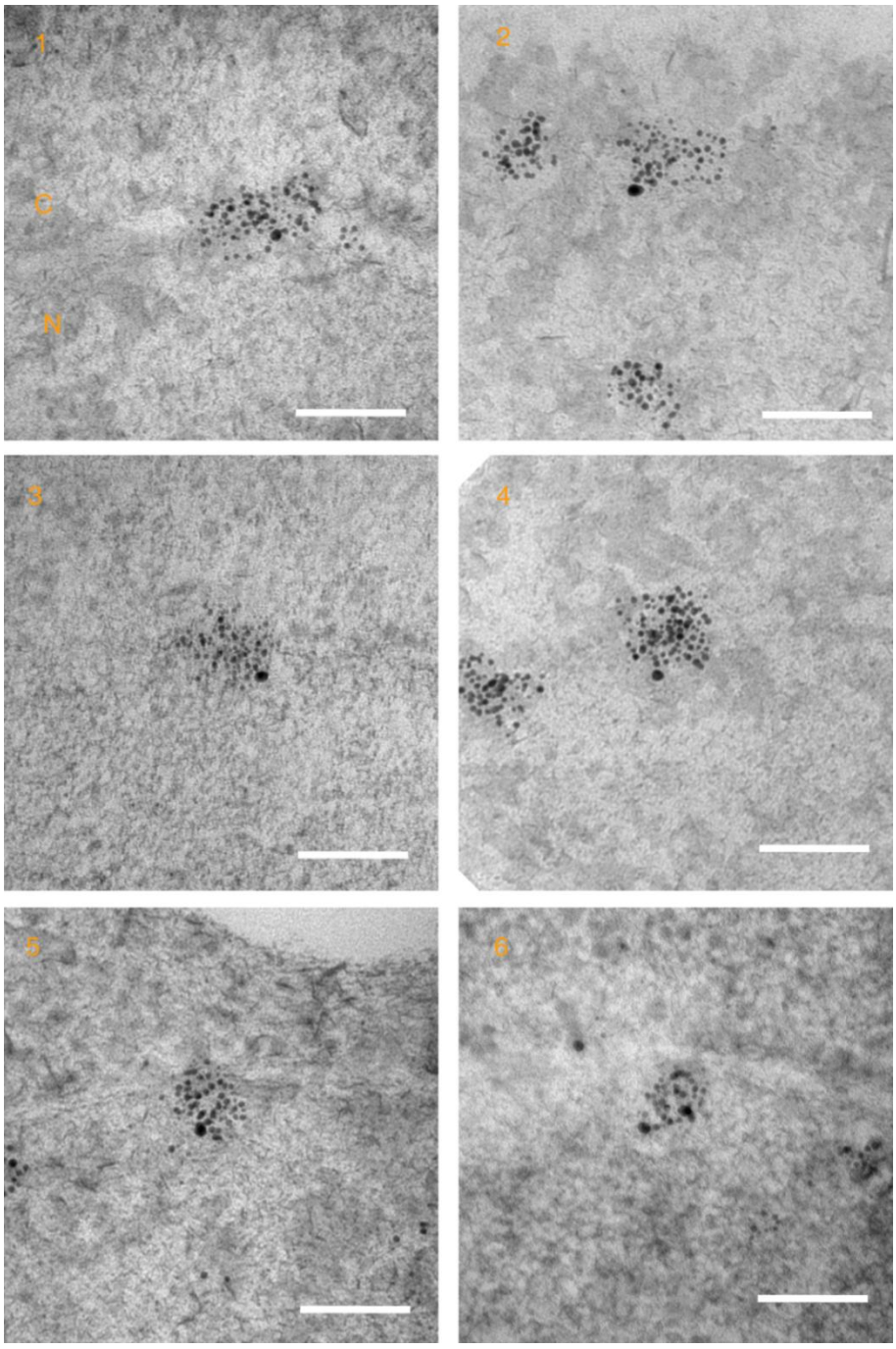

Figure 3.3.3 Late translocation of Kap121 dependant cargo. High pressure frozen freeze substituted yeast is labelled for GLFG (small gold particles) and for Kap121 (Spo12-NLS-GFP) (larger gold particles). Images are ordered by distance of Kap121 dependent import labelling from the NPC central plane. Here, the Kap121 dependent import labelling is inside the nucleus still seemingly associated with the NPC. C, cytoplasm; N, Nucleus. Scale bar represents 100nm.

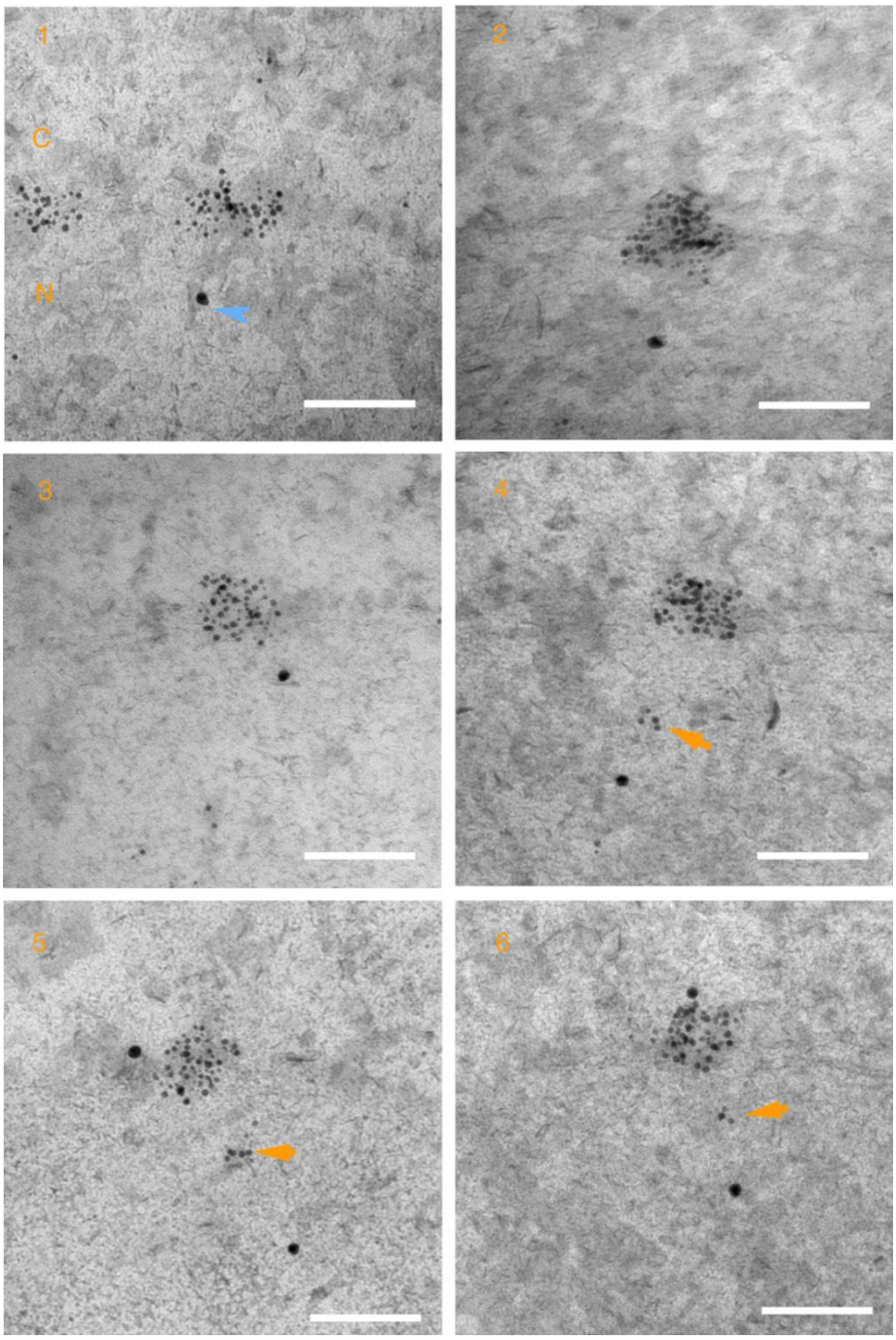

Figure 3.3.4 Translocated Kap121 dependant cargo. High pressure frozen freeze substituted yeast is labelled for GLFG (small gold particles) and for Kap121 (Spo12-NLS-GFP) (larger gold particles). Images are ordered by distance of Kap121 dependent import labelling from the NPC central plane. Here the Kap121 dependent import labelling is well into the nucleus. Note subset of GLFG labelling ~100nm into the nucleus in Images 4, 5 and 6 this is an area that could be the NPC distal basket ring. This labelling is seemingly in line with the Kap121 dependent import labelling and the larger set of GLFG labelling. C, cytoplasm; N, Nucleus. Orange arrow points to subpopulation of GLFG labelling. Blue arrow points to possible channel. Scale bar represents 100nm.

Figures 3.3.1-3.3.4 show Kap121 dependant import cargo-NLS. The main steps in the import are:

i. approach to NPC and its GLFG repeats
ii. movement towards the central plane of the pore (Figure 3.3.1)
iii. cargo-NLS at central plane of NPC (Figure 3.3.2)
iv. movement into the basket region (Figure 3.3.3)
v. disassociation from the NPC returning to its usual state ready for more translocation events (Figure 3.3.4).

Figure 3.3.1 shows early stages of cargo-NLS import, showing the labelling for cargo-NLS as it approaches the NPC and labelling for the NPC's GLFG domains (Figure 3.3.1). Next, the labelling for cargo-NLS can be seen at the edge of the GLFG labelling (Figure 3.3.1, Images 1-4). As the cargo-NLS labelling gets closer to the central plane it is still at the peripheral of the labelling of the GLFG domains (Figure 3.3.1, Images 5 and 6). The GLFG labelling appears to be less extended into the cytoplasm. This may represent a collapse of GLFG domains (Figure 3.3.1, Images 5 and 6). Whilst the labelling for cargo-NLS is on the cytoplasmic side it would appear that labelling for the GLFG repeats is also mostly cytoplasmic.

Figure 3.3.2 shows the cargo-NLS labelling in or close to the central plane of the NPC. The labelling for the GLFG domains looks to be less extended into the cytoplasm compared to pores with the cargo-NLS labelling into the cytoplasm (Figure 3.3.1, Image 1). The labelling for the GLFGs appears to be closer to the central plane in Figure 3.3.2, Images 5 and 6. This could represent the completion of the collapse of Nup116 towards its C-terminal anchor which is reported at the central plane (J. Fiserova personal communication). Some GLFG labelling appears to be extending into the nucleus (Figure 3.3.2, Images 1-3), ahead of the cargo-NLS labelling. This increase in nuclear GLFG labelling could represent extension of GLFG domains into the nucleus. The extension of GLFG repeats may be caused by the transfer of the cargo-NLS off the GLFG Nup, possibly to Nup53 which possesses a Kap121 binding domain (Marelli *et al* 1998). This is suggested as Kap-β1 has been shown to collapse the FG-domain of Nup153 in *Xenopus* (Lim *et al* 2007), and its disassociation of Kap-β1 by RanGTP allows re-extension of the FG domain of Nup153 in *Xenopus* (Lim *et al* 2007). It is not always the case that only GLFG domains are seen to 'collapse' (Figure 3.3.2, Image 4). Here cargo is at the midplane and there is quite a lot of cytoplasmic GLFG labelling. Possible explanations for this include inaccuracy of labelling or the NPC having a high translocation capacity. In the second case the translocation events may not all be viewed due to

there only being one section through the NPC and only labelling for one cargo. The cargo-NLS labelling is also often at the edge of the pore as observed previously in Fiserova *et al* (2010).

Figure 3.3.3 attempts to show the later events of translocation moving from the central plane to the inner basket region. The GLFG domains are less extended into the cytoplasm and extend into the nucleoplasm (Figures 3.3.3, Images 2, 5 and 6). Some NPCs have GLFG labelling on both nucleoplasmic and cytoplasmic sides (Figure 3.3.3, Image 3), however all have some level of nucleoplasmic labelling of GLFG domains. This cannot be said for the NPCs where the cargo-NLS labelling is cytoplasmic (Figure 3.3.5, Image 1). This nuclear GLFG labelling may show the pore setting up for an export event to recycle Kap121.

Figure 3.3.4 tries to show the disassociation from the NPC and labelling for cargo-NLS moving into the nucleus. The cargo-NLS labelling can be seen going it the nucleus in Figure 3.3.4. Labelling for cargo-NLS can be seen in what appear to be channels (blue arrow in Figure 3.3.4, Image 1) going into the nucleus. In Figures 3.3.4, Images 4, 5 and 6, there is some GLFG labelling between the main body of GLFGs in the NPC and the cargo shown by orange arrows. The area of labelling corresponds to the area of the nuclear basket. There is also SEM evidence for the nuclear basket to be GLFG labelled shown in Section 3.4. Figures 3.3.4, Images 5 and 6, have labelling for cargo-NLS at the cytoplasmic side and Figure 3.3.4, Image 6, is very similar to Figure 3.3.1. The NPCs in Figure 3.3.4 are less nucleoplasmic in labelling for GLFGs than in Figure 3.3.3. This could be due to export of Kap121 recycling it to the cytoplasm. The recycling method could be that GLFG domains are collapsing back to the midplane where the protein is anchored. It may then disassociate from Kap121, allowing extension back to cytoplasmic. After this recycling event the NPC's GLFG domains would again be cytoplasmic, as they were before the import event.

To quantify these initial results the position of the cargo-NLS was used to categorise the NPCs. An NPC was only used when the cargo was seemingly interacting with the NPC. The NPCs were put into the following categories:

- Cargo cytoplasmic; the cargo-NLS is ~60nm to the NPCs central plane on the cytoplasmic side (examples in Figure 3.3.1).
- Cargo at midplane; when the cargo-NLS is at the plane of the NE within the pore (examples in Figure 3.3.2).
- Cargo Nuclear; the cargo-NLS is ~60 nm to the central plane on the nucleoplasmic side (examples in Figure 3.3.3).

The NPC scored GLFG distribution was determined as in Section 3.1.

GLFG distribution	Cargo cytoplasmic	Cargo at midplane	Cargo nuclear	WT
mostly cytoplasmic (%)	73.333	30.000	13.333	55.300
both (%)	26.667	35.000	53.333	36.800
mostly nucleoplasmic (%)	0.000	35.000	33.333	7.900
sample number	15	20	15	152

Table 3.3.1 NPC scored GLFG distribution at different stages of Spo12-NLS-GFP import (a marker of Kap121 dependant import). This shows a shift from NPCs scored as mostly cytoplasmically GLFG labelled when cargo is cytoplasmic, both sided and mostly nucleoplasmic scored GLFG labelling when cargo at the midplane and more nuclear. WT has also been included to show the steady state GLFG distributions for comparison.

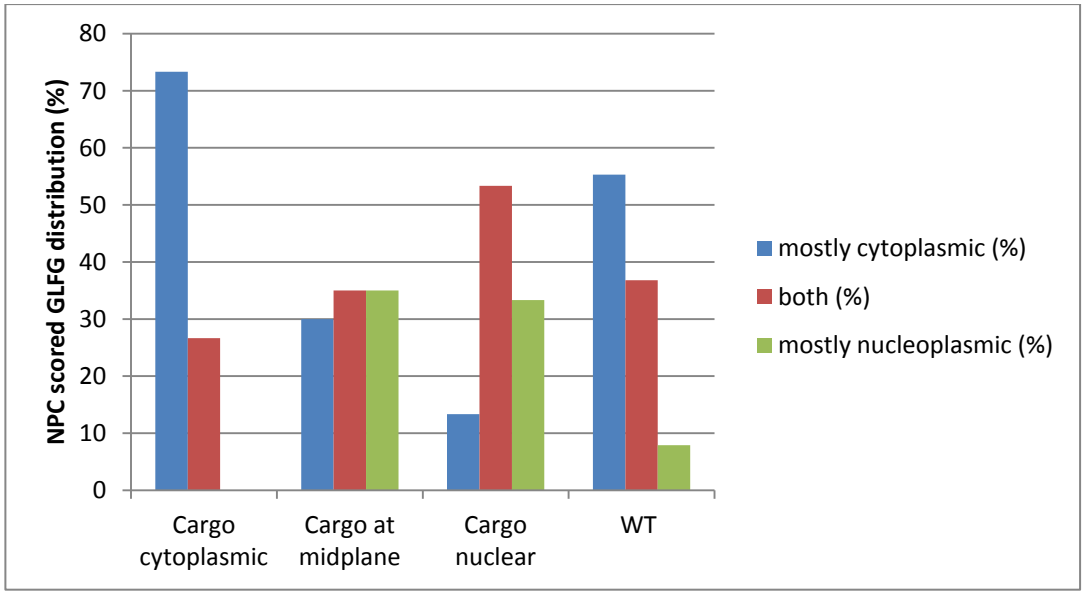

Chart 3.3.1 NPC scored GLFG distribution at different stages of Spo12-NLS-GFP a marker of Kap121 dependant import. This shows a shift in the scored GLFG distribution of NPCs from cytoplasmic to more both sided and nucleoplasmic as Kap 121 dependant import occurs. WT is included for comparison to a more steady state GLFG distribution.

These preliminary results (Chart 3.3.1) indicate that NPCs with a mostly cytoplasmic GLFG is the category with the largest proportion of pores (73%). These associate with the cytoplasmic Kap121 dependant cargo-NLS. When the cargo-NLS is at the midplane there are NPCs of all GLFG domain distributions. NPCs with cargo-NLS at the midplane can be compared to WT. This comparison

shows the percentage of nuclear labelled GLFG NPCs has increased from <10% in WT to 35% in NPCs with cargo at the midplane. This shows an increase in nuclear labelling when cargo-NLS is at the midplane. For NPCs with nuclear cargo, the NPC's GLFG domains are either mostly both sided (53%) or mostly nuclear (33%), with low amounts of mostly cytoplasmically labelled NPCs.

GFP is a small protein which can diffuse through the NPC without the aid of karyopherins and can therefore be used as a marker for the route of diffusion. The labelling for the GFP is ~8nm gold particles and the GLFGs are labelled with ~3nm gold particles. As the GFP is near the midplane there is no clear change in the GLFG distribution. Figures 3.3.5 Images 6, 7 and 9 have mostly cytoplasmic labelling. There did not appear to be a trend with how far the GFP was from the mid plane of the pore. The GFP labelling is seen to be in some cases in the middle of GLFG labelling Figures 3.3.5, Images 2, 4, 5, 7-12.

By comparing movement through the NPC of unconjugated GFP and Kap121 dependant cargo-GFP some differences can be observed. Kap121 dependant cargo-GFP labelling was most often found to be at the periphery of the GLFG labelling (as previously observed in Fiserova *et al* (2010)). This peripheral location could be due to the GLFG Nup collapsing towards its anchor, taking the NLS-cargo with it. Unconjugated GFP labelling was both at the edge of the GLFG labelling, and in the midst of the GLFG labelling. Kap121 dependant cargo-GFP labelling appeared to have an effect on the GLFG labelling localisation, based on its distance from the midplane/stage of translocation. The changes in GLFG localisation seen in Kap121 dependant cargo-GFP were not observed in unconjugated GFP labelling. This could suggest an interaction between GLFGs and Kap121.

Some possible improvements are:

- Further repetitions to increase the number of results available for analysis
- Sometimes NPCs were difficult to categorise, so there may be some subjective evidence, this could be improved by mapping the individual GLFG labels in pores categorised based on the cargo-NLS location.
- Serial sectioning of individual NPCs GLFG and cargo labelled; this may show any changes in GLFG repeat distribution in relation to a cargo NLS more clearly.
- Label for different cargo-NLSs to see if the distributions of GLFG domains (or other FG domains of other Nups if labelled for) change during import of different cargos.

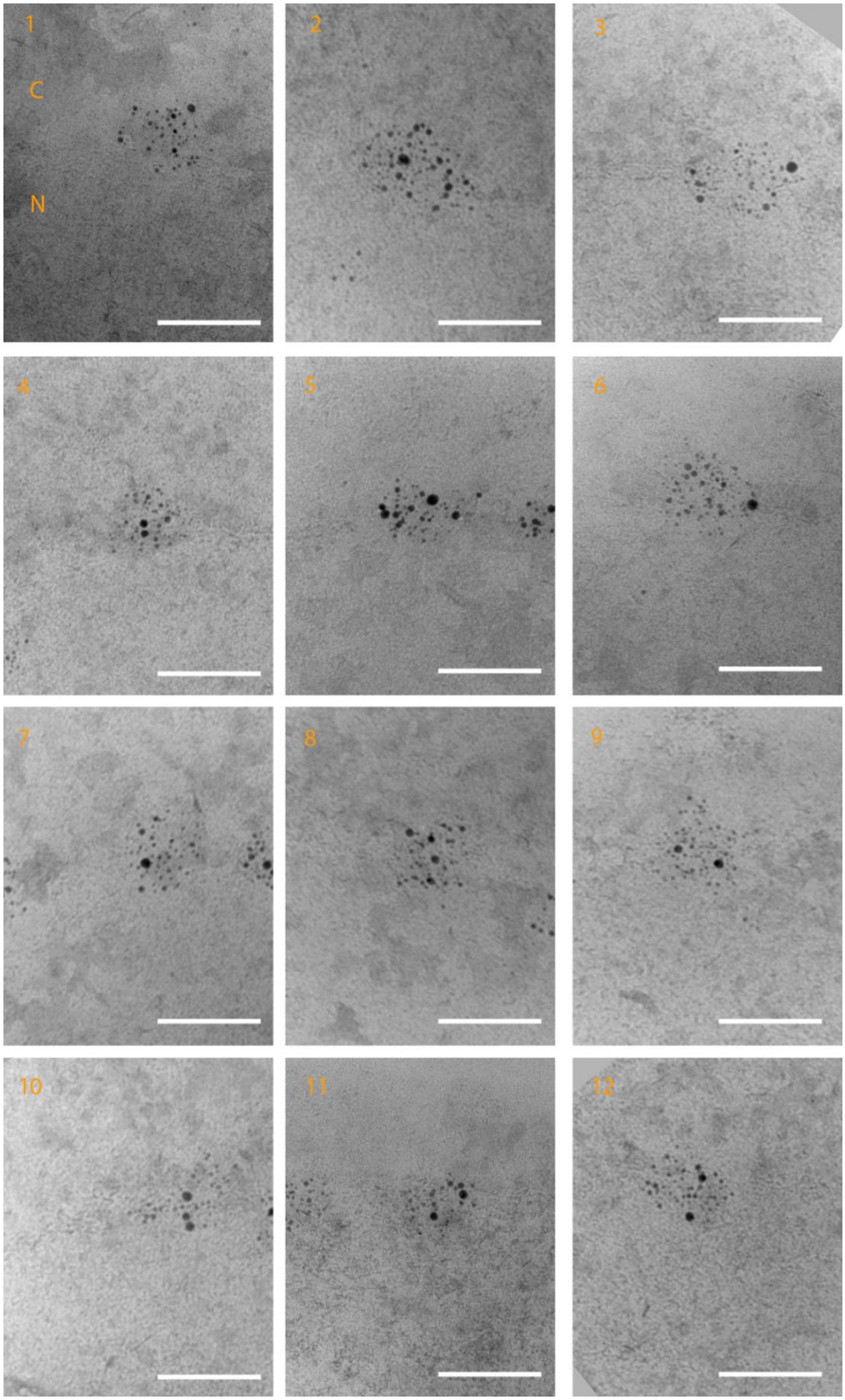

Figure 3.3.5 Diffusion of unconjugated GFP. High pressure frozen freeze substituted yeast labelled for GLFG (small gold particles) and for unconjugated GFP (larger gold particles). Images are ordered by distance of unconjugated GFP labelling from the NPC central plane. Note the GFP is often seen amongst the GLFG labelling. C, cytoplasm; N, Nucleus. Scale bar represents 100nm.

3.4 GLFG domains may be located to NPC associated filament structures

The aim of this work was to acquire structural information about the yeast NPC. There is currently limited information regarding the position of the GLFG repeat domains and it has been suggested that the GLFG Nup116 may be located to the cytoplasmic filaments (Kiseleva *et al* 2004). Scanning electron microscopy was used as this gives an image of the surface of the nuclei. In order for the electron beam to scan over the nuclei surface it must not be occluded by other cellular components. To ensure this was the case, nuclei were extracted from yeast cells by enzymatically digesting the cell wall, then osmotically lysing the cell. Selected samples were immunogold labelled for GLFG repeats, and then all were prepared for SEM observation by fixing, critical point drying and chromium coating. Using SEM, the extracted components of the yeast cell can then be viewed and intact nuclei can be seen (Figure 3.4.1). In Figures 3.4.2-3.4.9 WT samples were also indirectly 5nm gold labelled for GLFG repeats. This was to see what structures GLFG repeats of Nups form. This was done to try and help understand models of nuclear transport as they vary on the structural properties of the FG domains. Some models predict the FG domains interacting with each other, forming a hydrogel (Frey 2006; 2007; 2009), whereas other evidence suggests FG Nups act as polymer brushes (Lim *et al* 2007). With these results it should be remembered that extracting a nuclei from the cell into a buffer may have structural effects on the NPC. Also, the relatively long fixation times may not catch the NPCs in their most native conformation. Due to the relatively low numbers of NPCs observed it was not appropriate to undertake statistical analysis.

The extracted yeast nuclei were in varying states, with some better preserved than others. Figure 3.4.1 shows extracted nuclei from a temperature sensitive Prp20 deletion mutant SWY3733 at permissive temperature, the results obtained should be the same as for WT. The nucleus has many structures which are interpreted to be ribosomes, vesicles, endoplasmic reticulum (ER) and NPCs. Some of the false colouring was aided by images with higher magnification from this nucleus as in Figure 3.4.11. One observation is that the ER edge appears to be thicker than the rest of the ER and there are often flattened vesicle structures (in yellow) on the edge of the ER. There are many vesicle-like structures coloured purple in Figure 3.4.1. These vesicle-like structures are still attached to the nucleus after lysing the cell. This indicates the possibility that they are attached to the nucleus in some way.

GLFG labelling on the cytoplasmic face of the nucleus

The GLFG labelled WT nuclei show that the labelling of GLFG domains appears to be high on filaments of NPCs, shown by Figures 3.4.2, 3.4.4, 3.4.5, 3.4.6 and 3.4.7. The filaments on the NPC in Figure 3.4.2 emanate from what looks to be the top of the cytoplasmic ring, therefore they are likely to be cytoplasmic filaments. They appear to be highly labelled for GLFGs. The NPC associated filaments are not always observed to be GLFG labelled (Figure 3.4.3). Some suggestions for this could be:

(i) the NPC is still forming and the GLFG Nups yet present.
(ii) the labelling is not always consistent, possibly due to damage in lysing the yeast cell.
(iii) misinterpretation of NPCs .
(iv) transient association of GLFGs with or into cytoplasmic filaments.
(v) GLFG repeats are lost from the cytoplasmic side as occasionally observed in TEM (possibly during translocation).

The GLFG labelling sometimes appears to coincide with the internal filaments (IF, Figure 3.4.4). These internal filaments would appear to be continuous with the cytoplasmic ring (CR, Figure 3.4.4). Figure 3.4.4 also has what appear to be cytoplasmic filaments. These appear to be on top of the cytoplasmic ring. The cytoplasmic filaments are not extending over the NPC, allowing internal filaments to be seen. The NPCs can be identified by the clusters of GLFG labelling (Figures 3.4.5 and 3.4.6). A further example of GLFG labelling the cytoplasmic filaments is the false coloured pore in Figure 3.4.6. Possible internal filaments are seen in Figure 3.4.7, these do not appear to be cytoplasmic filaments as they do not emanate from the top of the cytoplasmic ring. They appear to be continuous with the cytoplasmic ring or possibly attached under the cytoplasmic ring. The possible internal filaments are GLFG labelled. They meet in the centre of the NPC and appear to join (T). This joining of GFLG repeats in the centre of the NPC could be the transporter. The false coloured pore in Figure 3.4.7 has GLFG labelling surrounding it; this could be damaged cytoplasmic filaments.

Cytoplasmic and internal filaments appear to be labelled for GLFG repeats; filament labelling is shown by Figures 3.4.2, 3.4.4, 3.4.5, 3.4.6 and 3.4.7.

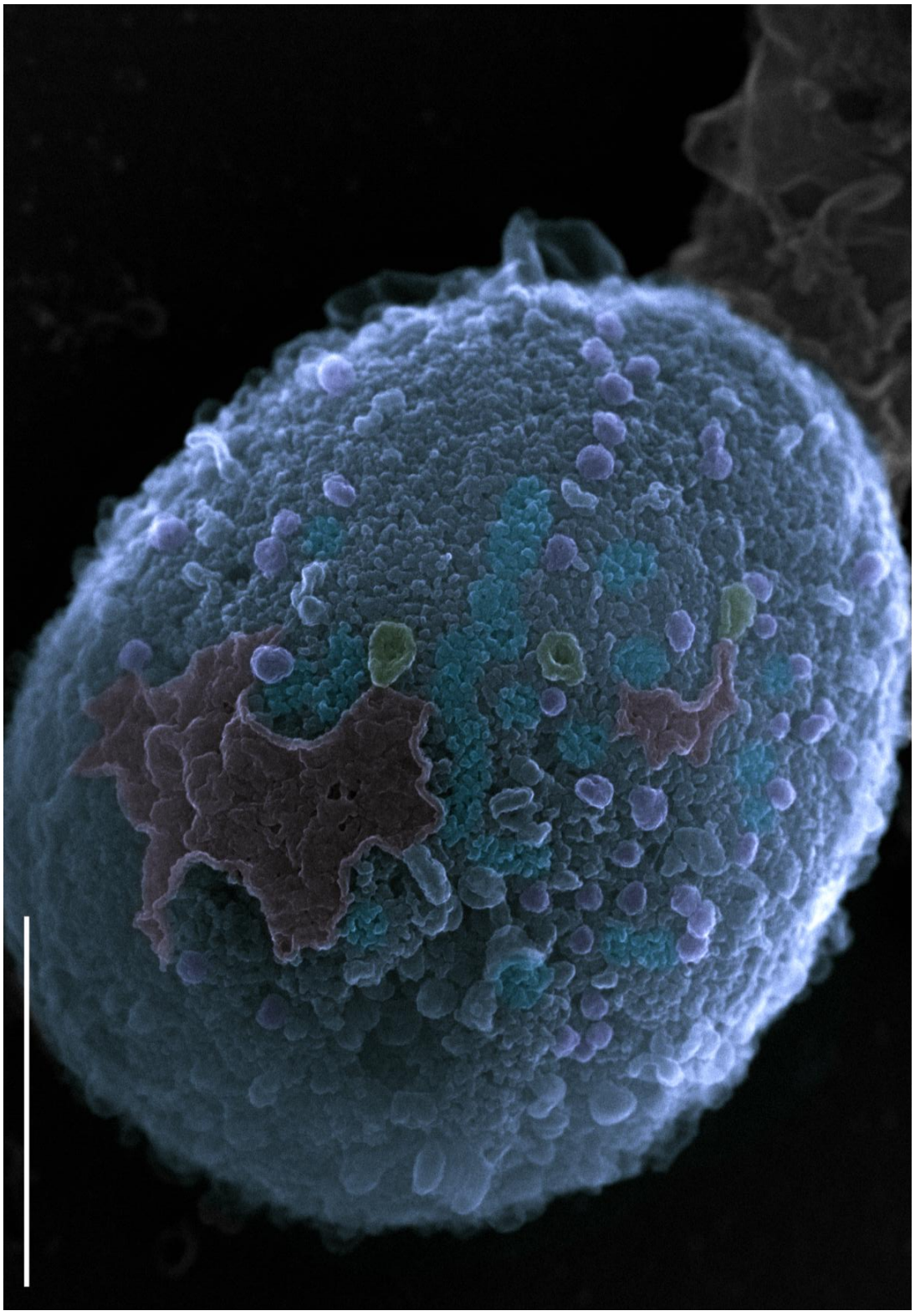

Figure 3.4.1 SEM image of yeast nucleus from enzymatically and osmotically lysed yeast cell. This image has been false coloured based on the structures believed to be present. Red, endoplasmic reticulum; yellow, flattened vesicle; purple, vesicles; blue, selected nuclear pore complexes. From a 3733 yeast cell grown at 24°C. Image taken at 40000X magnification with 30kV, scale bar 1µm.

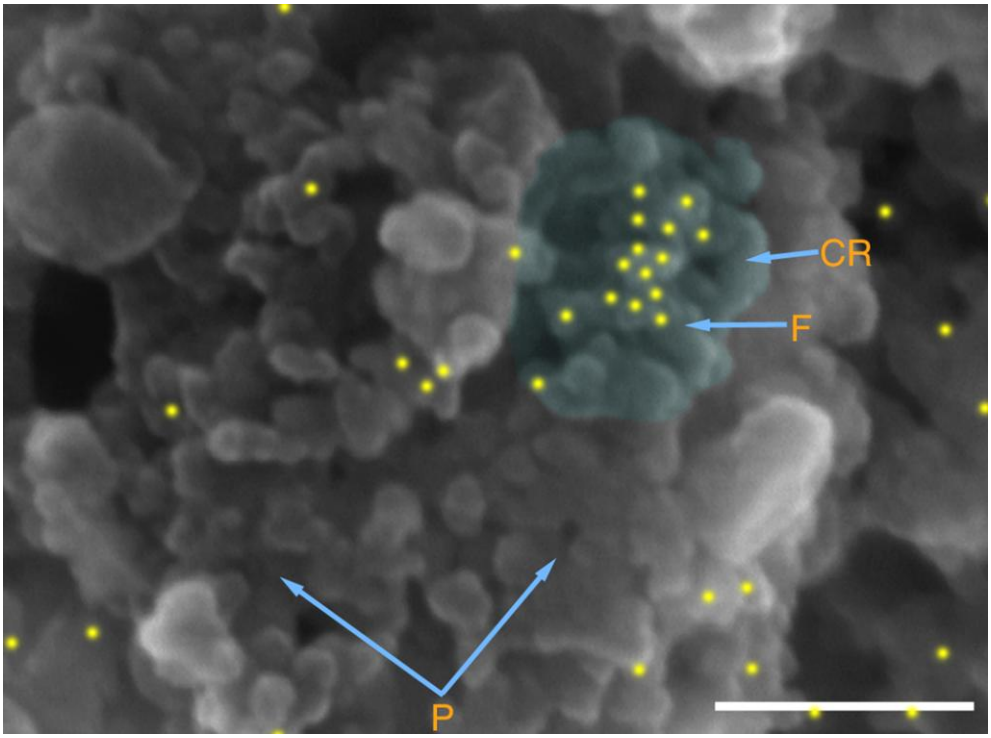

Figure 3.4.2 WT NPC with high level of filament labelling. Yeast nuclei from enzymatic osmotically lysed yeast. GLFG 5nm gold labelling (yellow). A structure that has been interpreted as the NPC has been coloured blue. The image has been adjusted through histogram for contrast and median filter of 1 pixel for noise reduction. CR, cytoplasmic ring; F, filament from top of CR therefore likely a cytoplasmic filament; P, potentially other NPCs. Image take at 300000X magnification with 10kV. Scale bar represents 100nm.

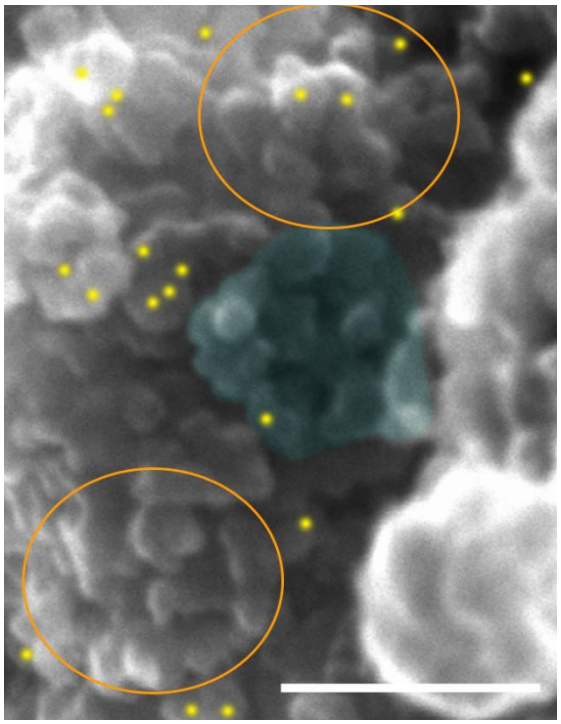

Figure 3.4.3 WT NPC with low level of GLFG labelling. Yeast nuclei from enzymatic osmotically lysed cells. Indirect GLFG 5nm gold labelling (yellow). The area interpreted as a NPC has been false coloured blue. Potential NPCs are circled in orange, these also have low levels of labelling. The image has been adjusted through histogram for contrast and median filter of 1 pixel for noise reduction. Image taken at 300000X magnification with 10kV. Scale bar represents 100nm.

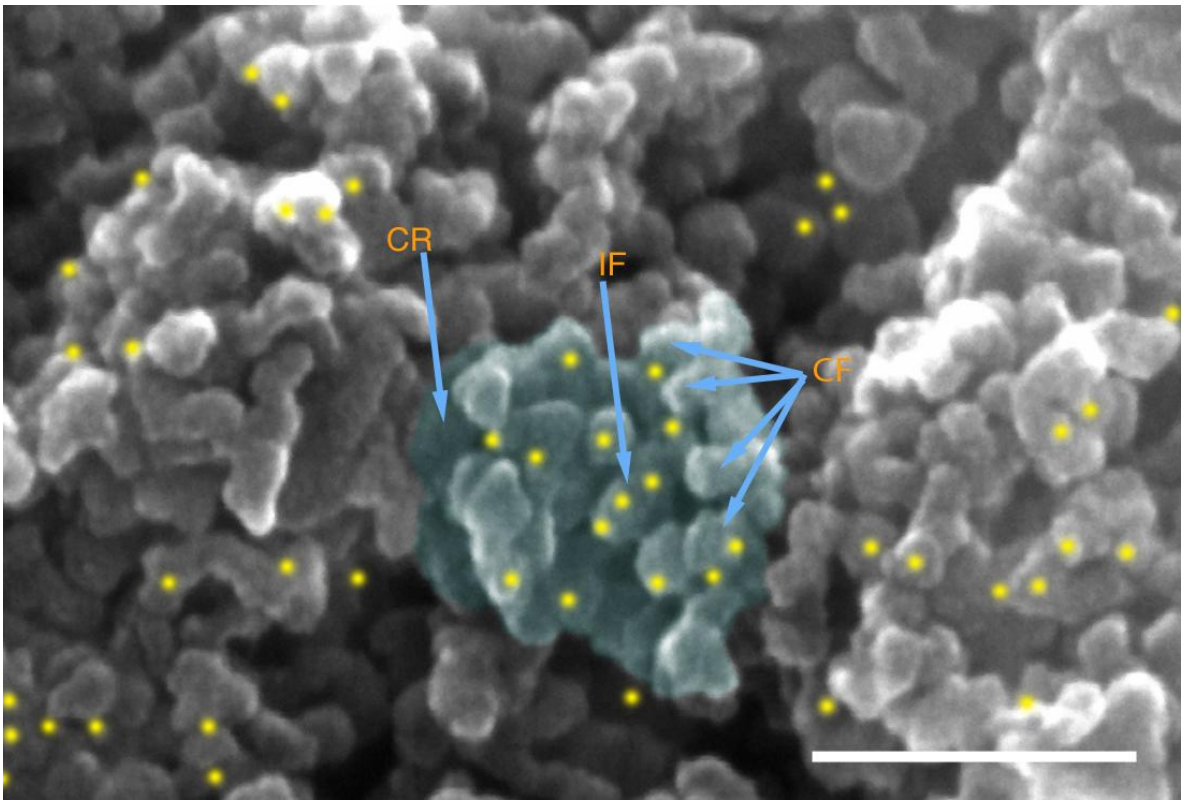

Figure 3.4.4 WT GLFG labelled NPC with seemingly different filaments. Yeast nuclei surface from enzymatic osmotically lysed yeast labelled for GLFG repeats. **T**he NPC is false coloured blue. There are seemingly at least two sets of filaments. Some filaments come from the top of the cytoplasmic ring and inner cytoplasmic ring periphery, in this example these are cytoplasmic filaments. Some internal filaments are seen to be labelled for GLFG repeats multiple times along a single filament. CR, cytoplasmic ring; CF, cytoplasmic filament. Image taken at 300000X magnification with 10kV. Scale bar represents 100nm.

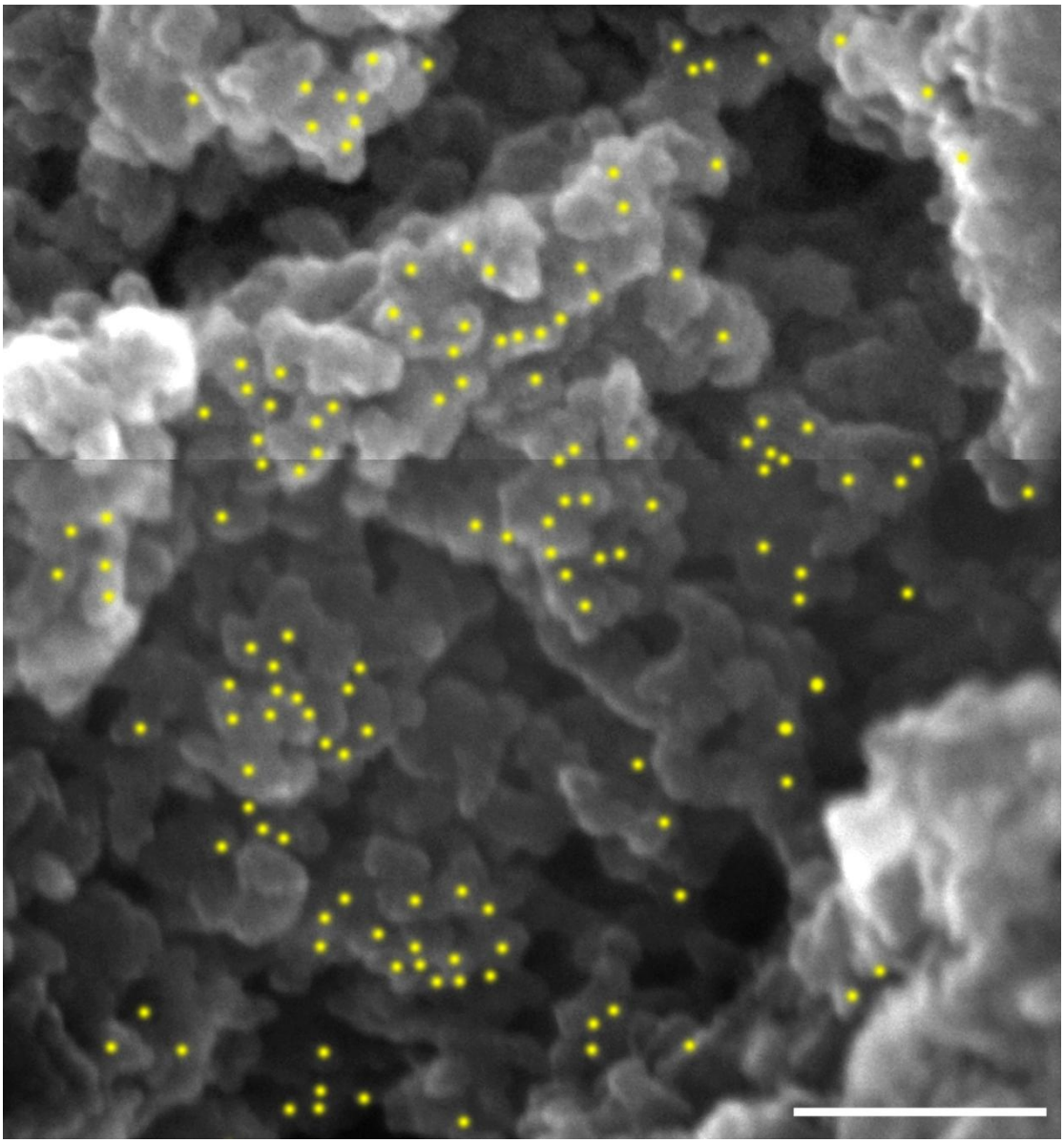

Figure 3.4.5 GLFG labelling quite specific to NPC-like structures. NPCs have not been false coloured or encircled to allow the reader to interpret NPCs. WT yeast nuclei surface from enzymatic osmotically lysed yeast labelled for GLFG repeats. This nuclei surface seems more damaged and flattened than in other figures (e.g. Figure 3.4.4), therefore NPC structures are not as clear. Image taken at 10kV, 300000X magnification scale bar 100nm.

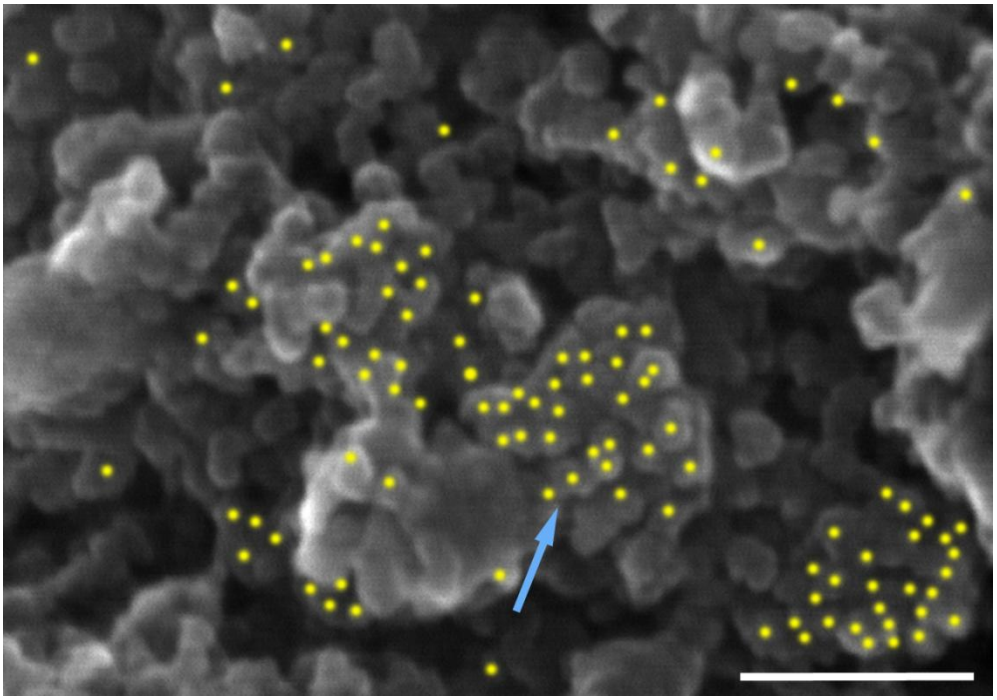

Figure 3.4.6 WT NPCs with GLFG repeats labelled which localizes often to filaments. Yeast nuclei surface from enzymatic osmotically lysed yeast labelled for GLFG repeats. NPC filaments appear to be highly labelled. Blue arrow points to a highly GLFG labelled possible cytoplasmic filament labelled. Scale bar represents 100nm. Image taken at 300000X magnification at 10kV.

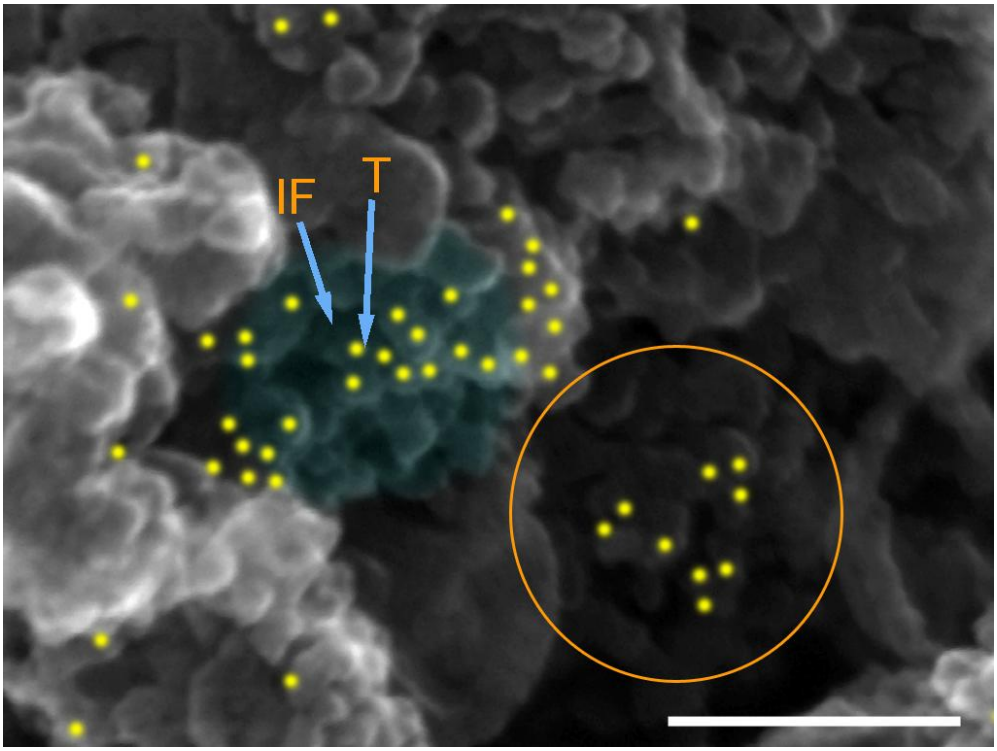

Figure 3.4.7 Internal filaments joining at the NPC centre labelled for GLFG repeats. Yeast nuclei surface from enzymatic osmotically lysed yeast labelled for GLFG repeats. False coloured in blue is an NPC. This NPC has labelling to the sides of the NPC and also on the filaments extending towards the centre of the NPC. Circled in orange is potentially another NPC. IF, internal filaments; T, possible transporter structure. Scale bar represents 100nm. Image taken at 300000X magnification with 20kV.

GLFG labelling on the inner nuclear face

The inner nuclear face could be seen when the nucleus fractured fortuitously, with part being left on the chip. It was often difficult to determine if the remaining material was from the nucleus. However, if NPC structures like in Figure 3.4.8 (encircled in orange) could be seen then it was likely to be the inner NE face. In Figure 3.4.8 (box 1) the top arrow points to filaments which appear to run at 90 degrees to each other. The lower arrow in box 1 shows more weave-like filaments. Box 3 (Figure 3.4.8) also has filaments possibly resembling a lamina-like structure. These filaments appear to be in a similar plane to the NPCs. These filaments could therefore be a putative lamina.

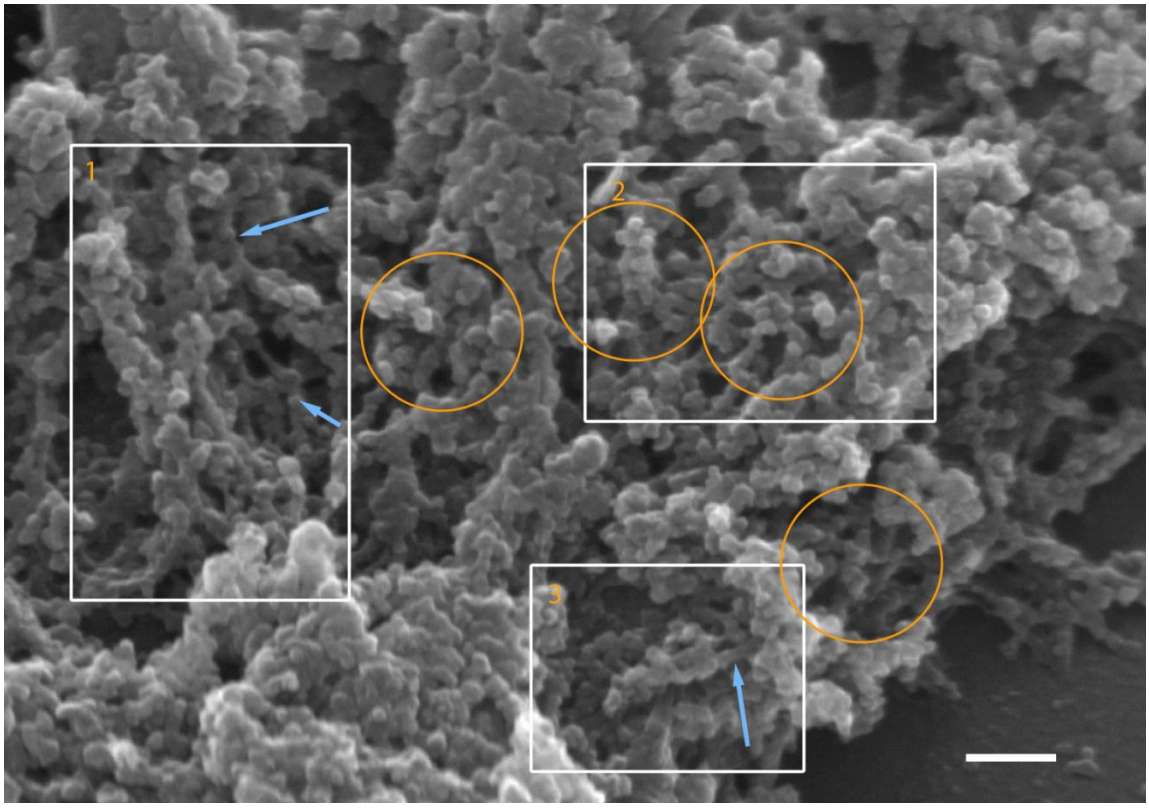

Figure 3.4.8 Burst yeast nuclei; showing inner nuclear membrane face of the nucleus. Structures resembling NPCs are circled in orange. Arrows point in box 1 and 3 to filaments can be seen which resemble a lamin type structure. Box 2 is shown to a higher magnification in Figure 3.4.9. Image taken using 10kv. Scale bar 100nm.

Figure 3.4.9 is box 2 from Figure 3.4.8, but with a higher magnification and a backscattered image merged to show GLFG labelling. In Figure 3.4.9 the NPCs appear to have filaments which join together, possibly at a basket. The basket filaments and the distal basket ring are labelled by arrows. The NPC on the left in Figure 3.4.9 looks like there may be cargo translocating as there is

material (labelled Cg) on top of the distal ring. The basket filaments, which emanate from the nucleoplasmic ring and join at the distal basket of the NPC, have GLFG labelling. GLFG labelling on the filaments would appear to be higher in the NPC with possible cargo in translocation. The structure interpreted to be a distal basket is also labelled for GLFG domains in both of the NPCs highlighted in Figure 3.4.9. The basket on the right has the distal basket labelled, however the filaments are not highly labelled. This distal basket GLFG labelling correlates to TEM labelling studies (Figure 3.4.10). TEM of GLFG labelled NPCs show there is GLFG labelling in an area corresponding to the distal basket ring of the NPC. Interestingly, the anchorage point the GLFG Nups is likely to be near the midplane. The GLFG Nup116 anchor has been shown to be at the midplane (Fiserova unpublished data). Therefore this sub population of GLFG labelling away from the midplane may indicate that there is indeed a relaxed or extended coil domain lacking GLFG repeats and the collapsed cohesive GLFG containing coil at the end of the GLFG Nup, as suggested in Yamada *et al* (2010) (in this case at the distal basket ring). The GLFG labelling of the basket filaments and distal basket ring may be translocation state dependant as suggested by results from Section 3.3.

In Figure 3.4.9 filaments look like they are connecting the NPC with the inner face of the NE (at C). These filaments resemble the lamin fibres connecting to the NPC revealed by detergent extraction in *Xenopus* in Figure 4 in Goldberg and Allen (1996). In vertebrates the lamina has a structural role in the nucleus.

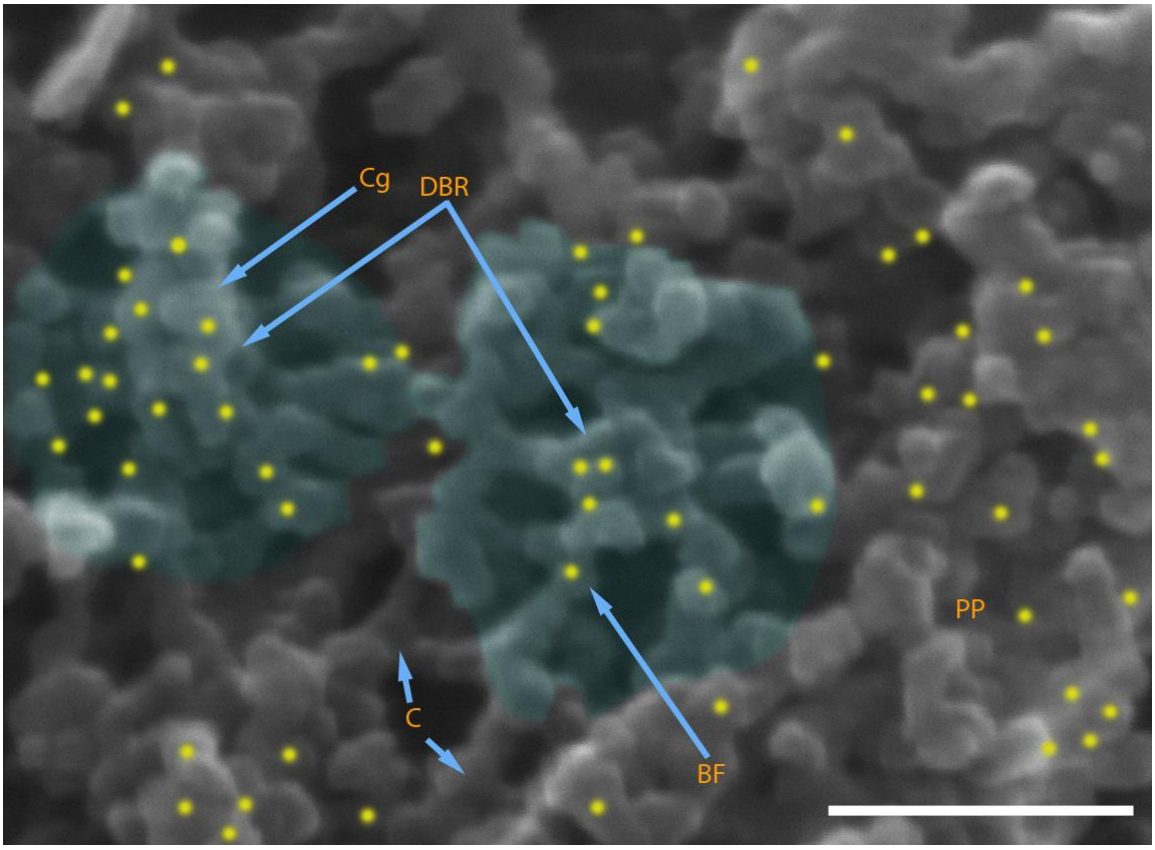

Figure 3.4.9 Nuclear basket filaments GLFG labelled, with connections to possible structural elements of the nucleus from the NPC. From enzymatic osmotically lysed yeast. Sample was indirectly GLFG 5nm gold labelled (yellow). The NPC on the furthest left appears to have something bound, possibly a cargo (Cg). C represents possible connections of the NPC with the inner face of the NE. The basket filaments (BF) can be seen converging at a structure which I suspect is the distal basket ring (DBR). PP labels a potential NPC. Image captured at 300000X magnification with 10 KV. Scale 100nm.

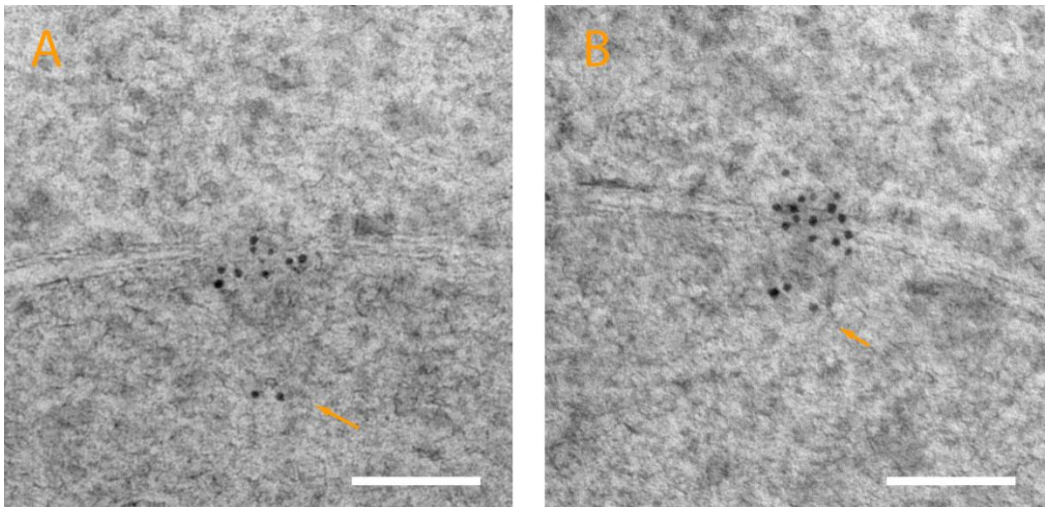

Figure 3.4.10 Subpopulation of GLFGs labelled in an area that could be the nuclear basket. Both (A) and (B) are oriented with cytoplasm at top and nucleoplasm at bottom. In (A) the subpopulation of GLFG labelling (arrowed) is further from the midplane to that of (B). Note that there is no GLFG labelling between the two areas of labelling. Scale bar 100nm.

Structural differences between the Prp20 mutant at 24˚C and 37˚C

The results of WT NPCs were compared with observed temperature sensitive Prp20 mutants. Prp20 mutants at the non-permissive temperature were defective in the nucleotide exchange activity of the RanGEF, Prp20. As a result RanGDP is not converted to RanGTP, causing a deficiency of the active RanGTP molecular switch. Deficiency of RanGTP should lower the rate of cargo disassociation leaving the NPC potentially stuck late translocation. The aim of this experiment was to see if there were any differences in NPC structure of the 37°C Prp20 mutant, using the 24˚C Prp20 mutant and WT as controls. The yeast cultures used were WT and temperature sensitive SWY3733. The mutation phenotype is present at the non-permissive temperature (37°C), and not present at the permissive temperature (24°C).

Red arrows in Figure 3.4.11 are possible internal filaments. In the 37 °C Prp20 mutant internal filaments can be observed as in Figure 3.4.12. They appear to be short, similar to those noted in Figure 3.4.11. The internal filaments can also be seen in Figure 3.4.13, these internal filaments are thinner than in Figure 3.4.12. It may be that they are stretching and possibly forming part of the transporter structure, thus making them thinner. The internal filaments can also be seen to be disordered like in Figure 3.4.13 (right NPC IF) and in Figure 3.4.14 (IF). This could be due to the sample preparation process, however Figures 3.4.13 and 3.4.14 are from the same nucleus, so a similar level of sample preservation could be expected. Internal filaments in the Prp20 mutant at non-permissive temperature (37°C) can be more easily seen than for WT and Prp20 mutant at permissive temperature (24°). This is because the thicker filaments, which usually cover the NPC do not allow us to see inside the NPC. This could mean that the mutation in Prp20 leading to the lack of regeneration of RanGTP is affecting cytoplasmic filament extension over the NPC.

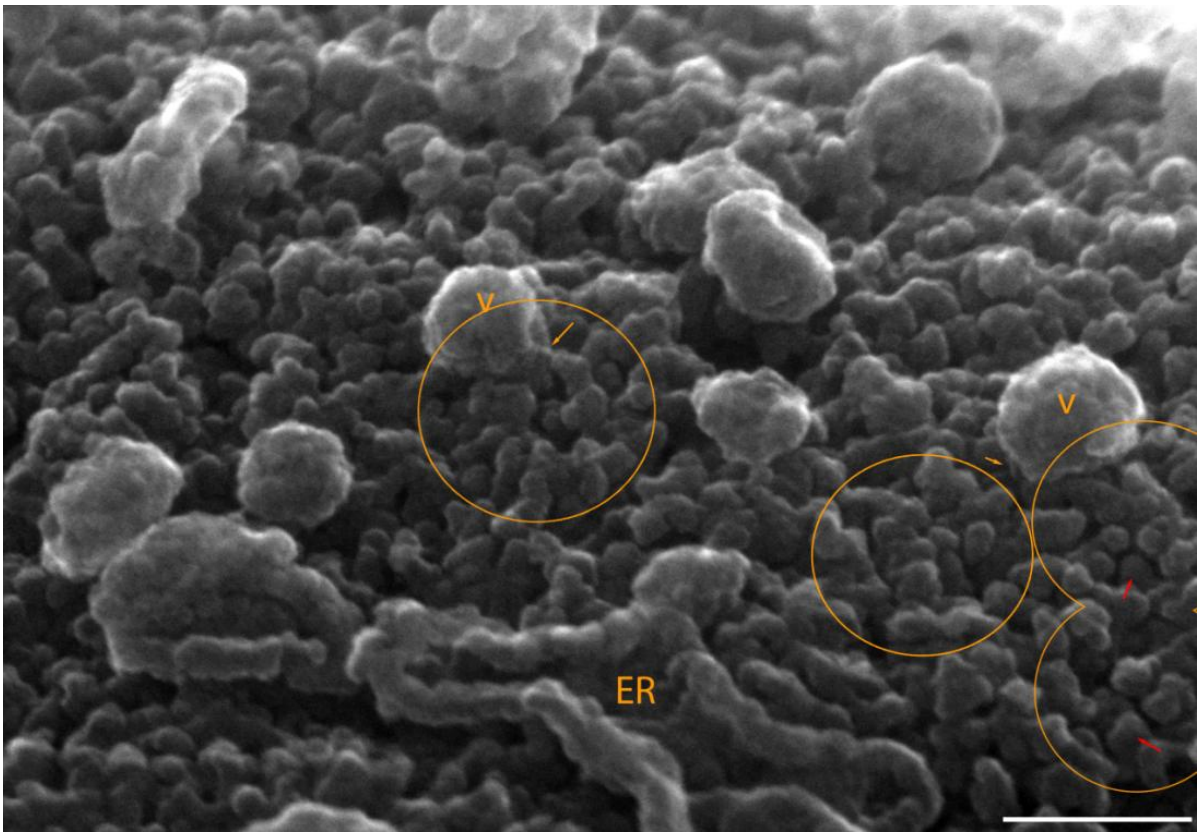

Figure 3.4.11 Nuclear surface of 3733 at 24°C, NPC with seemingly extended cytoplasmic filaments. Yeast nuclei surface from enzymatic osmotically lysed yeast. Orange arrows point to the possible NPCs connections with vesicles. Red arrows point to filaments very similar to those in Figure 3.4.16. ER, endoplasmic reticulum; V, vesicle. Image taken at 200000X magnification with 30kv.

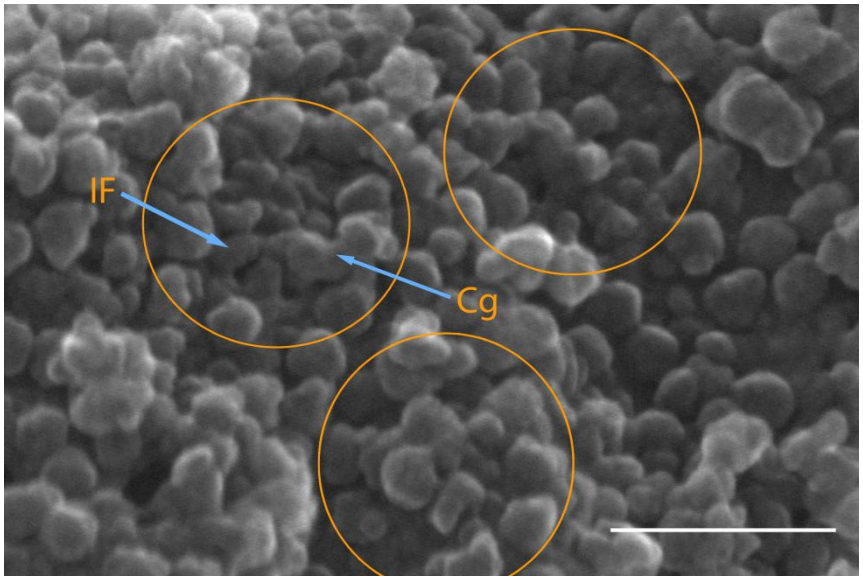

Figure 3.4.12 A NPC with internal filaments that do not join in the NPC centre. 3733 yeast grown at 37˚C. Nuclei surface from enzymatic osmotically lysed yeast. Cg points to potential cargo in transit e.g. mRNA. The NPC with this potential cargo has well defined internal filaments (IF) which look short and do not connect in the middle of the NPC. Image taken at 300000X magnification with 30kv. Scale bar represents 100nm.

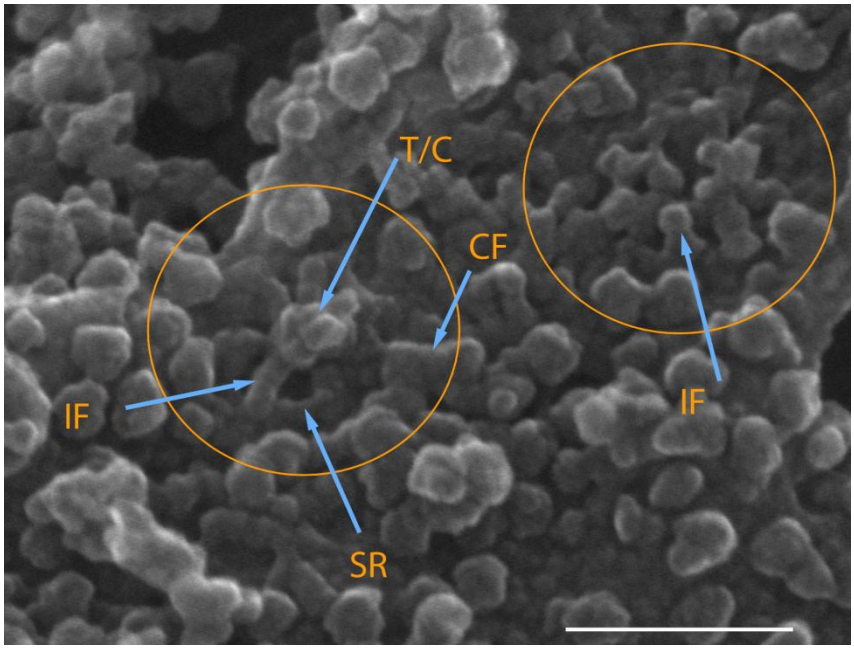

Figure 3.4.13 Nuclear surface of 3733 at 37°C, one NPC with internal filaments appearing ordered and joining in NPC centre at transporter structure. Yeast nuclei surface from enzymatic osmotically lysed yeast. The left NPC has well defined internal filaments (IF) which look to connect in the middle (T/C). This could be joining at or forming a transporter, alternatively it could be possible cargo translocating. These filaments have a thinner diameter than those in Figures 3.4.12 and 3.4.16; they are possibly stretching. Image taken at 300000X magnification with 30kv, scale bar represents 100nm.

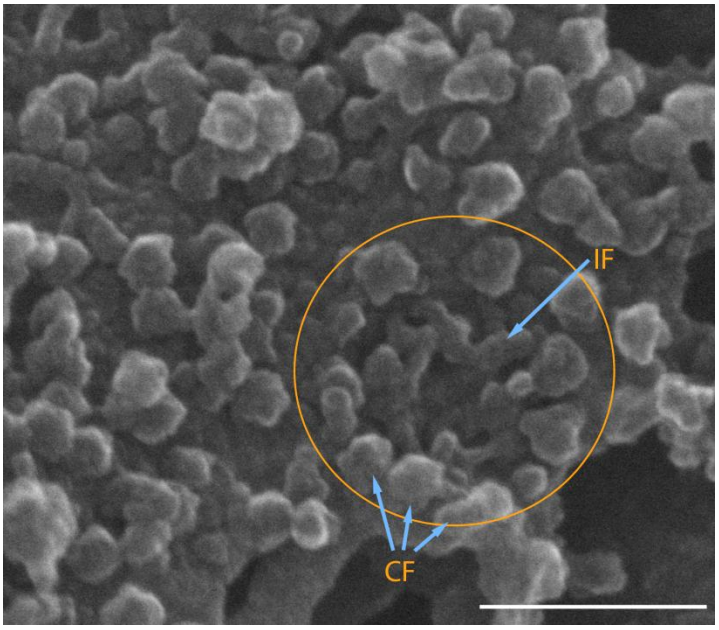

Figure 3.4.14 Mutant 3733 at 37°C with disrupted internal filaments. Yeast nuclei surface from enzymatic osmotically lysed yeast. This NPC has filaments (IF) emanating from similar locations as those shown in Figures 3.4.16 and 3.4.17, but they seem more disrupted. There also seems to be an outer group of filaments these are possibly cytoplasmic filaments. OF, outer filaments; IF, internal filaments. Image taken at 300000X magnification at 30KV. Scale bar represents 100nm.

Possible NPC connections to vesicle-like structures

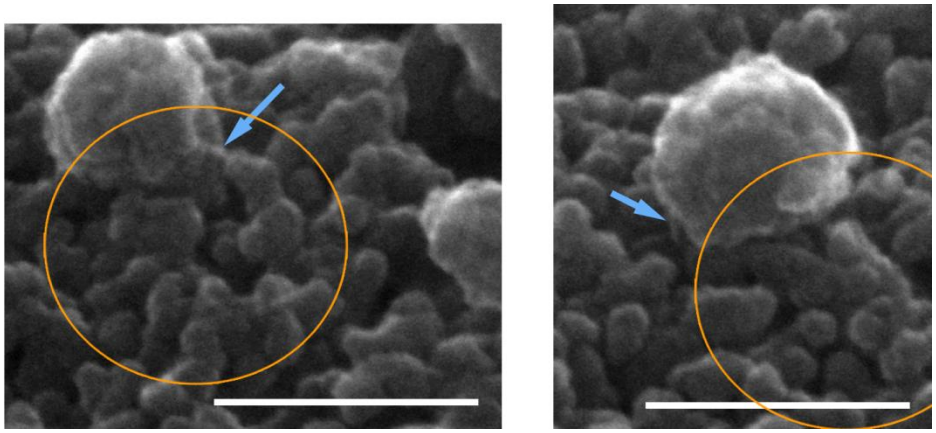

Figure 3.4.15 NPC connections to vesicle-like structures. Encircled in orange are possible NPCs. Blue arrows point to possible vesicle-NPC connections. Scale bar 100nm.

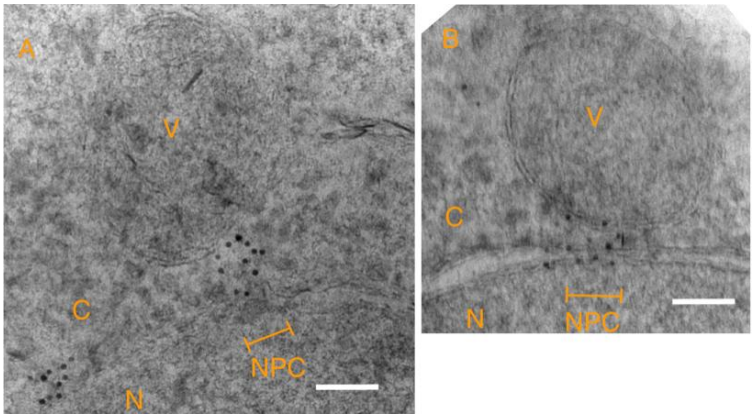

Figure 3.4.16 TEM of GLFG repeat labelling extending from NPCs towards vesicle-like membrane structure. Observed using TEM, high pressure frozen, freeze substituted GLFG indirect immunogold labelled WT yeast. Immuno gold labelled for GLFG repeats V, Double membrane vesicle (potential mitochondria); NPC, Nuclear pore complex; C, cytoplasm; N, nucleus. Scale bars represent 100nm.

Figure 3.4.11 is a higher magnified nuclear surface image of Figure 3.4.1. It shows some NPCs from 3733 at permissive temperature (24°C). There appear to be long cytoplasmic filaments covering the NPC, one of which looks to be making a connection to a vesicle (highlighted by left image, Figure 3.4.15). Another vesicle-like structure appears to have a connection to a different NPC highlighted in the right image (Figure 3.4.15). These vesicles or membrane structures could be the same vesicles or membrane structures as observed by TEM (Figure 3.4.16). In the TEM results GLFG labelling extends from the pore to a membrane structure. In the Prp20 temperature sensitive mutants at the non-permissive temperature (37°C) similar connections can be seen to vesicle-like structures (Figure 3.4.11 and some highlighted in Figure 3.4.15). These could be tethering the vesicles-like structures to NPCs and the nucleus. In the TEM results, the area of GLFG labelling would seem thicker than the structure seen in the SEM images. This could be due to the

sample preparation process for SEM, which may cause some connections to be lost or it to take a more compact shape than in vivo. There appears to be a higher number of vesicles-like structures on the surface of the 37°C 3733 nucleus than the 24°C 3733 nucleus in Figures 3.4.17 and 3.4.18, this could be due to sample preparation. A larger sample size with a WT at 37˚C as a control would need to be collected to show this.

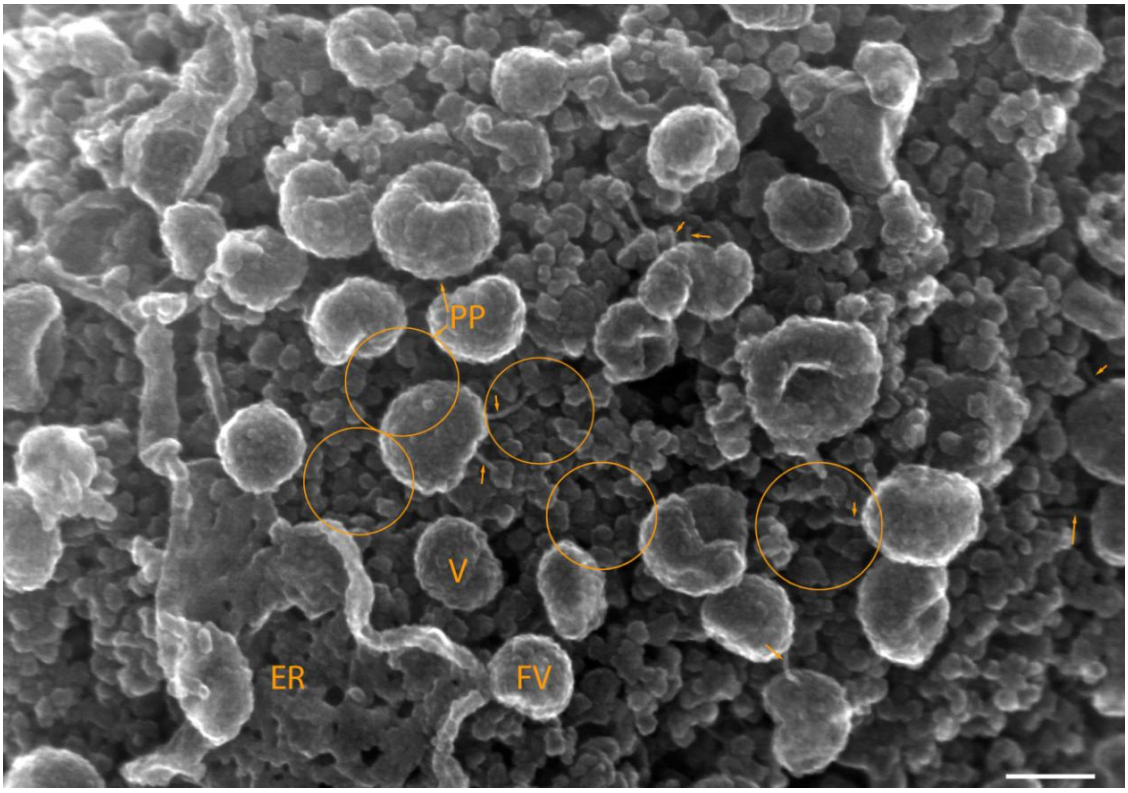

Figure 3.4.17 Nuclear surface of 3733 at 37°C, showing NPCs and vesicle- like structures with fine filaments connected to possible NPC related structures. Yeast nuclei surface from enzymatic osmotically lysed yeast. Arrows from PP show potential NPCs behind the vesicles. Lone orange arrows point to connections from vesicles to the nucleus and in many areas which could potentially be a NPC. At the edge of the ER there is a flattened vesicle. This could be involved in extending the ER, similar structures are also shown in Figure 3.4.1. Also shown in yellow is a vesicle (V) which appears in an NPC. FV, flattened vesicle; PP, potential NPCs behind vesicles; ER endoplasmic reticulum; V, vesicle seemingly in an NPC. Image taken with 30kv.

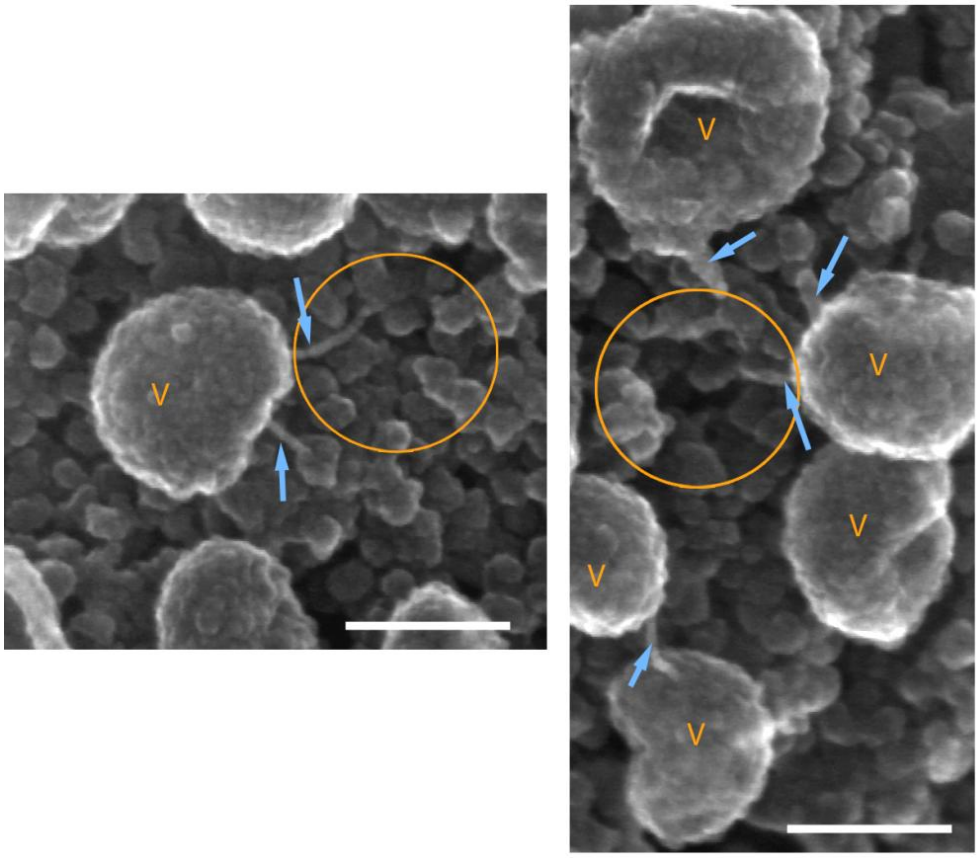

Figure 3.4.18 Possible vesicle-like structures connected via fine filamentous-like structures to NPC resembling structures. V, vesicle-like structure; encircled in orange is NPC resembling structure; blue arrows point to thin filament-like structures connecting vesicle-like structure to NPC-like structures. Scale bars represent 100nm. Images from Figure 3.4.17.

Chapter 4 Discussion

In this chapter the results given in Chapter 3 are discussed in relation to existing models for import. It is found that the evidence supports the reversible collapse and forest models, however is not explained by the hydrogel model. An adapted model for the import of Kap121 dependant cargo, which uses aspects of both the reversible collapse and forest models, is proposed. It is possible that a similar model may apply to import of other molecules.

4.1 Yeast NPC structure

Previous SEM experiments of yeast are shown by Kiseleva *et al* (2004). This gives evidence for a cytoplasmic ring, cytoplasmic filaments and nucleoplasmic ring with a possible basket attached (however seemingly damaged by nuclei fracturing). Evidence is also given for a central transporter structure which may be linked by internal filaments in yeast (Kiseleva *et al* 2004). The NPC structure is largely conserved in a wide variety of eukaryotic organisms from *Xenopus* to plants.

SEM is used to show the surface structure of the NPCs. It is important to see these structures to help show how the NPC 'works'. The SEM of yeast nuclei presented in Section 3.4 gives supporting evidence for a highly conserved NPC structure. Structures observed were:

- Cytoplasmic ring.
- Cytoplasmic filaments, seen attached to the top of the cytoplasmic ring and sometimes observed extending into the centre of the pore. These are GLFG labelled and therefore likely to have GLFG domains.
- Internal filaments, seem to be continuous with the cytoplasmic ring. GLFG labelling suggests they have GLFG domains.
- Transporter, possibly made from GLFG labelled internal filaments.
- Basket filaments, observed on the nucleoplasmic face, joining at a distal basket ring. GLFG labelling suggests the basket ring has GLFG domains.

- Possible NPC-putative lamina connections; filaments joining up with the area near the basket filament anchorage site. This connection may be connecting the NE to the NPC.

As filaments of the NPC seem to have GLFG labelling it may be that GLFG Nups and possibly other FG Nups form them. Alternatively, they may just associate with these filaments, potentially in a transient manner.

Some NPCs were observed with low levels of GLFG labelling on the cytoplasmic side. This could be a 'young NPC' which has not yet had its GLFG Nups added. It could also be inconsistent labelling or misinterpretation of NPCs. This observation could possibly indicate a transient association of GLFGs with or into cytoplasmic filaments, with the GLFGs moving from the cytoplasmic filaments, possibly to basket filaments and the distal basket ring.

Cytoplasmic filaments are sometimes observed in 3-D reconstructions such as in the study by Stoffler *et al* (2003) of the *Xenopus* NPC. However, due to the cytoplasmic filaments' flexible or dynamic structure they appear as 'stubs' near their anchorage point where flexibility or 'dynamicness' is limited. This is partially overcome in Beck *et al* (2004) where classes of *Dictyostelium discoideum* NPCs are used to make 3-D reconstructions. In some 3-D reconstructions cytoplasmic filaments are not observed, for example in the study of the yeast NPC by Yang *et al* (1998). There is evidence for the existence of yeast cytoplasmic filaments from TEM thin sections (Fahrenkrog *et al* 1998). FESEM of yeast nuclei showed cytoplasmic filaments (Kiseleva *et al* 2004). Immuno FESEM show these cytoplasmic filaments are possibly Nup116 (GLFG Nup) labelled (Kiseleva *et al* 2004). TEM studies have also shown Nup116 to occupy additional positions in the central plane and on the nucleoplasmic side (Ho *et al* 2000; Rout *et al* 2000). Results from Section 3.4 show the cytoplasmic filaments to be present in yeast and appear to be GLFG domain labelled.

Cytoplasmic internal filaments are observed using FESEM in *Xenopus* by Goldberg and Allen (1996). These internal filaments are attached to the underside of the cytoplasm ring, they extend towards the centre of the NPC where they join (Goldberg and Allen 1996). FESEM of yeast nuclei also show internal filaments possibly joining at a transporter (Kiseleva *et al* 2004). However, these structures are not as clear as in *Xenopus*. Averaging methods such as those used by Akey *et al* (1993) and Alber *et al* (2007[2]) do not resolve internal filaments, probably due to their variability. Internal filaments in this study were observed joining in the middle of the NPC in yeast. In the middle of the NPC is a structure known as the transporter. It is debated whether the transporter structure is a functional structure or cargo in transit.

- Evidence for cargo: Plugging of NPCs is shown by AFM when transport is arrested at 4°C. Unplugging is observed when at 25°C, which is more permissive of transport and NPCs are observed less plugged (Stoffler *et al* 2003). The electron density resembles that of cargo (Beck *et al* 2007).
- Evidence for a functional structure of the NPC: A study of the FG Nup's predicted structure shows how the collapsed cohesive FG domains of FG Nups could make up the transporter (Yamada *et al* 2010). These collapsed cohesive coil domains are attached to the NPC by predicted relaxed or extended coil domains of FG Nups.

In Section 3.4 GLFG labelled internal filaments were observed joining at the centre of the NPC. This is where the structure corresponding to the transporter is located. The area where the internal filaments join is GLFG labelled. This would be expected with the prediction of FG collapsed cohesive coil domains suggested by Yamada *et al* (2010) to form the transporter structure. Kiseleva *et al* (2004) shows, for the GLFG Nup57 temperature sensitive mutant at 37°C, a loss of transporter and internal filaments and cytoplasmic filaments. This indicates GLFG domains may be important in transporter structure possibly contributing to it. Joining of internal filaments at the NPC centre was also observed in the Prp20 mutant at the non-permissive temperature 37°C (however these samples did not undergo GLFG labelling). These results suggest:

i. the internal filaments observed are GLFG Nups.
ii. the transporter is at least partially made of GLFG domains.

These structures may also contain other FG domains, however experiments such as labelling for the other FG domains would need to be performed in order to prove this. Not all of the NPCs had internal filaments which joined at the centre. In these NPCs the transporter structure appears to be absent. The possible GLFG labelling of internal filaments indicates that the internal filaments observed in other studies such as Goldberg and Allen (1996), Kiseleva *et al* (2004) and Fiserova *et al* (2009) may be observing GLFG or other FG Nups.

Nucleoplasmic filaments and distal basket ring (DBR)

In *Xenopus,* eight nucleoplasmic filaments are attached to the periphery of the nucleoplasmic ring between each bipartite subunit (Goldberg and Allen 1996). The DBR is formed from the nucleoplasmic filaments joining together (Goldberg and Allen 1996). Yeast also have a basket structure evidenced by thin section TEM (Fahrenkrog *et al* 1998) and FESEM, however, these appear damaged. In Section 3.4 the yeast nucleoplasmic face can be seen. This face of the NE was

difficult to observe; nuclei fracture experiments were performed, however, NPCs were often damaged. Occasionally the yeast nuclei fractured fortuitously under normal isolation and immuno labelling conditions allowing the inner nuclear face to be observed. Structures resembling nucleoplasmic filaments and distal basket rings could be seen. Immunogold labelling for GLFGs showed that the basket filaments and distal basket ring are likely to be GLFG labelled. TEM results from Section 3.1 show GLFG labelling in an area that may correspond to the distal basket ring. This labelling is away from its likely anchor domain at the midplane with an unlabelled region in between. This unlabelled region (between GLFG labelling and its likely anchor) may correspond to the predicted relaxed or extended coil domain of Nup116 in Yamada *et al* (2010). The GLFG labelling away from the likely anchor corresponds to the collapsed coil FG containing region of Nup116 shown in Yamada *et al* (2010). Thin section TEM immunogold labelling for Nup116 in Ho *et al* (2000) also show one of the locations of Nup116 (a GLFG Nup) to be on the nucleoplasmic side, possibly in an area corresponding to the nucleoplasmic basket and distal basket ring (Ho *et al* 2000).

Prp20

At the non-permissive temperature the mutants used were defective in the nucleotide exchange activity of the RanGEF, Prp20. As a result RanGDP is not converted to RanGTP, causing a deficiency of the active RanGTP molecular switch.

Prp20 yeast at the non-permissive temperature, 37˚C, show filaments extending towards the centre of the pore. These filaments appear to be internal filaments. They are often not observed in WT as they are occluded by the cytoplasmic filaments extending over the NPC. This indicates that cytoplasmic filaments in the Prp20 mutant at 37°C do not appear to cover the NPC channel. This could mean that these cytoplasmic filaments have been removed during sample preparation, or cytoplasmic filaments have shortened towards their anchor. It has previously been observed that RanGTP causes extension of the cytoplasmic filaments and it is suggested this may be a role in altering NPC conformation for import with GDP, or export with GTP (Goldberg *et al* 2000). It could be that in Prp20 mutant yeast the lack of RanGDP to RanGTP conversion is causing the cytoplasmic filaments to shorten, allowing us to see into the pore and view its internal filaments. This shortening of cytoplasmic filaments may be because the NPC is in an import conformation. Walther *et al* (2002) showed that the cytoplasmic filaments are dispensable for import. Prp20 mutant results at the non-permissive temperature hint that the cytoplasmic filaments shorten

(whilst NPC possibly locked in a late import state) and so may not play an active role and are dispensable for import.

Due to the difficulties in observing the yeast NPCs in SEM it is hard to get large numbers to compare. The observations are therefore based on low numbers of NPCs and the results should be confirmed with further observation in yeast, alternatively other species could be investigated. Evidence is given through the TEM results (Section 3.1) that in the Prp20 mutant at 37°C NPCs are possibly found more frequently than in WT to be in a late import conformation, with a shift in the GLFG labelling from cytoplasmic to nucleoplasmic. This is further supported by labelling cargo (Spo12-NLS-GFP) and observing a GLFG domain shift towards nucleoplasmic as the cargo translocates. It has also previously been observed by cryoelectron tomography that there are changes in the cytoplasmic filaments, distal basket ring and central channel (Beck *et al* 2004). These changes in NPC structures are possibly due to translocation of cargo because the classes are defined by the central transporter, which may be partially cargo. Beck *et al* (2004) showed two potential classes of NPC, which could be the cytoplasmic filament (CF) class and luminal spoke ring (LR) class. The LR class has cytoplasmic filaments extending and connecting to the transporter via an elongated density and the DBR has an opening (Beck *et al* 2004). In the LR class cytoplasmic filaments are only observed at their base and the DBR has more mass bound (Beck *et al* 2004). These classes could possibly be partially explained by GLFG domain movement within the pore. There is possibly a shift to nucleoplasmic GLFG labelling when an import cargo complex is likely to be bound. The mass could be lost to the basket filaments. Evidence for this is given by GLFG labelled DBR, and Beck *et al* (2004) shows a more massive NPC basket in LR class. This could represent the GLFG domains, possibly other FG domains and cargo near or associated with the DBR. In Beck *et al* (2004) the cytoplasmic filaments are defined in the CF class, but in the LR class only the base of the cytoplasmic filaments can be seen. This could be observing the shift from a more import-like form in the LR class and export form in the CF class. If Prp20 mutants at 37°C were observed on the nucleoplasmic side and GLFG labelled it may indicate that there is an increase in DBR size and increase in GLFG labelling.

Connections of NPCs to membrane structures

Observed in Section 3.4 were fine filament structures extending towards vesicle-like structures. These filaments often emanated from NPC-like structures. Sections 3.1 and 3.2 showed the extension of GLFG repeats from the NPC to membrane structures, so one possible candidate for these structures seen in Section 3.4 are GLFG Nups. If more yeast nuclei were labelled for GLFG

repeats then these fine filament structures may be identified using SEM. Results in Sections 3.1 and 3.2 showed that in the WT pores GLFG repeats were observed 'reaching' to membrane structures in the cytoplasm. This leads to the idea that pores are involved in vesicle recruitment or membrane recruitment for membrane growth. Some vesicle-like structures appear to have internal membranes and look very much like mitochondria as they appear similar to some mitochondria observed in Garofalo *et al* (2007) and the isolated mitochondria as in Fortsch *et al* (2011). This could imply that NPCs localise the mitochondria, possibly by tethering to the NPCs. Reasons for tethering the mitochondria could include:

i. Providing energy for the nucleus by phosphotransfer for its functions such as efficient nucleocytoplasmic transport (Dzeja 2002).
ii. For mitochondria nuclear signalling such as for apoptosis (Garofalo *et al* 2007).
iii. Regulating mitochondria such as in the cell cycle; when NPCs are clustered at the spindle pole bodies during cell division (Winey *et al* 1997) it may ensure some mitochondria are also inherited in the new bud.

This possible NPC-mitochondria tethering could be established using TEM, and possibly SEM, by double immunogold labelling for mitochondria and GLFGs. Live cell imaging, (such as with spinning disk microscopy) may also suggest if mitochondria are located to NPCs and if their dynamics are linked.

As GLFG domains appear to be present in spindle pole bodies (SPB) (Section 3.2) they may play a role in cell division. GLFG domains are seen reaching from the SPB towards a vesicle-like structure. This may indicate a shared role with GLFGs in NPCs (which are also seen reaching towards vesicle-like structures). A mitochondria has been observed very close to a SPB in Mcintosh and O'Toole (1999). It is not clear which protein is GLFG labelled in the SPB and it may be a novel component of the SPB.

Putative yeast lamina

Yeast apparently lack a nuclear lamina, however the lamina is shown to be connected to NPCs in *Xenopus* (Goldberg and Allen 1996) and NPC distribution is shown to be controlled by Lamin A in Drosophila (Furukawa *et al* 2009). Therefore, if yeast have no lamina their NPCs would be expected to be in a more random distribution. There is evidence suggesting that NPC distribution in yeast is non-random and found to cluster especially in mitotic and late anaphase cells (Winey *et al* 1997). These clusters are mobile (Belgareh and Doye 1997). Likewise, plants had been thought

to have no lamina, however Fiserova *et al* (2010) shows using SEM that tobacco has organised filamentous proteins underlying the inner nuclear membrane and interconnecting NPCs. This is shown to be similar to lamina structures observed in *Xenopus* (Fiserova *et al* 2010).

The results stated above indicate that there could be a putative yeast lamina. Woven filament structures have previously been observed in *Xenopus* (Figure 4.1) (Goldberg and Allen 1992). Results in Section 3.4 show some evidence for the presence of similar woven filamentous structures on the nucleoplasmic face of the nucleus in yeast (Figure 4.1). There are also filaments running at 90 degrees to each other around the plane of the NE. Goldberg and Allen (1996) show by detergent extraction that the lamina in *Xenopus* connects to the NPC (Figure 4.2). Results in Section 3.4 show filaments seemingly connecting to the NPC (Figure 4.2). Additionally, the NPC is seen to stay intact after osmotically lysing the cell, indicating some level of nuclear structural integrity. Nuclear structural integrity is suggested to be provided by the lamina in vertebrates (Broers *et al* 2006), therefore it may be keeping the yeast nucleus intact after lysing the cell. These results speculatively indicate the presence of a putative yeast nuclear lamina. Salt and detergent extraction of yeast nuclei may help reveal a lamina-like structure (if present). If lamin candidates were identified in yeast these could be labelled for using immuno-SEM.

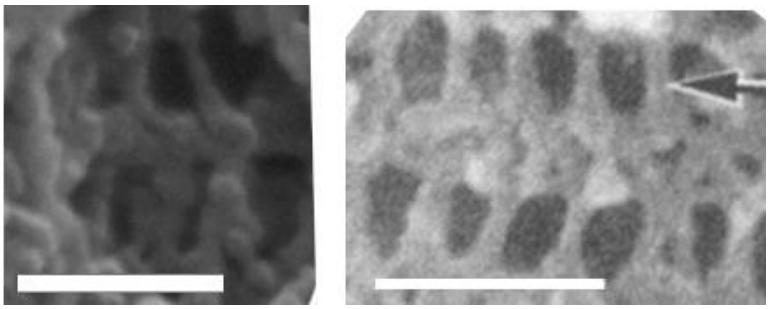

Figure 4.1 Possible similar NE lattice yeast (Left) and *Xenopus* (Right) (image on right from Goldberg and Allen (1996)). Scale bar 100nm.

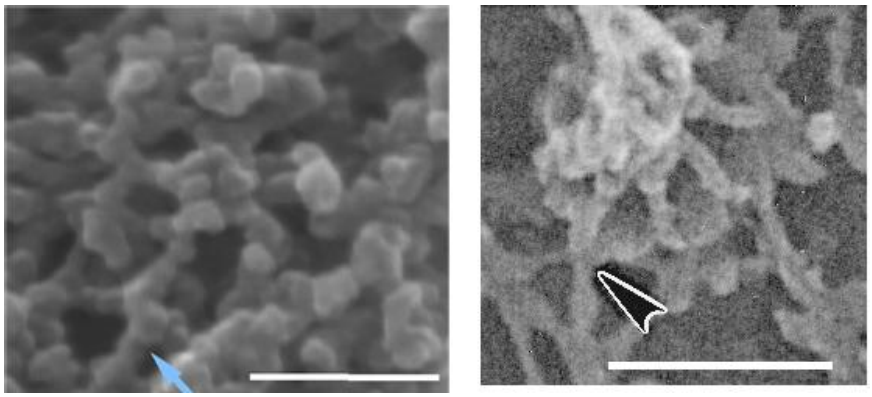

Figure 4.2 Possible similar lamin connections to the NPC in yeast (left) and *Xenopus* (right). (Image on right from Goldberg and Allen (1992)). Left image: blue arrow is to possible lamina-NPC connection. Right image: detergent extraction in *Xenopus* revealing possible lamina-NPC connections (arrow) to the NPC. Scale bar 100nm.

4.2 Discussion of results in relation to existing models of translocation

This project has centred around the NPC's GLFG Nups and their structure, localisation and dynamics during translocation. The results from labelling GLFG domains potentially show how dynamic the GLFG domains are. The antibody used was raised against the GLFG domain of Nup116, but also appears to recognise the GLFG domains of Nup57 and Nup49 on Western blots (S. Wente personal communication).

There are many models of translocation through the NPC. Paulillo *et al* (2005) shows FG domains of Nup153 and Nup214 to be flexible within the NPC. These are suggested in Paulillo *et al* (2005) to function in guiding cargo through the pore, which could possibly be explained by a reversible collapse. The reversible collapse model (based on in vitro TEM and AFM studies) suggests FG Nup153 collapses when a transport factor (Kap-β1) binds, 'reeling' it in to the centre midplane of the NPC (Lim *et al* 2007). This collapse is shown to be reversed by RanGTP addition, which disassociates Kap-β1 from FG binding (Lim *et al* 2007). The hydrogel model by Frey *et al* (2007) is based on the selective phase model (Ribbeck and Gorlich 2001). A FG hydrogel is suggested to be formed in the NPC by weak hydrophobic interactions between FG repeats. Transport factors are suggested to be able to enter this hydrogel due to hydrophobic patches on their surface, which compete for FG binding. The FG Nups' domains have been studied to try and understand their structural configuration. This predicts some FG Nup domains to be cohesive as in the hydrogel model, and some FG domains to repel, forming potentially collapsible brushes, as predicted by the reversible collapse model (Yamada *et al* 2010).

The location of the C-terminal anchor domain of GLFG Nups has previously been studied by thin section TEM (Rout *et al* 2000). However, this does not give any information about the position of the highly extended FG repeats. This report shows the extent of GLFG labelling in relation to the C-terminal in averaged NPCs. It also shows the variation between individual NPCs. In particular, the GLFG labelling is either on the nucleoplasmic side, cytoplasmic side or on both. From the averaging data it was shown that the GLFG labelling in WT has a bias towards the cytoplasmic side. Serial sectioning was used to confirm the GLFG distribution across more of the 3-D volume of individual NPCs. This confirmed that individual NPCs had different distributions of GLFG labelling, which was

on the nucleoplasmic or cytoplasmic side or on both sides. NPCs also varied on how far the GLFG labelling extends into the nucleus and cytoplasm.

The GLFG distribution in the asymmetric FG Nups (Nup42ΔFG, Nup159ΔFG, Nup60ΔFxF, Nup1ΔFxFG, Nup2ΔFxFG) of yeast mutants 2971 and 3064 (which has an additional symmetric FG domain deletion in Nsp1 (Nsp1ΔFGΔFxFG deletion)) are localised more to the NPC edge than in WT. WT has higher levels of GLFG labelling in the centre of the NPC than the FG deletion mutants. The cohesive FG domains of Nups with relaxed or extended non-cohesive coils are predicted in Yamada *et al* (2010) to contribute to the transporter structure in the centre of the NPC. The FG deletion mutants 2971 and 3064 both have the FG domain deletion Nup1ΔFxFG. Nup1 is suggested to partially make the transporter (Yamada *et al* 2010). By deleting the FxFG domain of Nup1 the transporter structure may not form as easily, therefore the other Nups which may constitute it (including GLFG Nups) may collapse to the edge of the NPC. This could be tested by FG deletion mutant of only Nup1 to see if the GLFG labelling is still closer to the edge and less in the centre of the NPC than WT. It may show that a high concentration of FG domains in the NPC is needed for clustering of FG domains. The central plane may not be as densely packed with FG domains, due to much of the FG mass missing in 2971 and 3064. Therefore, only the edges near their anchorage point are occupied.

WT, 2971 and 3064 all had a cytoplasmic GLFG labelling bias. In 3064 there is a slight shift in the GLFG labelling from the cytoplasm to the nucleoplasm compared to WT and 2971. As the only difference between 2971 and 3064 is the Nsp1ΔFGΔFxFG deletion this shift in GLFG labelling may be caused by deleting the Nsp1 FG domain. It is interesting that there is a difference in GLFG labelling as the GLFG domains of Nups have not been removed, only the FG domains of Nups have been deleted. The FG repeats therefore seem to be influencing the distribution of GLFG repeats. This could be through crowding as suggested in Yamada *et al* (2010). These mutants (2971 and 3064) have a large mass of FG domains deleted so would be less crowded in the NPC.

Investigated next was whether different NPCs possessed a steady state of GLFG domain distribution or whether the variation was due to there being functionally different NPCs. For instance some NPCs could be specialised for import and some for export. One explanation for the different GLFG distributions between NPCs could be due to them being frozen and fixed and therefore captured at different stages of translocation events. To test this, Prp20 mutants were used to see if this altered the GLFG distribution. At the non-permissive temperature the mutants used were defective in the nucleotide exchange activity of the RanGEF, Prp20. As a result RanGDP

is not converted to RanGTP, resulting in a deficiency of the active RanGTP molecular switch. RanGTP is responsible for cargo disassociation as well as cargo export complex formation. In the Prp20 mutant at the non-permissive temperature (37˚C) there was a shift in the GLFG labelling from the cytoplasmic side towards the nucleoplasmic side. This should be confirmed with a study of WT at 37˚C as a control.

Possible explanations for these observations include:

(i) NPC locked in a late import state: this would be due to reduced levels of RanGTP, reducing the efficiency of disassociation of transport receptor-cargo receptors leading to the attenuation of cargo on the nucleoplasmic side.

(ii) Not being able to regenerate RanGTP could lead to limited export.

It should also be taken into account that the many other cellular roles of Prp20 and the effects on GLFGs within the pore may not be caused directly by the lower level of RanGTP regeneration. Evidence from Ryan *et al* (2003) showed temperature sensitive mutants of the Ran cycle stopped new NPC assembly. Therefore, NPCs observed in the Prp20 mutant may be 'old' NPCs and not newly forming/formed NPCs.

In the Prp20 mutant the GLFG labelling shifted from the cytoplasmic to the nucleoplasmic side. We suggest that this is because when RanGTP is limited and the import complexes fail to disassociate the NPC gets stuck in a late import conformation. To see if there is a shift in GLFG domain labelling during specific transport a transport cargo was examined. The transport route of Spo12-NLS-GFP (a marker for Kap121 import) was attempted to be observed. This was done by double labelling experiments for GLFGs and the GFP conjugated to Spo12. The following was observed:

- Spo12-NLS-GFP approaching the pore with its GLFG labelling mostly in the cytoplasm. This is most like the scored GLFG distribution steady state of WT.
- The Spo12-NLS-GFP moving into the central plane at the edge of the NPC. This is accompanied by less extension of the GLFG labelling. This possibly shows a collapse towards the central plane of the pore where the GLFG Nup116 for example is anchored by its C-terminal domain (J. Fiserova personal communication). The location of the Spo12-NLS-GFP at the edge of the NPC has previously been observed by Fiserova *et al* (2010). This peripheral localisation could be due to the collapse of the GLFG domains, possibly initiated when they bind to Kap121. The subsequent collapse of the GLFG domain may

carry the Kap121 import complex to its anchorage site at the edge of the NPC. The Kap121 import complex is now located near to or at the central plane. The GLFG localisation appears to extend into the nucleus ahead of the Kap121 import complex (located around the central plane). This suggests that import complexes are not carried all the way through the channel by FG domains (Paulillo *et al* 2005), where nuclear GLFG extension would be expected to remain with the cargo. A reason for this nuclear GLFG extension could be passing the cargo on, for example to the Kap121 binding domain of Nup53 (Marelli *et al* 1998). This may allow re-extension of GLFG domains as is shown to happen with the human FG Nup153 when RanGTP is added, possibly removing its transport factor (Kap-β1) (Lim *et al* 2007).

- Spo12-NLS-GFP moving into the nucleus from the central plane. GLFG labelling still mostly in the midplane and in the nucleus. This is similar to the GLFG distribution in Prp20 mutants at non-permissive temperature. Therefore the Prp20 mutant's NPCs at non-permissive temperature may be caught in late import. This could be confirmed by Prp20 mutants with different cargos having conjugated GFP. This may then show accumulation of cargo if and where the cargo has arrested. This is likely to show where RanGTP disassociates the import cargo complex. Once the cargo label is no longer associated with the NPC labelling for GLFGs returns to being mostly cytoplasmic. Observed in some pores between the main body of GLFG labelling in the NPC and cargo is a small amount of GLFG labelling. This area could correspond to the distal basket ring which is seen to be GLFG labelled in Section 3.4. The cargo can sometimes be seen to be going into what could be interpreted as channels.

One observation was that the Kap121 dependent import labelling is not seen to be within the area GLFG labelled and is instead at the edge of the GLFG labelling and at the edges of the NPC. Unconjugated GFP was then observed in translocation. Notably the unconjugated GFP labelling was found amidst the GLFG repeat labelling and seemingly random distribution in the NPC. Previous studies (Fiserova *et al* 2010) have shown that markers for Kap121 mediated import in WT occurred close to the edge of the NPC, compared to diffusion of unconjugated GFP which had no preference for the area of channel that it diffused through. This labelling of Spo12-NLS-GFP at the edge of labelled GLFG domains, and unconjugated GFP labelling amidst labelled GLFG domains would not be expected with the hydrogel model. This is because in the hydrogel model the transport factor is suggested to break into the FG, or in this case GLFG hydrogel, so the transport receptor-cargo complex would be observed in it more than an inert protein (such as GFP). Fiserova

et al (2010) shows how Kap121 mediated transport was affected in GLFG deletion mutants (ΔNΔC ΔNup100GLFG and ΔNup145GLFG). This showed Kap121 cargo complex translocation becomes uniform and loses its bias towards the edge. Possible explanations for this could be:

i. As Kap121 dependant cargo labelling was seen at the edge it could be GLFGs creating an entropy barrier against Kap121 dependant cargo, preventing it freely diffusing through GLFG domains. Therefore removing GLFG domains may allow Kap121 to translocate through any part of the NPC.
ii. The GLFG Nups are 'reeling' in the Kap121 cargo complex to their anchorage point as suggested in the reversible collapse model by Lim *et al* (2007). Therefore removing GLFG Nups stops 'reeling' in towards anchorage points and Kap121 dependant Spo12-NLS-GFP has to diffuse through the NPC.

GLFG domains can restructure or reposition within the pore and can potentially become much more nucleoplasmic in response to limited RanGDP to RanGTP conversion in the Prp20 mutant, possibly arresting cargo in the NPC. The GLFG domains seem to become more nucleoplasmic when the cargo is at the midplane or just into the nucleus whilst still within the confines of the pore. This could be where RanGTP may disassociate the import complex. Then, Spo12-NLS-GFP labelling moves away from the NPC down possible channels and GLFGs can be seen associated with an area corresponding to the distal basket ring (also shown in SEM results). The GLFG domains may play a role in opening (and closing) the distal basket ring or may have been involved in pushing Kap121 towards the nucleus. Then, once cargo is disassociated, some GLFGs may still be left associated to the distal basket ring.

The GLFG labelling extension into the nucleus ahead of Spo12-NLS-GFP labelling is surprising and would not be expected with FG Nups carrying or guiding the cargo through the NPC as suggested by Paulillo *et al* (2005). A possible explanation for this GLFG extension ahead of the Spo12-NLS-GFP translocation could be that once at the midplane of the NPC there is possible import cargo disassociation by RanGTP, allowing GLFG Nup restructuring and extension in the nucleoplasmic direction. However, this possible restructuring and extension of GLFG labelling is observed in the Prp20 mutant where there may be lower RanGTP levels, so import cargo may still be bound to the NPC. This suggests that the loss of cargo from the GLFG domains is not RanGTP dependant. Instead, Kap121 may be passed to Nup53 by competition for binding. This competition for the Kap121-Spo12-NLS-GFP complex is suggested as Nup53 possesses a Kap121 binding site (Marelli *et al* 1998). Nup53's Kap121 binding domain is close (30AAs, <10 nm) to where it is potentially

inserted or tightly associated with the membrane (Patel and Rexach 2008), therefore this Nup53-Kap121 interaction is thought to be at the edge of the NPC (Yamada *et al* 2010). Mutations in Nup53 cause Kap121 mediated import to be inhibited (Marelli *et al* 1998). It is therefore likely to be involved in Kap121 import. This passing of the transport receptor complex from collapsed GLFGs may allow the GLFG domains to once again extend, this time in the nucleoplasmic direction ready to bind Kap121 to recycle it back to the nucleoplasm. RanGTP could then release Kap121 from Nup53 (Marelli *et al* 1998).

Griffis *et al* (2002) showed that Nup98, which is the only vertebrate GLFG Nup, is a dynamic component of the NPC and is mobile within the nucleoplasm, associating with novel structures the NPC and GLFG body. This may indicate a similar role of GLFG Nups in yeast and vertebrates.

Nuclear Envelope herniations in FG Nup deletion mutants

The observation of the herniations in deletion Nup NPCs has previously been observed (Wente 1997). Results in Section 3.1 show that labelling for the GLFG domains could be seen in these herniations, indicating that components of the NPC may be removed from the NE into a herniation. This could therefore be a process of removing defective NPCs or causing NPC assembly defects. Other explanations for these 'herniation' structures could include the mutation having deleterious effects on the pore's ability to bind these membrane vesicles and incorporate them in the NE as a way of membrane growth and so is much slower at this step. A further possibility is that in the creation of these vesicle structures the mutation has impaired the ability of the NPC to push away the structures, consequently causing defective vesicle formation. Observed changes in GLFG distribution, together with the observation in Wente and Blobel (1993) that the temperature sensitive GLFG Nup116 null mutants cause herniations, imply that it could be the loss of some asymmetric FG domains affecting the functionality of the GLFG Nup116.

The herniations in Wente and Blobel (1993) are filled with electron dense material, as in Figure 3.1.9 A. It is suggested in Wente and Blobel (1993) that the pores lowered the entropy barrier in deletion mutants, which allows a membrane to grow over the pore, thus creating a herniation.

4.3 Import Model

The model of import proposed by this study is based on the following observations:

i. GLFG domains appear to localise to NPC associated filamentous structures.
ii. In Prp20 mutants GLFG domains shift from a cytoplasmic to a nucleoplasmic location. Therefore, GLFG domains are mobile and more nucleoplasmic when (possibly) caught in late import. Additionally, cargo loss from GLFG domains, which allows potential elongation of GLFG Nups into the cytoplasmic side, may not be caused by RanGTP.
iii. Spo12-NLS-GFP marker for Kap121 dependant import showed retraction of GLFGs towards the central plane. Then when Spo12-NLS-GFP is at the midplane there is possibly GLFG labelling extension into the nucleoplasm.

Below, a model of import is proposed for the steps of nuclear import involving GLFG domains. In it, steps C-G are proposed on the basis of GLFG labelling nucleoplasmic extension, which may be pushing cargo out. However, as extension occurs whilst cargo is still seemingly at the midplane it is suggested to be there to 'catch' Kap121 after disassociation of the import complex and recycle it back to the cytoplasm.

Proposed model of import

(A) Initial binding of importin-cargo complex to GLFG domain.
(B) Collapse of GLFG Nup 'reeling' importin-cargo complex to near the GLFG Nups anchor domain, near the midplane at the NPC periphery, as in the reversible collapse model (Lim *et al* 2007) based on Nup153 in *Xenopus*.
(C) Importin-cargo complex passes from GLFG, possibly due to competitive binding from other Nups (in the case of Kap121 binding by Nup53). This pass of import cargo complex from GLFG Nup may allow extension of GLFG Nup into the nucleoplasm as importin cargo complex no longer bound.
(D) Disassociation of import complex by RanGTP (in the example of Kap121 potentially from Nup53).
(E) Importin may rebind GLFG domains.

(F) GLFG domains again collapse towards the anchor near the midplane at the NPC periphery.

(G) Importin passed by competitive binding from Nup e.g. Nup53 allowing GLFG domains to extend cytoplasmically

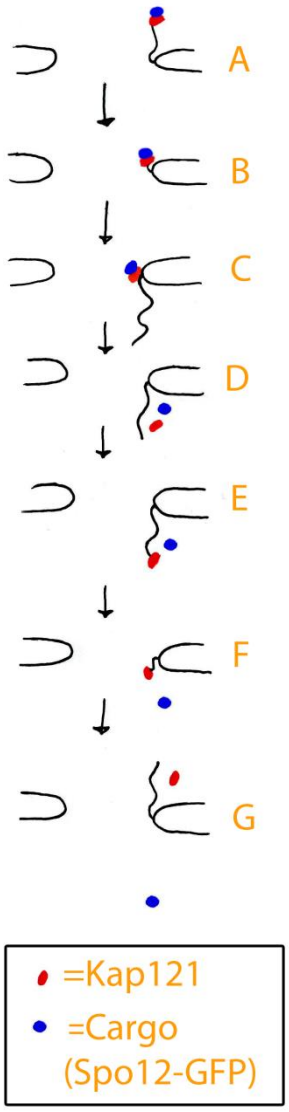

Figure 4.3 Proposed model of import based on Kap121 import. This model suggests GLFG Nups 'reeling' Kap-cargo complex in (B). At midplane Kap cargo complex is possibly passed (C). Extension of GLFG domains is to the nucleoplasmic side as Kap cargo complex is no longer GLFG bound. Cargo is disassociated by RanGTP Kap, possibly exported in similar collapse and disassociation event.

This model does not explain how the direction of extension (cytoplasmically or nucleoplasmically) is controlled. It has been shown that the GLFG Nup Nup116C is localised on both cytoplasmic and nucleoplasmic sides with an asymmetric majority 54% on the cytoplasmic side, 18% at the midplane and 27% on the nucleoplasmic side (Ho *et al* 2000). It may therefore be the anchor moving positioning the GLFG domains during translocation and this may control which way they extend.

To get more experimental evidence and further establish the mechanism by which the NPC translocates molecules, tagged cargos which use different Kaps could be observed. Alternatively, the mRNA export factors Gle1 and Dbp5, which translocate through the centre of the NPC (Fiserova *et al* 2010), could be studied to see if the GLFG (or other FG) repeats restructure in response to export of mRNA or other Kap cargo complexes. Kaps, in addition to cargos, could be labelled to see how GLFG domain distribution is affected by their translocation and by their recycling. This may indicate whether GLFG domains extend into the nucleoplasm to 'catch' the Kap after disassociation of the Kap cargo complex and collapse to recycle the Kap back to the cytoplasm. To test if in the Prp20 mutant cargo is being attenuated in late import, experiments could be carried out using cargo with conjugated GFP in a Prp20 mutant. This may also show where the cargo is disassociated from the NPC by RanGTP as the cargo should arrest where disassociation takes place. Atomic force microscopy could be used to confirm a collapse of the GLFG Nup116 in response to Kap121. This could be done in a similar way to in Lim *et al* (2007), where the spatial range of nanodot tethered cNup153 response to addition of Kap-β1 is measured. To see if Kap121

is passed from GLFG to Nup53, Nup53 deletion mutants with Kap121 dependant cargo labelled could be examined. If deleting Nup53 prevents passing Kap121 from GLFGs then NPCs would be expected at state C in the proposed model. This could be expected as GLFG domains may not be extending due to a collapse caused by Kap121 binding, they are then unable to extend nucleoplasmically due to a limited (or complete lack of) ability to pass a Kap121-cargo complex on.

Serial sectioning could be further utilised to make reconstructions of individual NPCs with GLFGs and cargos mapped. Ultrathin serial sectioning at ~10nm would allow ~10 sections through a NPC, allowing individual NPC reconstruction. This would then allow GFLG distribution changes (in the x and y axis) to be observed in individual NPCs. Serial sectioning NPCs could also be performed using immunolocalisation of other Nups. The N-terminal of the GLFG Nups and other FG Nups could also be labelled for by tagging the ends specifically or making specific antibodies against the ends. This could possibly show movement in the ends of the FG Nups in relation to cargo. This may show if specific GLFG Nups extend out cytoplasmically then nucleoplasmically in response to a cargo. Labelling accuracy for GLFGs could be improved by using direct gold conjugates to anti-GLFG or fab fragments.

4.4 Conclusions

Mapping the GLFG domains within the NPC shows them to be highly variable, have a cytoplasmic bias and be able to extend large distances from the NPC. FG deletion mutants have higher percentages of GLFG labelling towards the NPC edge than WT and lower percentages towards the middle than WT, indicating FG domains affect GLFG domain positioning. GLFG domain labelling is observed ‘reaching’ to membrane structures from the NPC. Serial sectioning of individual NPCs was used to confirm the GLFG distribution. This confirmed that individual NPCs had different distributions of GLFG labelling, which was on the nucleoplasmic or cytoplasmic side, or on both sides. Mutants which are defective in the nucleotide exchange activity of the RanGEF, Prp20, have a deficiency of the active RanGTP molecular switch. This causes a shift in the GLFG labelling from the cytoplasmic side towards the nucleoplasmic side. Similarly the import of Kap121-dependant import cargo seems to cause a shift from cytoplasmic to nucleoplasmic labelling. This is observed

as the cargo reaches the midplane of the NPC. FESEM shows GLFG labelling to be associated with filaments (cytoplasmic, internal and nucleoplasmic) and possibly also the transporter.

A List of Figures

B List of Tables

C List of Charts

Bibliography

Akey C.W. and Rademacher M, 1993, Architecture of the *Xenopus* nuclear pore complex revealed by three-dimensional cryo-electron microscopy, The Journal of Cell Biology, Volume 122:1-19

Akey C.W, 1995, Structural plasticity of the nuclear pore complex, Journal of Molecular Biology, Volume 248 L:273-293

Alber[1] F, Dokudovskaya S, Veenhoff L.M, Zhang W, Kipper J, Devos D, Suprapto A, Karni-Schmidt O, Williams R, Chait B.T, Sali A. and Rout M.P, 2007, Determining the architecture of molecular assemblies, Nature, Volume 450:683-694

Alber[2] F, Dokudovskaya S, Veenhoff L.M, Zhang W, Kipper J, Devos D, Suprapto A, Karni-Schmidt O, Williams R, Chait B.T, Sali A. and Rout M.P, 2007, The molecular architecture of the nuclear pore complex, Nature, Volume 450:695-701

Allen N.P.C, Patel S.S, Huang L, Chalkley R.J, Burlingame A, Lutzmann M, Hurt E.C and Rezach M, 2002, Deciphering networks of protein interactions at the nuclear pore complex, Molecular and Cellular Proteomics, Volume 1:930-946

Andrade M.A, Perez-Iratxeta C. and Ponting C.P, 2001, Protein repeats: Structures, functions and evolution, Journal of Structural Biology, Volume 134, 117-131

Bailer S.M, Balduf C. and Hurt E, 2001,The Nsp1p carboxy-terminal domain is organised into functionally distinct coiled-coil regions required for assembly of nucleoporins subcomplexes and nucleocytoplasmic transport, Molecular and Cellular Biology, Volume 21:7944-7955

Bayliss R, Littlewood T. and Stuart M, 2000, Structural basis for the interaction between FxFG nucleoporin repeats and importin-β in nuclear trafficking, Cell, Volume 102:99-108

Beck M, Forster F, Ecke M, Plitzko J.M, Melchior F, Gerisch G, Baumeister W. and Medalia O, 2004 Nuclear pore complex structure and dynamics revealed by cryoelectron tomography, Science Volume 306:1387-1390

Beck M, Lucic V, Forster F, Baumeister W. and Medalia O, 2007, Snapshots of the nuclear pore complexes in action captured by cryo-electron tomography, Nature, Volume 449:611-615

Belgareh N. and Doye V, 1997, Dynamics of nuclear pore distribution in nucleoporins mutant yeast cells, The Journal of Cell Biology, Volume 136:474-759

Broers J.L.V, Ramaekers F.C.S, Bonne G. Yaou R.B. and Hutchison C.J, 2006, Nuclear lamins: Laminopathies and their role in premature ageing, American Physiological Society Volume 86:967-1008

Chaves S.R. and Blobel G, 2001, Nuclear import of Spo12p, A protein essential for meiosis, The Journal of Biological Chemistry, Volume 276:17712-17717

Cingolani G, Prtosa C, Weis K. and Muller C.W, 1999, Structure of importin-β bound to the IBB domain of importin-α, Nature, Volume 399:221-229

Conti E, Uy M, Leighton L, Blobel G. and Kuriyan J, 1998, Crystallographic anaylsis of the recognision of a nuclear localisation signal by the nuclear import factor karyopherin α, Cell, Volume 94:193-204

Conti E. and Lzaurralde E, 2001, Nucleocytoplasmic transport enters the atomic age, Current Opinion in Cell Biology, Volume 13:310-319

Conti E, Muller C.W. and Stewart M, 2006, Karyopherin flexibilty in nucleocytoplasmic transport, Current opinion in Structural Biology, Volume 16:237-244

Cronshaw J.M, Krutchinsky A.N, Zhang W, Chait B.T. and Matunis M.J, 2002, Proteomic analysis of the mammalian nuclear pore complex, Journal of Cell Biology, Volume 158:915-927

Dasso M, 2002, The Ran GTPase: theme and variations, Current Biology, Volume 12:R502-R508

Delphin C, Guan T, Melchior F. and Gerace L, 1997, RanGTP targets p97 to RanBP1, a filamentous protein localised at the cytoplasmic periphery of the nuclear pore complex, Molecular Biology of the Cell, Volume 8:2379-2390

Denning D.P, Patel S.S, Uversky V, Anthony F.L. and Rexach M, 2003, Disorder in the nuclear pore complex: The FG repeat regions of the nucleoporins are natively unfolded, PNAS, Volume 100:2450-2455

Devos D, Dokudovskaya S, Alber F, Williams R, Chait B.T, Sali A. and Rout M.P, 2004, Components of coated vesicles and nuclear pore complexes share a common molecular architecture, PLoS Biology, Volume 2:2085-2093

Devos D, Dokudovskaya S, Williams R, Alber F, Eswar N, Chait B.T, Rout M.P. and Sali A, 2005, Simple fold composition and modular architecture of the nuclear pore complex, PNAS, Volume 103:2172-2177

Dzeja P.P, Bortolon R, Perez-Terzic C, Holmuhamedov L.E. and Terzic A, 2002, Energetic communication between mitochondria and nucleus directed by catalyzed phosphotransfer, PNAS, Volume 99:10156-10161

Englmeier L, Olivio J.C. and Mattaj I.W, 1999, Receptor-mediated substrate translocation through the nuclear pore complex without nucleotide triphosphate hydrolysis, Current Biology, Volume 9:30-41

Fahrenkrog B, Hurt C.E, Aebi U. and Pante N, 1998, Molecular Architecture of the Yeast Nuclear Pore Complex: Localization of Nsp1p Subcomplexes, Journal of Cell Biology,Volume 143:577-588

Fiserova J, Kiseleva E. and Goldberg M.W, 2009, Nuclear envelope and nuclear pore complex structure and organisation in tobacco BY-2 cells, The Plant Journal, Volume 59:243-255

Fiserova J, Richards S.A, Wente S.R. and Goldberg M.W, 2010, Facilitated transport and diffusion takes distinct spatial routes through the nuclear pore complex, Journal of Cell Science Volume 123:2773-2780

Fiserova J. and Goldberg M, 2010, Immunoelectron Microscopy of Cryofixed Freeze-Substituted *Saccharomyces cerevisiae,* Methods in Molecular Biology, Volume 657, Part 2:191-204

Fontoura B.M.A, Blobel G. and Yaseem N.R, 2000, The nucleoporin Nup98 is a site for GDP/GTP exchange on Ran and termination of Karyopherin β2-mediated nuclear import, The Journal of Biological Chemistry, Volume 275:31298-31296

Fortsch J, Hummel E, Krist M, Westermann B, The myosin-related motor protein Myo2 is an assential mediator of bud-directed mitochondrial movement in yeast,Journal of Cell Biology, Volume 3:473-488

Frey S, Richter R.P. and Gorlich D, 2006, FG-rich repeats of nuclear pore proteins form a three-dimensional meshwork with hydrogel-like properties, Science, Volume 314:815-817

Frey S. and Gorlich D, 2007, A saturated FG-repeat hydrogel can reproduce the permeability properties of the nuclear pore complexes, Cell, Volume 130:512-523

Frey S. and Gorlich D, 2009, FG/FxFG as well as GLFG repeats form a selective permeability barrier with self healing properties,EMBO, Volume 28:2554-2567

Fried H. and Kutay U, 2003 Nucleocytoplasmic transport: taking an inventory, Cellular and Molecular Life Sciences, Volume 60:1659-1688

Furukawa K, Ishida K, Tsunoyama T, Toda S, Osoda S, Horigome T, Fisher P.A. and Sugiyama S, 2009, A-type and B-type lamins initiate layer assembly at distinct areas of the nuclear envelope in living cells, Experimental Cell Research, Volume315:1181-1189

Garofalo T, Tinari A, Matarese P, Giammarioli M.A, Manganelli V, Ciarlo L, Misasi R, Sorice M. and Malorni W, 2007, Do mitochondria act as cargo boats in the journey of GD3 to the nucleus during apoptosis, Federation of European Biochemical Societies Volume 581:3899-3903

Goldberg M.W. and Allen T.D, 1992, High resolution scanning electron microscopy of the nuclear envelope demonstration of a new regular, fiberous lattice attached to the baskets of the nucleocytoplasmic face of the nuclear pores, Journal of Cell Biology, Volume 119:1429-1440

Goldberg M.W. and Allen T.D, 1996, The nuclear pore complex and lamina: three-dimensional structures and interactions determined by field emission in-lens scanning electron microscopy, Journal of Molecular Biology, Volume 257:848-865

Goldberg M.W, Solovei I. and Allen T.D, 1997, Nuclear pore complex structure in birds, Journal of Structural Biology, Volume 119:284-294

Goldberg M.W , Rutherford S.A, Hughes M, Cotter L.A, Bagley S, Kiseleva E, Allen T.D. and Clarke P.R, 2000. Ran alters the nuclear pore complex conformation, Journal of Molecular Biology, Volume 300:519-529

Goldberg M.W, 2004, Import and export at the nuclear envelope, Symposia of the Society for Experimental Biology, Volume 56:115-133

Gorlich[1] D, Pante N, Kutay U, Aebi U. and Bischoff F.R, 1996, Identification of different roles for RanGDP and RanGTP in nuclear protein import, EMBO Journal, Volume 15:5584-5594

Gorlich[2] D, Henklein, Laskey R.A and Hartmann E, 1996, A 41 amino acid motif in importin-α confers binding to importin-β and hence transit into the nucleus, EMBO, Volume 15:1810-1817

Griffis E.R, Altan N, Lippincott-Schwartz J. and Powers M.A, 2002, Nup98 is a mobile nucleoporin with transcriptional dependant dynamics, Molecular Biology of the Cell, Volume 12:1282-1297

Hinshaw J.E, Carragher B.O. and Milligan R.A, 1992 architecture and design of the nuclear pore complex, Cell, Volume 69:1133-1141

Ho A.K, Shen X.T, Ryan K.J, Kiseleva E, Levy A.M, Allen T.D. and Wente S.R, 2000, Assembly and preferential localisation of Nup116 on the cytoplasmic face of the nuclear pore complex by interaction with Nup82, Molecular and Cellular Biology, Volume 20:5736-5748

Jarnik M. and Aebi U, 1991, Towards a more complete 3-D structure of the nuclear pore complex, journal of structural biology, Volume 107:291-308.

Kiseleva E, Allen T.D, Rutherford S, Bucci M, Wente S.R. and Goldberg M.W, 2004, Yeast nuclear pore complexes have a cytoplasmic ring and internal filaments, Journal of Structural Biology, Volume 145:272-288

Kiseleva E, Goldberg M.W, Daneholt B. and Allen T.D, 1996, RNP export is mediated by structural reorganisation of the nuclear pore basket, Journal of Molecular Biology, Volume 260:304-311

Kobe B, 1999, Autoinhibition by an internal nuclear localisation signal revealed by the crystal structure of mammalian importin-α, Nature Structural and Molecular Biology, Volume 6:388-397

Krishnan V.V, Lau E.Y, Yamada J, Denning D.P, Patel S.S, Colvin M.E. and Rexach M.F, 2008, Intramolecular cohesion of coils mediated by phenylalanine-glycine motifs in the natively unfolded domain of a nucleoporin, PLOS Computational Biology, Volume 4:1-13

Lee S.J, Matsuura Y, Liu S.M. and Murray S, 2005, Structural basis for nuclear import complex dissociation by RanGTP, Nature, Volume 435:693-696

Lim R.Y.H, Huang N.P, Koser J, Deng J, lau K.H.A, Schwarz-Herion K, Fahrenkrog B. and Aebi U, 2006, Flexible phenylalanine-glycine nucleoporins as entropic barriers to nucleocytoplasmic transport, PNAS, Volume 103:9512-9517

Lim R.Y.H, Fahrenkrog B, Koser J, Schwarz-Herion K, Deng J. and Aebi U, 2007, Nanomechanichial basis of selective gating by the nuclear pore complex, Science, Volume 318:640-643

Lim R.Y.H, Ueli A. and Fahrenkrog B, 2008, Towards reconciling structure and function in the nuclear pore complex, Histochemical Cell Biology, Volume 129:105-116

Lovine M.K. and Wente S, 1997, A Nuclear Export Signal in Kap95p is Required for Both Recycling the Import Factor and Interaction with the Nucleoporin GLFG Repeat regions of Nup116 and Nup100p, The Journal of Cell Biology, Volume:137:797-811

Macara I.G, Transport into and out of the nucleus, 2001, Microbiology and Molecular Biology Reviews Volume 65:570-594

Marelli M, Aitchison J.D. and Wozniak R.W, 1998, Specific Binding of the Karyopherin Kap121 to a Subunit of the Nuclear Pore Complex Containing Nup53p, Nup59p, and Nup170p, Journal of Cell Biology, Volume 143:1813-1830

Masia F, Langbein W, Watson P. and Paola B, 2009, Resonant four-wave mixing of gold nanoparticles for three-dimensional cell microscopy, Optical Letters, Volume 34:1816-1818

Oka M, Asally M, Yasuda Y, Ogawa Y, Tachibana T. and Yoneda Y, 2010, The mobile FG nucleoporin Nup98 is a cofactor for Crm1-dependent protein export, Molecular Biology of the Cell, Volume 21:1885-1896

Patel S.S, Belmont B.J, Sante J.M. and Rexach F. Michael, Natively unfolded nucleoporins gate protein diffusion across the nuclear pore complex, 2007, Cell, Volume 129:83-96

Patel S.S. and Rexach M.F, Discovering Novel Interactions at the Nuclear Pore Complex Using Bead Halo, 2008, Molecular and Cellular Proteomics, Volume 7:121-131

Paulillo S.M, Phillips E.M, Koser J, Sauder U, Ullman K.S, Powers M.A. and Fahrenkrog B, 2005, Nucleoporin domain topology is linked to the transport status of the Nuclear Pore Complex, Journal of Molecular Biology, Volume 351:784-798

Rabut G, Doye V. and Ellengerg J, 2004, Mapping the dynamic organisatiuon of the nuclear pore complex inside single living cells, Nature Cell Biology, Volume 6:1114-1121

Ribbeck K. and Gorlich D, 2001, Kinetic analysis of translocation through the nuclear pore complexes, EMBO, Volume 20:1320-1330

Rout M.P. and Blobel G, 1993, Isolation of the yeast nuclear pore complex, Journal of Cell Biology,Volume 123:771-783

Rout M.P, Aitchison J.D, Suprapto A, Hjertaas K, Zaho Y. and Chait B.T, 2000, The yeast nuclear pore complex: composition, architecture and transport mechanism, Volume 148:635-651

Rout M.P, Aitchison J.D, Magnasco M.O. and Chait B.T, 2003, Virtual gating and nuclear transport: the hole picture, Trends in Cell Biology, Volume 13:622-628

Ryan K.J, McCaffery M and Wente S.R, 2003, the Ran GTPase cycle is required for yeast nuclear pore assembly, The Journal of Cell Biology, Volume 160:1041-1053

Ryan K.J, Zhou Y. and Wente S.R, 2007, The karyopherin Kap95 regulates nuclear pore complex assembly into intoact nuclear envelopes in vivo, Molecular Biology of the Cell, Volume 18:887-898

Scheffzek K, Klebe C, Fritz-Wolf K, Kabsch W. and Wittinghofer A, 1995, crystal structure of the nuclear Ras-related protein Ran in its GDP-bound form, Nature, Volume 374:378-381

Seki T, Hayashi N. and Nishimoto T, 1996, RCC1 in the Ran pathway, Journal of Biochemistry, Volume 120:207-214

Stewart M, 2007, Molecular mechanism of the nuclear protein import cycle, Nature molecular cell biology, Volume 8:195-208

Stoffler D, Goldie K.N, Feja B. and Aebi U, 1999, Calcium-mediated structural change of native nuclear pore complexes monitored by time-lapse atomic force microscopy, Journal of Molecular Biology, Volume 287:741-752

Stoffler D, Feja B, Fahrenkrog B, Walz J, Typke D. and Aebi U, 2003, Cryo-electron tomography provides novel insights into nuclear pore architecture: implications for nucleocytoplasmic transport. Journal of Molecular Biology, Volume 328:119-130

Strambio-de-Castillia C, Blobel G and Rout M.P, 1995, Isolation and characterization of nuclear envelopes from the yeast *Saccharomyces*. Journal of Cell Biology, Volume 131:19-31

Strambio-de-Castillia C, Blobel G and Rout M.P, 1999, Proteins connecting the nuclear pore complex with the nuclear interior Volume 144:839-855

Strawn L.A, Shen T , Shulga N, Goldfarb D.S and Wente S.R, 2004, Minimal nuclear pore complexes define FG repeat domains essential for transport, Nature cell biology, Volume 6:197-206

Tran E.J. and Wente S.R, 2006, Dynamic Nuclear pore complexes: life on the edge, Cell, Volume 125:1041-1053

Walther T.C, Fornerod M, Pickersgill H, Goldberg M, Allen T.D and Mattaj I.W, 2001, The nucleoporin nup153 is required for nuclear pore basket formation, nuclear pore complex anchoring and import of a subset of nuclear proteins, The EMBO Journal, Volume 20:5703-5714

Walther T.C, Pickergill H.S, Cordes V.C, Goldberg M.W, Allen T.D, Mattaj I.W. and Fornerod M, 2002, The cytoplasmic filaments of the nuclear pore complex are dispensable for selective nuclear protein import, The Journal of Cell Biology, Volume 158:63-77

Wente S.R. and Bobel G, 1997, A temperature-sensitive Nup116 null mutant forms a nuclear envelope seal over the yeast nuclear pore complex thereby blocking nucleocytoplasmic transport, The Journal of Cell Biology, Volume 123:275-284

Winey M, Yarar D, Giddings T.H. and Mastronarde D.N, 1997, Nuclear pore complex number and distribution throughout the *Saccharomyces cerevisiae* cell cycle by three-dimensional reconstruction from electron micrographs of nuclear envelopes, Molecular biology of the Cell, Volume 8:2119-2132

Yamada J, Phillips J.L, Patel S, Goldfien G, Calestagne-Morelli A, Huang H, Ryan R, Acheson J, Krishnan V.V, Newsam S, Gopinathan A, Lau E.Y, Colvin M.E, Uversky V.N. and Rexach M.F, 2010, A bimodal distribution of two distinct categories of intrinsically-disordered structures with separate functions in FG nucleoporins, Molecular and Cellular Proteomics in press

Yang Q, Rout M.P. and Akey C.W, 1998, Three-dimensional architecture of the isolated yeast nuclear pore complex: functional and evolutionary implications, Molecular Cell, Volume 1,223-234

Yang W, Gelles J. and Musser S.M, 2004, Imaging of single-molecule translocation through nuclear pore complexes, PNAS, Volume 101:12887-12892.

Yokoyama N, Hayashi N, Seki T, Pante N, Ohba T, Nishii K, Kuma K, Hayashida T, Miyata T, Aebi U. Fukui M. and Nishimoto T, 1995, A giant nucleopore protein that binds Ran/TC4, Nature, Volume 376:184-188.

Zolotukhin A.S. and Felber B.K, 1999, Nucleoporins Nup98 and Nup214 participate in nuclear export of human immunodeficiency virus type 1 Rev, Journal of Virology, Volume 73:120-127

Acknowledgements

I would like to thank Martin for all his help with everything, Jindriska for trying to share her infinite knowledge with me, Ritu for giving me good references and being generally nice to me, Georgia for making me do presentations, and Helen, Tim and Christine for putting up with me. Thank you and sorry to anyone from Biology that I have forgotten.

Finally thanks to Nicola for nagging me to work.

(And probably my family for being wonderful (ish)).